Università degli Studi di Ferrara

DOTTORATO DI RICERCA IN FARMACOLOGIA E ONCOLOGIA MOLECOLARE

CICLO XXI

COORDINATORE Prof. Pier Andrea Borea

Voltage-dependent anion channels: different isoforms for different functions

Settore Scientifico Disciplinare MED/04

Dottorando	**Tutore**
Dott. Diego De Stefani	Prof. Rosario Rizzuto

Anni 2006/2008

Contents

Abstract

The Voltage-dependent anion channel (VDAC) is the most abundant protein of the outer mitochondrial membrane (OMM) and mediates the flow of ions and metabolites between the cytoplasm and the mitochondrial network. Here we reveal novel and unexpected roles of this protein in the regulation of Ca^{2+} signaling, cell death and autophagy, throwing light on the differential contribution of the three mammalian isoforms in these cellular processes. In particular, we show that: i) VDAC is physically linked to the endoplasmic reticulum Ca^{2+} release channel inositol-1,4,5-trisphosphate receptor (IP_3R), through the molecular chaperone grp75 and the functional coupling of these channel directly enhances Ca^{2+} accumulation in mitochondria; ii) the different VDAC isoforms share common Ca^{2+} channelling properties in living cells but VDAC1 is the only isotype selectively coupled to the ER Ca^{2+} releasing machinery, thus laying the foundations for a preferential route specifically transmitting Ca^{2+}-mediated cell death signals between the two organelles; iii) VDAC2 is selectively required for the induction of the autophagic process through the establishment of specific protein-protein interactions and the consequent assembly of macromolecular complexes at the OMM level involved in nutrient sensing mediated by the mammalian Target Of Rapamycin (mTOR) signaling pathway. These data highlight the pleiotropic functions of VDAC and its role as central regulator of cell patho-physiology.

Abstract (italiano)

Il Voltage-dependent Anion Channel (VDAC) è la proteina più espressa a livello della membrana mitocondriale esterna dove regola il flusso di ioni e piccoli metaboliti fra il citoplasma e lo spazio intermembrana. In questo lavoro vengono svelati nuovi ed inattesi ruoli di questa proteina nella regolazione del segnale Ca^{2+}, della morte cellulare e dell' autofagia, ed in particolare sul ruolo specifico che le tre diverse isoforme di questo canale giocano in questi processi. In particolare abbiamo dimostrato che: i) VDAC è in grado di interagire fisicamente con il canale di rilascio per il Ca^{2+} sensibile all'inositolo-1,4,5-trifosfato (IP_3R) del reticolo endoplasmatico attraverso la proteina adattatrice grp75 e che l'accoppiamento funzionale fra questi due canali stimola direttamente l'accumulo di Ca^{2+} nella matrice mitocondriale; ii) nonostante tutte le diverse isoforme di VDAC condividano simili proprietà canale nei confronti dello ione Ca^{2+}, VDAC1 è l'unica isoforma associata in modo specifico ai siti di rilascio del reticolo endoplasmatico e che questa interazione è probabilmente alla base della trasmissione di segnali specifici fra un organello e l'altro che mediano la morte cellulare; iii) VDAC2 è selettivamente coinvolto nell'induzione del processo autofagico grazie a specifiche interazioni proteiche e all'assemblaggio di complessi molecolari a livello della membrana mitocondriale esterna coinvolti nella dalla via di segnalazione del sensore di nutrienti mTOR (mammalian Target Of Rapamycin). Questi dati evidenziano le molteplici funzioni della proteina VDAC e il suo ruolo di fondamentale regolatore di processi sia patologici che fisiologici.

Introduction

The mitochondrion represents a unique organelle within the complex endomembrane systems that characterize any eukaryotic cell. Complex life on earth has been made possible through the "acquisition" of mitochondria which provide an adequate supply of substrates for energy-expensive tasks. Higher multicellular organisms have indeed high energy requirements necessary to carry out complex functions, such as muscle contraction, hormones and neurotransmitters synthesis and secretion, in addition to basal cellular metabolism (biomolecules synthesis and transformation, maintenance of ionic gradients across membrane, cell division). Mitochondria can fulfill this huge energy demand thanks to their extraordinary biosynthetic capacities: every day, mitochondria of a single human being can recycle up to 50 Kg of ATP. To further underline the relevance of these subcellular structures, one can also consider how these organelles have affected the physiology of the whole organism: lungs, heart and circulatory system have evolved essentially to provide molecular oxygen to mitochondria, which consume about 98% of the total O_2 we breathe. However, beyond the pivotal role they play in ATP production, a whole new mitochondrial biology has emerged in the last few decades: mitochondria have been shown to participate in many other aspects of cell physiology such as amino-acid synthesis, iron-sulphur clusters assembly, lipid metabolism, Ca^{2+} signaling, reactive oxygen species (ROS) production and cell death regulation. Hence, it is consequent that any mitochondrial dysfunction will inevitably lead to disease. Indeed, many pathological conditions are associated with organelle failure, including neurodegenerative diseases (Alzheimer's, Parkinson's, Hungtinton's), motoneuron disorders (amyotrophic lateral sclerosis, type 2A Charcot-Marie-Tooth neuropathy), autosomal dominant optic atrophy, ischemia-reperfusion injury, diabetes, ageing and cancer.

Understanding how mitochondria can sense, handle and decode various signals from the cytosol and other subcellular compartments represents a new exciting challenge in biomedical sciences.

Mitochondria: the basics

The mitochondrion is a double membrane-bounded organelle thought to be derived from an α-proteobacterium-like ancestor, presumably due to a single ancient invasion occurred more than 1.5 billion years ago. The basic evidence of this endosymbiont theory (Dyall et al., 2004) is the existence of the mitochondrial DNA (mtDNA), a 16.6 Kb circular double-stranded DNA molecule with structural and functional analogies to bacterial genomes (gene structure, ribosome). This mitochondrial genome encodes only 13 proteins (in addition to 22 tRNAs and 2 rRNAs necessary for their translation), all of which are components of the electron transport chain (mETC) complexes (I, III and IV), while the whole mitochondrial proteome consists of more than 1000 gene products. Thus, one critical step in the transition from autonomous endosymbiont to organelle has been the transfer of genes from the mtDNA to the nuclear genome. At the same time, eukaryotes had to evolve an efficient transport system to deliver nuclear-encoded peptides inside mitochondria: TIM (Transporters of the Inner Membrane), TOM (Transporters of the Outer Membrane) and mitochondrial chaperones (such as hsp60 and mthsp70) build up the molecular machinery that allows the newly-synthesized unfolded proteins to enter mitochondrial matrix (Mokranjac and Neupert, 2005).

Mitochondria are defined by two structurally and functionally different membranes: the plain outer membrane, mostly soluble to ions and metabolites up to 5000 Da, and the highly selective inner membrane, characterized by invaginations called *cristae* which enclose the mitochondria matrix. The space between these two structures is traditionally called intermembrane

space (IMS), but recent advances in electron microscopy techniques shed new light on the complex topology of the inner membrane. Cristae indeed are not simply random folds but rather internal compartments formed by profound invaginations originating from very tiny "point-like structures" in the inner membrane (Mannella, 2006). These narrow tubular structures, called *cristae junctions*, can limit the diffusion of molecule from the intra-cristae space towards the IMS, thus creating a micro-environment where mETC complexes (as well as other proteins) are hosted and protected from random diffusion.

As mentioned before, mitochondria are the main site of ATP production. When glucose is converted to pyruvate by glycolysis, only a small fraction of the available chemical energy has been stored in ATP molecules: mitochondria can "release" the remaining amount of energy with an outstanding efficiency (from a single glucose molecule mitochondria produce 15 times more ATP than glycolysis). The main enzymatic systems involved in this process are the tricarboxylic acid (TCA) cycle and the mETC. Products from glycolysis and fatty acid metabolism are converted to acetyl-CoA which enters the TCA cycle where it is fully degraded to CO_2. More importantly, these enzymatic reactions generate NADH and $FADH_2$ which provide reducing equivalents and trigger the electron transport chain. mETC consists of five different protein complexes: complex I (NADH dehydrogenase), complex II (succinate dehydrogenase), complex III (ubiquinol cytochrome c reductase), complex IV (cytochrome c oxidase) and complex V that constitutes the F_1F_0-ATP synthase. Electrons are transferred from NADH and $FADH_2$ through these complexes in a stepwise fashion: as electrons move along the respiratory chain, energy is stored as an electrochemical H^+ gradient across the inner membrane, thus creating a negative mitochondrial membrane potential (estimated around -180 mV against the cytosol). H^+ are forced to reenter the matrix mainly through complex V which couples this proton driving force to the phosphorylation of ADP into ATP, according to the chemiosmotic principle. ATP is then released to IMS through the electrogenic Adenine Nucleotide Translocase (ANT) which exchange ATP with ADP to provide new substrate

for ATP synthesis. Finally, ATP can easily escape the IMS thanks to the mitochondrial porin of the outer membrane, VDAC (voltage dependent anion channel) (Duchen, 2004). However, in the last two decades interest in mitochondrial biology has literally revamped, since the discovery of their prominent role in triggering cell death through apoptosis (Liu et al., 1996).

Calcium signaling: the general framework

In all eukaryotic cells, the cytosolic concentration of Ca^{2+} ($[Ca^{2+}]_c$) is tightly controlled by complex interactions among pumps, channels, exchangers and binding proteins, and relatively small and/or local changes in its concentration modulate a wide range of intracellular actions. $[Ca^{2+}]_c$ in resting condition is maintained around the value of 100nM, significantly lower than extracellular $[Ca^{2+}]$ (1mM). This condition is guaranteed by the low permeability of the plasma membrane to ions and by the activity of the Plasma Membrane Ca^{2+}-ATPase (PMCA, which pumps Ca^{2+} outside the cells) and of the Na^+/Ca^{2+} exchanger (NCX). This fine regulation of $[Ca^{2+}]$ allows this ion to act as one of the most important second messenger in signal transduction pathways. (Hajnoczky et al., 2000; Hajnoczky et al., 2002)

The increase of intracellular $[Ca^{2+}]$ can be elicited through two fundamental mechanisms: i) the Ca^{2+} mobilization from intracellular stores, mainly the endoplasmic reticulum (ER) and Golgi apparatus, or ii) the entry from the extracellular milieu. The main route inducing Ca^{2+} release from intracellular stores involves the IP_3 Receptor (IP_3R), a transmembrane protein located on the ER and Golgi membrane, which exposes on the cytosolic face the IP_3 binding site, while it forms a Ca^{2+} channel in the transmembrane domain. When extracellular soluble agonists binds a G-coupled protein receptor, different isoforms of phospholipase C (PLC) are activated producing inositol-1,4,5-trisphosphate (IP_3) from the hydrolysis of phosphatidylinositol 4,5 bisphosphate (PIP_2). The binding of IP_3 to its receptor induces its opening and the release of Ca^{2+} from ER and Golgi. IP_3R is not the only protein involved in Ca^{2+} release: ryanodine Receptor (RyR), for example, is a

6

transmembrane protein located on the ER membrane and it is activated by the alchaloid ryanodine and by Ca^{2+} itself, while Sphingolipid Ca^{2+} release-mediating protein of the ER (SCaMPER) is activated by sphingosine-1-phosphate (Mao et al., 1996). Intracellular store depletion consequent to the opening of the IP_3R triggers the activation of an inward rectifying Ca^{2+} current from the extracellular spece named capacitative Ca^{2+} entry (CCE). The molecular determinants of CCE have been identified in the very last few years and include an ER Ca^{2+} sensing protein (STIM) and specialized Ca^{2+} channels in the plasma membrane (Ora, for a recent review (Oh-hora and Rao, 2008)). The second mechanism inducing intracellular Ca^{2+} increases involves the opening of the plasma membrane Ca^{2+} channels, which are traditionally grouped into three classes: the Voltage Operated Ca^{2+} channels (VOCs) which open following a decrease of membrane potential (Bertolino and Llinas, 1992), the Receptor Operated Ca^{2+} channels (ROCs), also called ligand gated channels, which open following the binding of an external ligand (McFadzean and Gibson, 2002) and the Second Messenger Operated Channels (SMOCs) which open following the binding of a second messenger on the inner surface of the membrane (Meldolesi and Pozzan, 1987). Once activated its downstream targets, Ca^{2+} has to be rapidly removed from cytosol to restore the resting conditions. So, the Ca^{2+} signal is terminated by the combined activity of Ca^{2+} extrusion mechanisms, such as PMCA and NCX, and mechanisms refilling the intracellular stores, like Sarco-Endoplasmic Reticulum Ca^{2+} ATPases (SERCAs). It has long been known that mitochondria can rapidly accumulate Ca^{2+} down the electrochemical gradient established by the translocation of protons across the inner mitochondrial membrane (IMM), which is expressed as a membrane potential difference ($\Delta\psi_m$) of -180mV (negative inside) under physiological conditions (Mitchell, 1966). However, the accurate measurements of $[Ca^{2+}]$ in resting cells revealed values well below the affinity of the mitochondrial transporters. Thus, the role of mitochondria in Ca^{2+} homeostasis was considered marginal (i.e. limited to conditions of cellular Ca^{2+} overload), till the development of specific and reliable probes directly reported major swings of mitochondrial $[Ca^{2+}]$ (Rizzuto et al.,

1992b). While enlivening the interest in mitochondrial Ca^{2+} homeostasis, these data raised an apparent contradiction between the prompt response of the organelle and the low affinity of the transporter. Based on a large body of experimental evidence, it is now generally accepted that the key to the rapid Ca^{2+} accumulation rests in the strategic location of a subset of mitochondria, close to the opening Ca^{2+} channel. While, based on cell morphology, such proximity is expected, and indeed often observed, in neuronal prolongings, a close proximity between ER-resident Ca^{2+} channels and mitochondria in non-excitable cells implies the assembly of a dedicated signaling unit at the organelle interphase.

ER/mitochondria crosstalk: local microdomains support mitochondrial Ca^{2+} uptake

Mitochondrial Ca^{2+} transport: general concepts

The capacity of isolated mitochondria to rapidly accumulate Ca^{2+} across their membranes was a relatively early notion in bioenergetics and cell biology, already established in the 1960s (deluca vasington) when research carried out by various groups demonstrated that energized mitochondria can rapidly take up Ca^{2+} from the medium (for reviews, see (Saris and Carafoli, 2005)). Indeed, based on the chemiosmotic theory, the translocation by protein complexes of H^+ across an ion-impermeable inner membrane generates a very large H^+ electrochemical gradient and mitochondria employ the dissipation of this proton gradient not only to run the endoergonic reaction of ATP synthesis by the H^+-ATPase but also to accumulate cations into the matrix. Ca^{2+} fluxes across the ion-impermeable inner membrane is, in fact, not mediated by pumps or exchangers, but by a "uniporter" (possibly a gated channel, although the molecular identity and nature of the uniporter remains unknown) that provides a pathway for the accumulation of Ca^{2+} into the mitochondrial matrix, driven by the electrochemical potential gradient across the inner mitochondrial membrane, usually estimated at ~180 mV negative to the cytosol (Gunter et al.,

1998). If Ca^{2+} accumulation were governed solely by thermodynamic parameters, equilibrium, according to the Nernst equation, would be reached only when Ca^{2+} in the matrix reaches values 10^6 higher than in the extramitochondrial space, i.e. in the cytosol. As a consequence, most researchers by the end of 70's were convinced that these organelles comprised the key intracellular Ca^{2+} stores in living cells. The scenario changed dramatically at the beginning of the 1980s, when it was not only discovered that the total Ca^{2+} content of mitochondria in situ was negligibly low, but also that the Ca^{2+} mobilization from internal compartments elicited by receptor activation involved another cellular organelle, the endoplasmic reticulum (ER) (Streb et al., 1983).

In those years, while Ca^{2+} emerged as the ubiquitous, fundamental second messenger known to every biology student, it became immediately evident that mitochondria were not the active store in these signaling pathways. Indeed, the messenger shown to be produced upon stimulation of G protein coupled or growth factor receptors, IP_3, acts on ion channels located in the ER (Prentki et al., 1984). Moreover, the latter organelle (and not mitochondria) was shown to contain the molecular elements of a Ca^{2+} store: a pump (to accumulate Ca^{2+} against electrochemical gradient), a channel (to rapidly release it), and buffering proteins (to increase the total amount of ion that can be stored). For this reason, the concept of mitochondria as cellular Ca^{2+} stores was largely dismissed. In support of the notion that mitochondria cannot act as intracellular Ca^{2+} store, it should be noted that both resting and stimulated values of $[Ca^{2+}]_c$ appeared to be well below the affinity of the mitochondrial uniporter for Ca^{2+} (an apparent K_d of 20 to 30 μM under conditions thought to mimic the cytoplasm, estimated in the earlier work with isolated organelles). Indeed, the availability of indicators that could be easily loaded into most cell types and calibrated into accurate $[Ca^{2+}]$ estimates allowed us to verify that in living cells not only resting values (~0.1 μM), but also those briefly reached after physiological stimulation (1–3 μM), mitochondria could not, at least in principle, accumulate significant amounts of Ca^{2+}. The general consensus thus became that the well

established capacity of mitochondria to accumulate Ca^{2+} would be significant only in conditions of high-amplitude, prolonged $[Ca^{2+}]_c$ increases, i.e. in the Ca^{2+} overload that is observed in various pathological conditions (such as, for example, excitotoxic glutamate stimulation of neurons), convinced the majority of specialists that these organelles had little to do with physiological Ca^{2+} handling (Schinder et al., 1996). In contrast with this view, biochemical work demonstrated that three important mitochondrial enzymes intervening in key steps of intermediate metabolism (the pyruvate-, α-ketoglutarate- and isocitrate-dehydrogenases) are regulated by Ca^{2+}, a notion that would imply that $[Ca^{2+}]_m$ should vary in the physiological life cycle of a cell (Hansford, 1994; McCormack et al., 1990). However, given that no direct experimental evidence could support the notion that the Ca^{2+} concentration in the mitochondrial matrix rapidly changes upon cell stimulation, this observation did not modify the general perception of mitochondria as relatively inactive bystanders in the complex scene of cellular Ca^{2+} homeostasis.

This situation was completely reversed by the direct demonstration, at the beginning of the last decade, that mitochondria can rapidly accumulate Ca^{2+} under physiological conditions in living cells (Rizzuto et al., 1992a), and that Ca^{2+} accumulation modulates mitochondrial metabolic efficiency (Jouaville et al., 1999b), affects calcium signaling (Tinel et al., 1999), and can be a key factor in the activation o programmed cell death, matter of course a revitalized interest in this process.

Measurement of $[Ca^{2+}]_m$ in living cells lay the foundation of the "Hotspot Hypothesis"

The concept that mitochondria undergo major changes in matrix $[Ca^{2+}]$ also in physiological conditions awaited the direct, reliable measurement of this parameter in intact living cells. This was first achieved in the 1990s, by targeting to mitochondria a Ca^{2+}-sensitive photoprotein, aequorin (Rizzuto et al., 1992a), and allowed us to demonstrate that in a broad variety of systems that rely on different Ca^{2+} signalling machineries (i.e. IP$_3$Rs for HeLa cells, hepatocytes or astrocytes, RyRs for cardiac and skeletal muscle cells, plasma membrane channels for neurons and chromaffin cells),

10

$[Ca^{2+}]_c$ rises evoked by physiological stimulations are always paralleled by rapid $[Ca^{2+}]_m$ increases, which reach values well above those of the bulk cytosol (up to the millimolar range in chromaffin cells (Montero et al., 2000)). These studies showed that mitochondria in situ are much more efficient at taking up Ca^{2+} than predicted from their apparently low Ca^{2+} affinity, a notion that now is widely accepted. Similar conclusions could be reached also with fluorescent indicators, such as the positively charged Ca^{2+} indicator rhod-2 (that accumulates within the organelle) (Csordas et al., 1999) and the more recently developed GFP-based fluorescent indicators. With the latter probes, endowed with a much stronger signal than the photoprotein, single-cell imaging of organelle Ca^{2+} can be carried out. Thus it is possible to match the accurate estimates of $[Ca^{2+}]_m$ values, obtained with the photoprotein, with detailed spatiotemporal analyses of $[Ca^{2+}]_m$ transients. With these tools in hands, not only the notion was confirmed that mitochondria promptly respond to cytosolic $[Ca^{2+}]$ rises, but also that the $[Ca^{2+}]_c$ oscillations, the typical response to agonists of many cell types, are paralleled by rapid spiking of $[Ca^{2+}]_m$, thus providing a frequency-mediated signal specifically decoded within the mitochondria, as clearly shown in hepatocytes (Thomas et al., 1995), cardiomyocytes (Robert et al., 2001), and HeLa cells.

The obvious discrepancy between the low affinity of mitochondrial Ca^{2+} uptake mechanisms (expected based on the properties of their Ca^{2+} transporters established in vitro) together with the low concentration of global Ca^{2+} signals observed in cytoplasm (where Ca^{2+} elevations rarely exceed 2–3 μM), and the efficiency of mitochondrial Ca^{2+} uptake in intact cells (where$[Ca^{2+}]$ rise, in a few seconds, to values above 10 μM, and in some cell types up to 500 μM) led to the formulation of the "hotspot hypothesis". This hypothesis proposes that mitochondria preferentially accumulate Ca^{2+} at microdomains of high $[Ca^{2+}]$ that largely exceed the values reported in the bulk cytosol and meet the low affinity of the uniporter. This is achieved through a close interaction between the mitochondria and the ER, the intracellular Ca^{2+} store.

11

The key experiment that gave rise to the Ca^{2+} "hotspot" hypothesis was published in 1993 (Rizzuto et al., 1993). This experiment showed that perfusion of permeabilized cells with buffered $[Ca^{2+}]$ similar to those measured in the cytoplasm of stimulated (through activation of G protein-coupled receptors) intact cells induced a relatively inefficient Ca^{2+} loading of mitochondria, thus confirming the notion of a low-affinity uptake system. Conversely, discharge of Ca^{2+} from the ER triggered by the direct perfusion of IP_3 (thus causing the opening of the physiological Ca^{2+} release pathway also in permeabilized cells) induce mitochondrial Ca^{2+} uptake almost as efficiently as in intact stimulated cells. Because IP_3 itself had no effect on isolated mitochondria, this experiment (repeated later in many cell types and with different protocols) suggested that release of Ca^{2+} through the IP_3-gated ER channel created a microenvironment of $[Ca^{2+}]$ close to the mitochondria that was much higher than that measured in the bulk cytosol and high enough to activate the low affinity Ca^{2+} uniporter. In other words, "privileged," local signaling between the Ca^{2+} store (the ER) and mitochondria appeared to be the key to the participation of this organelle in intracellular Ca^{2+} homeostasis. It is important to underlines that the rapid dissipation of the local gradients by simple diffusion ensures a decrease in the rate of mitochondrial Ca^{2+} uptake and thus prevents excessive Ca^{2+} accumulation and mitochondrial damage. Additional strong evidence in support of the hotspot model is the relative insensitivity of the mitochondrial Ca^{2+} uptake rate, at least in some cell types, to cytoplasmic Ca^{2+} buffering. In cardiac cells, for example, concentrations of the Ca^{2+} chelator EGTA sufficient to practically abolish the cytosolic Ca^{2+} transient in response to caffeine are much less effective at inhibiting Ca^{2+} increases within mitochondria (Griffiths et al., 1998), which suggests that the distance is so small that Ca^{2+} diffuses from ER release channels into the mitochondria more rapidly than it can be buffered by EGTA.

The capacity of mitochondria to sense the microenvironment at the mouth of the IP_3-sensitive channel, and thus the high $[Ca^{2+}]$ generated by their opening upon cell stimulation is achieved through a close interaction between the mitochondria and the ER, that could be directly

demonstrated using targeted chimeras of green fluorescent recombinant protein (GFP) and a high-resolution imaging system. By imaging green fluorescent protein (GFP) constructs targeted to the it was estimated that 5-20% of the mitochondrial surface is in close apposition to ER in living HeLa cells. In keeping with the idea of "local" Ca^{2+} cross-talk between the mitochondria and the ER, it was recently demonstrated, through fast single-cell imaging of mitochondrial $[Ca^{2+}]m$ with targeted Ca^{2+}-sensitive GFPs (pericams and cameleons), that $[Ca^{2+}]_m$ increases originate from a discrete number of sites and rapidly diffuse through the mitochondrial network (Szabadkai et al., 2004). This concept, originally put forward through experiments carried out in HeLa cells, was confirmed in many cell systems, ranging from hepatocytes (in which this morpho-functional arrangement was shown to participate in the regulation of Ca^{2+} release through the IP$_3$Rs) to neurons, in which mitochondria were shown to be strategically placed to sense, and modulate, defined plasma membrane Ca^{2+} microdomains (e.g. those generated in synaptic regions).

The molecular and cellular definition of the ER/mitochondria contacts

Close appositions between ER and mitochondria have been observed in electron micrographs (EM) of fixed samples in many different cell types while experiments performed by our group had eventually confirmed the physical and functional coupling of these two organelles in living cells, by labelling the two organelles with targeted spectral variants of GFP (mtBFP and erGFP) (Rizzuto et al., 1998a). These experiments revealed the presence of overlapping regions of the two organelles (thus establishing an upper limit of 100 nm for their distance) and allowed to estimate the area of the contact sites as 5-20% of total mitochondrial surface. More recently, electron tomography techniques allowed to estimate an even smaller distance (10-25 nm) as well as the presence of trypsin-sensitive (hence proteinaceous) tethers between the two membranes (Csordas et al., 2006).

Unfortunately, very few of the relevant scaffolding or signaling proteins of the ER/mitochondria contacts have been identified, despite the growing interest on the topic.

13

Nevertheless, novel candidates are rapidly being isolated and it can be envisaged that the molecular characterization will rapidly proceed, thanks to the validation of biochemical approaches in the isolation of a subcellular fraction containing the putative ER/mitochondria contacts. Indeed one of the major apparent known technical pitfall of subcellular fractionation, i.e. the "contamination" of the mitochondrial fraction with ER vesicles, has been demonstrated to be due to the actual co-segregation of stably associated mitochondrial and ER membranes. This has led to a more accurate separation, through density gradient centrifugations, of pure mitochondria from the so-called "mitochondria-associated membrane" (MAM), which have been originally shown to be enriched in enzymes involved in lipid transfer between ER and mitochondrial membranes (e.g. the import of phosphatidylserine (PS) into mitochondria) (Stone et al., 2008; Vance, 1990, 2008). The shaping of the ER-mitochondrial network can be affected by binding proteins and physiological ligands; recently Hajnoczky and coworkers demonstrated that exposure to TGFβ affects Ca^{2+} transfer to the mitochondria through an impairment of the ER-mitochondrial coupling, thus supporting the notion of a highly dynamic regulation of inter-organelle communication (Pacher et al., 2008).

This actively adapting interconnection stems also from the observation that these organelles are intrinsically highly dynamic structures continuously moving (Saotome et al., 2008; Yi et al., 2004a) and remodelling in their shape. As a consequence, the molecular determinants of this dynamism, such as for example, the family of "mitochondria-shaping proteins" (Drp1, mitofusins, Opa1 etc.) constitute potential modulators of ER/mitochondria crosstalk. Along this line, Scorrano and coworkers have recently pointed out the crucial role of the mitofusin (MFN 1 and 2), in particular the isoform 2 is thought to be important for ER-mitochondrial interactions engaging them in both homo and etero-complexes(de Brito and Scorrano, 2008). They also showed that genetic ablation of MFN2 causes an increase in the distance between the two organelles with a consequent impairment of mitochondrial Ca^{2+} uptake, thus further supporting the high $[Ca^{2+}]$ microdomains theory. Moreover the ER-mitochondrial apposition performed by MFN 2 predispose

14

mitochondria to high Ca^{2+} microdomains and to the consequent overloading, leading eventually to apoptosis by excessive Ca^{2+} transfer.

Mitochondrial Ca^{2+} channels of the inner mitochondrial membrane

The molecular machinery of mitochondrial Ca^{2+} transport is still largely obscure. Indeed, accumulation into the matrix, and consequent release, occur via the activity of transport mechanisms that were functionally characterized in the 70s but were never molecularly identified despite the extensive efforts in this direction. We and other groups extensively worked on this topic and what emerged was that the outer mitochondrial membrane membrane (OMM, although traditionally considered freely permeable) is a critical determinant of the mitochondrial Ca^{2+} accumulation (Csordas et al., 2002; Rapizzi et al., 2002a). Thus, the mitochondrial Ca^{2+} uptake machinery will be brefly discussed, concentrating on the influx and efflux mechanism of the IMM.

The Mitochondrial Calcium Uniporter (MCU)

Mitochondrial Ca^{2+} uptake plays a key role in the regulation of many cell functions, ranging from ATP production to cell death. However, the molecular mechanism underlying this phenomenon has not yet been completely explaned, indeed, while the contribution of OMM Ca^{2+} channels (VDAC) has been well characterized, little is known about the so called Mitochondrial Ca^{2+} Uniporter (MCU). MCU is an highly selective ion channel located in the mitochondrial inner membrane, with a dissociation constant $\leq 2nM$ over monovalent cations, reaching saturation only at supraphysiological $[Ca^{2+}]_c$. Ca^{2+} crosses the inner mitochondrial membrane through the MCU thanks to the considerable driving force represented by the negative transmembrane potential. Also Sr^{2+} and Mn^{2+} are conducted by MCU and the relative ion conductance can be resumed as follows: $Ca^{2+} \approx Sr^{2+} \geq Mn^{2+} \approx Ba^{2+}$. Studies performed on isolated mitochondria allowed the identification of some regulatory molecules acting on MCU, in particular the most effective inhibitors are the

hexavalent cation Rutenium Red (RuR) and its related compound RuR360; MCU is also modulated by aliphatic polyamines, such as spermine and aminoglycosides, and by the adenine nucleotides, in the order of effectiveness ATP>ADP>AMP (whereas the nucleoside adenosine is ineffective) (Litsky and Pfeiffer, 1997) as well as several plant-derived flavonoids (Montero et al., 2004). RuR could represent a potentially important tool for the MCU identification, but it showed some major drawbacks: indeed, it binds a broad array of glycoproteins and it is completely cell-impermeant so that, even at high concentrations (50mM), it is almost ineffective in reducing the mitochondrial Ca^{2+} transients elicited by cell stimulation. Another important regulator of MCU is Ca^{2+} itself. As demonstrated by Moreau and its group, in fact, MCU has a biphasic dependence on cytosolic Ca^{2+} concentration ($[Ca^{2+}]_c$): $[Ca^{2+}]_c$ increase can both activate or inactivate mitochondrial Ca^{2+} uptake. MCU activation by Ca^{2+} is mediated by the Ca^{2+}-dependent Calmodulin activation and by the following activation of its effector, Calmodulin-dependent Protein KinaseII (CaM kinaseII), as demonstrated by the impairment of mitochondrial Ca^{2+} uptake induced by KN-62, an inhibitor of CaM kinaseII. On the other hand, $[Ca^{2+}]_c$ increase then inactivates the uptake pathway. These two processes follow an accurate kinetic: the uptake induction occurs with a time constant of 6 seconds, while the inactivation occurs with a time constant of 17 seconds. This mechanism allows the mitochondrial Ca^{2+} oscillation, but it prevents an excessive mitochondrial Ca^{2+} accumulation when intracellular Ca^{2+} elevation is prolonged (Moreau et al., 2006). Further studies performed to clarify the mechanisms regulating Ca^{2+} homeostasis, suggest a role of the kinase- mediated network in the regulation of Ca^{2+} uptake: in particular, the different isoforms of protein kinase C (PKC), when overexpressed in HeLa cells, showed different effects on global Ca^{2+} signaling (e.g. PKCα, possibly through the previously reported PKC-mediated phosphorylation of IP_3Rs, reduces ER Ca^{2+} release (Ferris et al., 1991),while the other PKC isoforms act on mitochondrial homeostasis: PKCβ reduces mitochondrial Ca^{2+} transients, whereas PKCζ potentiates them) (Pinton et al., 2004). A recent paper

by Graier and coworkers suggested that the uncoupling proteins 2 and 3 (UCP2 and UCP3) of the IMM are essential for mitochondrial Ca^{2+} uptake since isolated liver mitochondria from UCP2 KO mice show no RuR-sensitive Ca^{2+} uniporter acivity (Trenker et al., 2007). However, attempts from other groups to reproduce these data failed (Brookes et al., 2008), thus the role of UCPs in mitochondrial Ca^{2+} uptake should be regarded with caution. Finally, circumventing the low affinity of the MCU, another mode of Ca^{2+} influx into mitochondria was described by Sparagna *et al.* (Sparagna et al., 1995), defined rapid mode of uptake or RaM. This route should allow mitochondria to uptake large amounts of Ca^{2+} in short pulses, at least 300 times faster than through the MCU. It should transport Ca^{2+} only for a brief period during the initial part of the pulse and then be inactivated by Ca^{2+} binding to an external binding site. These prerogatives thus imply a marginal role in the total uptake of Ca^{2+} in the matrix, but could possibly generate local $[Ca^{2+}]_m$ microdomains near the site of the transporter, that could represent hotspots for the regulation of Ca^{2+}-sensitive matrix processes. This work was not followed up, and thus the molecular identity, and even the existence, of RaM is even more elusive than MCU. Indeed, it is sensitive to the same regulatory mechanisms (e.g. it is also inhibited by RuR), so the possibility remains open that it is simply a different functional state of the MCU (Gunter et al., 2000).

Calcium extrusion pathways

The efflux pathways were extensively studied in isolated organelles, and their functional properties are fairly well characterized. The mitochondrial Na^+/Ca^{2+} exchanger (mNCX) is similar to that found in the plasma membrane; it allows Ca^{2+} efflux and it is inhibited by Sr^{2+}, Ba^{2+}, Mg^{2+} or Mn^{2+}, and by a variety of compounds of pharmacological interest such as diltiazem, verapamil and other blockers of the voltage-dependent calcium channels, and more specifically by CGP37157 [30]. As to the stechiometry of the exchange, Ca^{2+} was reported to be transported out of mitochondria against values greater than those predicted for passive leak, and thus a $Ca^{2+}/3Na^+$ was postulated (Baysal et al., 1994). The H^+/Ca^{2+} exchanger (mHCX) is prevalent in non-excitable

cells, and it extrudes Ca^{2+} against a gradient that is much higher than what thermodynamic parameters permit for an electroneutral H^+/Ca^{2+} exchanger (Jung et al., 1996; Pfeiffer et al., 2001). These efflux pathways can become saturated with high matrix Ca^{2+} load, such that sustained and rapid Ca^{2+} influx can still lead to mitochondrial Ca^{2+} overload.

Calcium release from cellular store: structure and function of the IP_3R

Many extracellular stimuli, such as hormones, growth factors, neurotransmitters, neutrophins, odorants, and light, function generating IP_3 through the phospholipase C isoforms, activated in different manners: G-protein coupled receptors (PLCβ), tyrosine-kinase coupled receptors (PLCγ), an increase in Ca^{2+} concentration (PLCδ) or activated by Ras (PLCε) (Litjens et al., 2007; Rebecchi and Pentyala, 2000). The final effector is the inositol 1,4,5 trisphosphate IP_3-sensitive receptor, a member of a superfamily of ion channels with six transmembrane domains, residing on the ER membrane. The opening of the channel is under dual control, by IP_3 and by Ca^{2+} itself, as will be discussed in more detail later.

From the structural point of view, several domains are recognized in the protein sequence, with different functions. These include the IP_3-binding domain (IP_3BD), i.e. the minimal sequence sufficient for IP_3 binding, located near the N-terminus of the protein (aa 226-578). Interestingly, this protein domain contains armadillo-repeat protein structures that are engaged in protein-protein interactions, and mediates intramolecular interactions with other IP_3R domains as well as the association with other regulatory proteins. N-terminally to the IP_3BD, i.e. within aa 1-222, a suppressor region is located that inhibits ligand binding and thus lowers the global receptor IP_3 affinity in the physiological range. In the C-terminal portion, hydrophobic residues form the C-terminal transmembrane/channel-forming domain (Furuichi et al., 1989; Mignery and Sudhof, 1990), and, between them, an internal coupling domain assures the signal of IP_3 binding is transferred to the channel-forming region, hence triggering its opening (Mikoshiba, 2007). Finally,

in their coupling/suppressor domains, the IP$_3$Rs possess consensus sequences for phosphorylation by numerous kinases, including Protein Kinase A (cAMP-dependent) (Bugrim, 1999), Protein Kinase B (Akt/PKB) (Khan et al., 2006), Protein Kinase G (cGMP-dependent) (Murthy and Zhou, 2003), calmodulin-dependent protein kinase II (CaMKII) (Bagni et al., 2000), protein kinase C (PKC) (Vermassen et al., 2004), and various protein tyrosine kinases (PTK) (Jayaraman et al., 1996).

Three isoforms of IP$_3$R encoded by different genes have been identified with different agonist affinities and tissue distribution (Furuichi et al., 1994; Iwai et al., 2005; Wojcikiewicz, 1995). Given that the affinity of the IP$_3$-binding core to its ligand is similar for the three isoforms, the tuning of the whole receptor's affinity appears to be due to the isotype-specific properties of the N-terminal suppressor domain (Iwai et al., 2007).

Ca^{2+} regulates channel activity in a biphasic manner, depending on Ca^{2+} concentration: at [Ca^{2+}] < 300nM, the ion exerts an activatory role, while it has an opposite inhibitory effect at [Ca^{2+}] > 300nM [44], thus allowing a fine dynamic feedback regulation during Ca^{2+} release (Iino and Endo, 1992). This biphasic regulation is particular evident for isoform 1, while the IP$_3$R-2 has a moderate Ca^{2+} sensitivity, and IP$_3$R-3 works at low cytosolic Ca^{2+} levels and it is not inhibited by high Ca^{2+} concentrations. In addition, also the ER Ca^{2+} content retains the capability to regulate the channel opening: in permeabilized hepatocytes, an increase in [Ca^{2+}]$_{er}$ enhances the sensitivity of IP$_3$R for its ligand, promoting also spontaneous Ca^{2+} release, but the nature of this direct regulation and the protein involved are still a matter of debate (Missiaen et al., 1992; Nunn and Taylor, 1992). In this context, the tight spatial relationship between ER and mitochondria, and the capacity of the latter to rapidly clear the high [Ca^{2+}] microdomain generated at the mouth of the IP$_3$R, makes mitochondria an active player in the control of IP$_3$R function. The first clear demonstration of this concept came from the fine work of Lechleiter and coworkers, who demonstrated that energized mitochondria, by regulating the kinetics of ER Ca^{2+} release, finely tune the spatio-temporal

patterning of Ca^{2+} waves in *Xenopus* oocytes (Jouaville et al., 1999a). Then, the observation that Ca^{2+} uptake by mitochondria controls the $[Ca^{2+}]$ microdomain at the ER/mitochondrial contacts and thus the kinetics of IP_3R activation/inactivation was extended to a variety of mammalian cell lines, e.g. hepatocytes (Hajnoczky et al., 1999), astrocytes (Boitier et al., 1999) and BHK-21 cells (Landolfi et al., 1998), thus highlighting its general relevance.

Whereas IP_3 and Ca^{2+} are essential for IP_3R channel activation, other physiological ligands, such as ATP, are not necessary but can finely modulate the Ca^{2+}-sensitivity of the channel (Smith et al., 1985). As for Ca^{2+}, the modulation of IP_3R by ATP is biphasic: at micromolar concentrations, ATP exerts a stimulatory effect, while inhibiting channel opening in the millimolar range (Bezprozvanny and Ehrlich, 1993; Iino, 1991).

Upon IP_3 production, IP_3Rs have been shown to cluster at the ER membranes: the size and composition of these clusters depend on the isoform involved, while the global IP_3 binding affinity is shared among the different isoforms (Iwai et al., 2005; Tateishi et al., 2005). Spontaneous clustering of IP_3Rs (in particular of IP_3R-2, due to its higher IP_3 affinity) have been proposed to be the underlying mechanism responsible for Ca^{2+} puffs observed in the cytoplasm (Mikoshiba, 2007). The merging of discrete and localized $[Ca^{2+}]_c$ increases, due to the opening of clustered IP_3Rs (Parker and Ivorra, 1990), are called "Ca^{2+} puffs" (Yao et al., 1995). Recruitment of neighboring IP_3Rs and combination of Ca^{2+} puffs results in Ca^{2+} waves, ensuring that the Ca^{2+} signal propagates to the entire cell (Rooney and Thomas, 1993), or limited to specific subcellular regions (Allbritton and Meyer, 1993). The effects triggered by tightly controlling the diffusion of a $[Ca^{2+}]_c$ signal elicited by IP_3R opening is well illustrated by pancreatic acinar cells. In this polarized cell type, the Ca^{2+} wave originates in the apical pole and may spread through the entire cell reaching the nucleus, determining gene transcription or cell death. Alternatively, the $[Ca^{2+}]_c$ signal can remain localized near the source, i.e. the apical pole, activating short-term effects such as secretion of enzyme-containing granules (Lee et al., 1997a; Lee et al., 1997b; Petersen et al., 1999; Thorn et al., 1993).

The fate of the $[Ca^{2+}]$ signal (remaining localized in the apical region, or reaching the basal region) depends on, at first, the effectiveness of the stimulus and the further action of different second messengers, and secondly, on the "firewall" effect given by mitochondria. Indeed, in this case mitochondria were shown to cluster between the apical and basal pole of the cell, thus forming a fixed "Ca^{2+} buffer" that must be overwhelmed by robust Ca^{2+} wave in order to reach the basolateral area. This occurs in case of supramaximal stimulations, but also when pathological challenges (e.g. alcohol or bile acids) synergistically act on the cells..

Enhancing ATP production or killing the cell: the yin/yang of mitochondrial calcium

The main physiological role of Ca^{2+} uptake was assessed to be the control of metabolic activity of the mitochondria, in terms of ATP production rate. Indeed, important metabolic enzymes localized in the matrix, the pyruvate-, α-ketoglutarate- and isocitrate-dehydrogenases (collectively called the Ca^{2+}-sensitive mitochondrial dehydrogenases, CSMDHs) are activated by Ca^{2+}, with different mechanisms: the first through a Ca^{2+}-dependent dephosphorylation step, the others via direct binding to a regulatory site (McCormack et al., 1990). Those three enzymes represent rate-limiting steps of the Krebs cycle thus controlling the feeding of electrons into the respiratory chain and the generation of the proton gradient across the inner membrane, in turn necessary for Ca^{2+} uptake and ATP production. These events were directly visualized in intact, living cells using a molecularly engineered luciferase probe (a chimeric photoprotein including the mitochondrial targeting sequence derived from subunit VIII of citochrome c oxidase). The probe revealed an increase in the [ATP] of the mitochondrial matrix following agonist stimulation and mitochondrial Ca^{2+} uptake (Jouaville et al., 1999a). Subsequent work revealed that this important example is only one of the mechanism controlling mitochondrial metabolism. Indeed, metabolite carriers of the inner membrane, such as aralar1 and citrin, possess a Ca^{2+} binding site in the portion of the protein

21

protruding in the intermembrane space, which is responsible for stimulation-dependent enhancement of substrate accumulation into the matrix (Lasorsa et al., 2003). This effect is lost if the Ca^{2+}-binding site is deleted from the carrier. Overall, these data indicate that a complex Ca^{2+}-sensing machinery, localized in different mitochondrial domains, underlies the coupling of aerobic metabolism to Ca^{2+}-mediated signals in the cytosol.

The interest in the process of mitochondrial Ca^{2+} homeostasis dramatically increased when it became apparent that also cell death is causally linked to organelle Ca^{2+} loading. On the one hand, it was clear that cellular Ca^{2+} overload, such as that caused by hyperstimulation of ionotropic glutamate receptors, leads to Ca^{2+} cycling across the mitochondrial membranes, collapse of the proton gradient and bioenergetic catastrophe, thus leading to cell death by necrosis. On the other hand, Ca^{2+} proved to sensitize cells to apoptotic challenges, acting on the mitochondrial checkpoint. This notion, subsequently confirmed by the study of other anti- and pro-apoptotic proteins, emerged from the analysis of the effect of Bcl-2 on Ca^{2+} signaling, as discussed later in this review. As discussed above Ca^{2+} binding to cyclophilin D positively regulates PTP opening (Basso et al., 2005a) and in turn cell death (Krieger and Duchen, 2002). Once opened, PTP allows the release in the cytosol of intermembrane-residing apoptotic factors, such as cytochrome c, AIF (apoptosis-inducing factor) and Smac/DIABLO, which can trigger apoptosis by both a caspase-dependent and a caspase-independent pathway (Giorgi et al., 2008). Physiological $[Ca^{2+}]_m$ oscillations do not induce PTP opening, but become effective with the synergistic action of pro-apoptotic challenges (such as ceramide or staurosporin) (Pinton et al., 2001b; Szalai et al., 1999).

As to differential effects of specific molecular effort, a deeper insight has been obtained for the IP_3R. The involvement of IP_3R in triggering apoptosis has been demonstrated in different cell types through IP_3R isoform-specific silencing in response to many apoptotic stimuli. In this intense research effort, type I and III isoforms were preferentially studied, while the role of IP_3R-2 in apoptosis, due to its low expression, limited to few human tissues, has not been clarified yet. In

CHO cells, that expressed all three IP$_3$R isoforms, IP$_3$R-3 was shown to strongly co-localize with mitochondria and its silencing depressed agonist-dependent mitochondrial Ca^{2+} signals and apoptosis, triggered by different activators of the extrinsic or intrinsic pathway. Altogether, these data suggested that, at least in this cell type, this isoform could be primarily involved in transferring Ca^{2+} to mitochondria in apoptosis (Mendes et al., 2005). In other cell types, the experimental evidence calls for a preferential role of type I IP$_3$R. In Jurkat T lymphoma cells, ablation of IP$_3$R-1 protects cells from apoptosis induced by different apoptotic stimuli (Jayaraman and Marks, 1997). Moreover, in this cell type the death ligand Fas-dependent killing by SW620 colon cancer cells, requires Ca^{2+} transmission from IP$_3$R to mitochondria: silencing of IP$_3$R-1 completely inhibited lymphocyte apoptosis, blocking apoptotic Ca^{2+} release (Steinmann et al., 2008). Thus, it appears reasonable to conclude that, while IP$_3$R-mediated release of Ca^{2+} from ER appears a key sensitizing step in various apoptotic routes, the precise molecular definition of this process awaits the fine clarification of the macromolecular complex assembled at the interphase between the two organelles, since significant differences may occur in various cell types and/or physiological conditions.

Voltage-dependent anion channels (VDAC)

Voltage-dependent anion channels (also known as mitochondrial porins) are the most abundant proteins of the outer mitochondrial membrane, and they are thus key players in many cellular processes, ranging from metabolism regulation to cell death. Indeed, every eukaryotic cell requires an efficient exchange of ions and metabolites between cytoplasm and mitochondria, and porins are the key molecular components that mediate this trafficking. VDAC is traditionally considered as a large, high-conductance, weakly anion-selective channel, fully opened at low potential (<20-30 mV), but switching to cation selectivity and lower conductance at higher potentials (the so called "closed" state) (Schein et al., 1976). Over the years, the physiological role

23

of the voltage-gating of VDAC has been quite controversial. How could a membrane that is so permeable as the outer mitochondrial membrane, maintain a membrane potential? Some have assumed that such a potential was not possible. Others have proposed a variety of ways to generate a potential. One of these, the existence of a Donnan potential, is a natural consequence of the presence of charged macromolecules in the intermembrane space and cytosol (Colombini, 1979). Since VDAC is not permeable to these, the free motion of their counterions will result in a potential across the outer membrane that depends on the ionic strength of the medium and the concentration of net charge carried by the macromolecules in the two compartments. Another proposal takes into account the motion of charged substrates associated with mitochondrial metabolism. Differential permeability of VDAC to metabolites would result in a transmembrane potential. Theoretically, sizable potentials could be generated (tens of millivolts) and this would depend on the level of mitochondrial metabolism. This would be a negative feedback process as an increase in metabolic rate would increase the potential resulting in channel closure and decrease access to metabolites. The fundamental question is: is there experimental evidence for such a potential? Cortese *et al.* measured the pH of the intermembrane space in isolated mitochondria and found that it was more acidic than the medium (Cortese et al., 1992). The difference was 0.4–0.5 pH units in the condensed form (large intermembrane space) and 0–0.2 pH units in the orthodox state (small intermembrane space). These values did not vary much with medium pH. Since protons are highly mobile a pH gradient could only be maintained by a potential across the outer membrane. A pH difference of 0.4–0.5 corresponds to a 20–30 mV potential negative in the intermembrane space. Our group have used pH-sensitive Yellow Fluorescent protein (YFP) targeted to mitochondrial intermembrane space in order to measure the pH within this region and in the cytosol of intact cultured mammalian cells (Porcelli et al., 2005). They find a pH difference: the cytosol was pH 7.4 and the intermembrane space 7.1. A pH difference of 0.3 corresponds to a 15–20 mV potential negative in the intermembrane space. These estimates are within the switching region of the channels when

reconstituted in phospholipid membranes (V_0 is about 25 mV). Moreover, a number of reports show that numerous cytosolic components can significantly modulate VDAC gating properties, including NADH (Lee et al., 1996), members of Bcl-2 protein family (Vander Heiden et al., 2001), metabolic enzymes (Pastorino and Hoek, 2008), chaperones (Schwarzer et al., 2002a) and cytoskeletal elements (Rostovtseva et al., 2008). An important question is whether this potential varies *in vivo* with changes in metabolic conditions. Jonas et al. measured the state of the VDAC channel in living cells: they found in the nerve terminal very little conductance in patch recordings likely made on the outer membrane of mitochondria (Jonas et al., 1999). This indicates that the channels are mainly closed and is consistent with measurements made of the permeability of the outer membrane of isolated mitochondria. The effects they report for the action of NADH and Bcl-xL on these patches shows that the conductances are sensitive to these agents as are VDAC channels (Lee et al., 1994; Malia and Wagner, 2007; Shimizu et al., 2000).

Yeast possesses only one channel forming isoform (but has also another VDAC gene that correctly inserts into OMM showing no channel activity), while higher multicellular organisms and mammals have three distinct VDAC genes (VDAC1, VDAC2 and VDAC3), with VDAC1 representing the best characterized one. These three isoforms show a good sequence homology (about 65 to 75% in similarity) and similar structure, with the only exception of VDAC2 that has a longer (11 aminoacids) N-terminal tail. Yeasts lacking VDAC gene cannot grow on non-fermentable medium, thus highlighting the relevance of this channel in mitochondrial function. Reintroduction of any of the mammalian VDAC genes in this yeast strain can promptly restore growth defects (Xu et al., 1999). Moreover, when reconstituted into liposomes, each isoform induced a permeability with a similar molecular weight cutoff (between 3,400 and 6,800 daltons based on permeability to polyethylene glycol). However, electrophysiological studies on purified proteins showed slight differences in channel properties. VDAC1 is the "prototypic" version whose properties are highly conserved among other species. VDAC2 also has normal gating activity but

may exist in 2 forms, one with a lower conductance and selectivity. VDAC3 can also form channels in planar phospholipid membranes but inserts very difficult in artificial membranes.

Very recently three different groups independently solved the 3D-structure of VDAC1 through X-ray crystallography or NMR studies. These data indicate that VDAC1 is β-barrel membrane protein composed of 19 β-strands with an a-helix N-terminal domain residing inside the pore (≈ 3 nm): this segment most likely represents the voltage sensor since it is ideally positioned to regulate the conductance of ions and metabolites passing through the VDAC pore (Bayrhuber et al., 2008; Hiller et al., 2008; Ujwal et al., 2008). VDAC can potentially regulate every aspect of mitochondrial physiopathology, since all metabolites entering and leaving mitochondria have to cross the OMM through this channel. Indeed, over the years VDAC has been shown to participate in a huge amount of cellular processes, ranging from the regulation of cellular metabolism, through its physical interaction with different hexokinase isoforms (HKI and HKII), a molecular event thought to underpin the aerobic glycolysis phenomenon in cancer cells (Pastorino and Hoek, 2008). Moreover, VDAC has been considered a master regulator of the apoptotic process: on one hand it was thought to be one of the main component of the mitochondrial Permeability Transition Pore (mPTP), the megachannel mediating the collapse of mitochondrial membrane potential ($\Delta\psi_m$) during apoptosis; on the other side it has long been believed a key mediator of Bax-mediated release of cytochrome c. However, despite the huge amount of work carried out on this protein, several recent papers have raised serious doubt about our functional understandings of this channel. Indeed, new approaches mainly based on mice knockout models failed to clearly confirm any of the above mentioned functions (Baines et al., 2007; Basso et al., 2005b; Bellot et al., 2007; Chiara et al., 2008; Galluzzi and Kroemer, 2007; Krauskopf et al., 2006; Rostovtseva et al., 2004) and rather suggest that a whole rethinking of VDAC roles is needed.

Autophagy

Autophagy, or cellular self-degradation, is a cellular pathway involved in protein and organelle degradation. This phenomenon was firstly described by Christian de Duve in the late 60's (Deter and De Duve, 1967), who also initiated the first experiments that provided the clear biochemical proof of the involvement of lysosomes in this process. However, a clear molecular understanding of this cellular event remained unresolved until the isolation of the first autophagy-deficient yeast mutants (Tsukada and Ohsumi, 1993) and the consequent genetic dissection of the pool of regulatory genes (the so-called ATG genes), thus ascribing autophagy among the tightly regulated and genetically programmed cellular processes. There are three primary forms of autophagy: chaperone-mediated autophagy (CMA), microautophagy and macroautophagy. CMA is a secondary response to starvation and, unlike the other two processes, involves direct translocation of the targeted proteins across the lysosomal membrane (Massey et al., 2006). Microautophagy is the least-characterized process but is used to sequester cytoplasm by invagination and/or septation of the lysosomal/vacuolar membrane (Wang and Klionsky, 2003). By contrast, the most prevalent form, macroautophagy, involves the formation of cytosolic double-membrane vesicles that sequester portions of the cytoplasm (Klionsky and Ohsumi, 1999). During macroautophagy, the sequestering vesicles, termed autophagosomes, are not derived from the lysosome/vacuole membrane. Fusion of the completed autophagosome with the lysosome or vacuole results in the delivery of an inner vesicle (autophagic body) into the lumen of the degradative compartment. Subsequent breakdown of the vesicle membrane allows the degradation of its cargo and eventual recycling of the amino acids and other nutrients. Although autophagy and autophagy-related processes are dynamic, they can be broken down into several discrete steps for the purpose of discussion: (1) induction; (2) cargo selection and packaging; (3) nucleation of vesicle formation; (4) vesicle expansion and completion; (5) retrieval; (6) targeting, docking and fusion of the completed

vesicle with the lysosome; and (7) breakdown of the intralumenal vesicle and its cargo and recycling of the macromolecular constituents. Briefly, one of the major regulatory components for sensing the extracellular milieu and transducing an appropriate signal to elements that allow autophagy to be induced is the mammalian Target of Rapamycin (mTOR), a highly conserved serine/threonine kinase that causes hyper phosphorylation of the Atg13 protein (Funakoshi et al., 1997). This form of Atg13 has a lower affinity for the kinase with which it interacts, Atg1, and the reduced interaction might inhibit autophagy (Kamada et al., 2000). Inhibition of Tor through starvation or treatment with rapamycin results in partial dephosphorylation of Atg13 and allows autophagic induction (Noda and Ohsumi, 1998). The mTOR signaling pathway regulation will be discussed in more details later. Then, bulk cytoplasm is randomly sequestered into the cytosolic autophagosomes, even if some reports show a specificity in the cargo selection (Onodera and Ohsumi, 2004). The subsequent vesicles nucleation process represents probably the least understood step in autophagy, but likely originates from a pre-autophagosomal structure (PAS) already present in the cytoplasm. Vesicle expansion and completion require an ubiquitin-like system mediating protein lipidation through the Atg8 protein (also known as LC3) (Ichimura et al., 2000). Only two proteins are known to remain associated with the completed autophagosomes, the specific receptor Atg19 and Atg8; other proteins that are involved in vesicle formation presumably recycle from the PAS or the vesicles during formation, thus enabling the retrieval of autophagy components. Of course, the timing of vesicle fusion with the lysosome must be tightly regulated, otherwise if the fusion process begins prior to completion of the double-membrane vesicle, the cargo will remain in the cytosol. The molecular machinery mediating this complex process however remains in part still obscure, even if several members of the SNARE protein family have been demonstrate to be necessary (Darsow et al., 1997). Lastly, the whole process must break down the single-membrane subvacuolar vesicles that result from fusion of the autophagosome with the lysosome, a step that mainly depends on the acidic pH of the organelle (Nakamura et al., 1997).

Autophagy covers several physiological functions, ranging from a basal housekeeping role to response to metabolic stress and regulation of cell death. Moreover, the relevance of this cellular process at whole organism level is underlined by the observation that the genetic ablation of many Atg genes often lead to organism death due to impaired cell differentiation (Sandoval et al., 2008), embryonic lethality or reduction in survival during neonatal starvation (Kuma et al., 2004). The repertoire of routine housekeeping functions performed by autophagy includes the elimination of defective or damaged proteins and organelles, the prevention of abnormal protein aggregate accumulation, and the removal of intracellular pathogens (Mizushima and Klionsky, 2007). Such functions are likely critical for autophagy-mediated protection against aging, cancer, neurodegenerative diseases, and infection. Although some of these functions overlap with those of the ubiquitin-proteosome system (the other major cellular proteolytic system) the autophagy pathway is uniquely capable of degrading entire organelles such as mitochondria, peroxisomes, and ER as well as intact intracellular microorganisms (Kim et al., 2007; Zhang et al., 2007). Further, the relative role of the autophagy-lysosome system in protein quality control (i.e. the prevention of the intracellular accumulation of altered and misfolded proteins) may be greater than previously thought. Moreover, autophagy is activated as an adaptive catabolic process in response to different forms of metabolic stress, including nutrient deprivation, growth factor depletion, and hypoxia. This bulk form of degradation generates free amino and fatty acids that can be recycled in a cell-autonomous fashion or delivered systemically to distant sites within the organism. Presumably, the amino acids generated are used for the de novo synthesis of proteins that are essential for stress adaptation. It is presumed that the recycling function of autophagy is conserved in mammals and other higher organisms, although direct data proving this concept are lacking. The amino acids liberated from autophagic degradation can be further processed and, together with the fatty acids, used by the tricarboxylic acid cycle (TCA) to maintain cellular ATP production. The importance of autophagy in fueling the TCA cycle is supported by studies showing that certain phenotypes of

autophagy-deficient cells can be reversed by supplying them with a TCA substrate such as pyruvate (or its membrane-permeable derivative methylpyruvate). For example, methylpyruvate can maintain ATP production and survival in growth factor-deprived autophagy-deficient cells that would otherwise quickly die (Lum et al., 2005). It can also restore ATP production, the generation of engulfment signals, and effective corpse removal in autophagy-deficient cells during embryonic development (Qu et al., 2007).

The mammalian Target of Rapamycin (mTOR)

mTOR is a highly conserved 289 kDa serine/threonine kinase that represents the main cellular nutrient sensor and regulates cell growth, cell cycle progression, nutrient import, protein synthesis and autophagy. The discovery of this kinase is rooted in a soil sample from Easter Island containing a bacterium (*Streptomyces hygroscopicus*) that produces the antifungal metabolite, rapamycin (from "Rapa Nui", the local name for Easter Island). Rapamycin binds to the FKBP12 protein to form a complex that interacts and inhibits several functions regulated by TOR (Wullschleger et al., 2006). Apart from yeast, where two *TOR* genes, *TOR1* and *TOR2*, have been identified, all eukaryotic genomes examined so far contain a single *TOR* gene. TOR belongs to a group of kinases known as the phosphatidylinositol-related kinases (PIKK) (Bhaskar and Hay, 2007). Members of the PIKK family contain a catalytic carboxy-terminal domain that has similarities with the catalytic domains of phosphatidylinositol-3 and phosphatidylinositol-4 kinases. Four functional domains are conserved in TOR proteins including the central FAT (FRAP, ATM, TTRAP) domain, the FRB (FKBP12-rapamycin binding domain) domain, the kinase domain and at the most C-terminal part of the protein the FATC domain. It has been suggested that these two domains may interact to expose the catalytic domain. The FATC domain is absolutely essential for TOR kinase activity. TOR exists in two different complexes TORC1 and TORC2 (Sarbassov et al., 2005a). In yeast, only TOR2 can form TORC2 and TORC1 is sensitive to rapamycin (Jacinto et al.,

2004). In other species, these two complexes are structurally and functionally conserved. Mammalian TORC1 (mTORC1) is composed of mLST8 (GβL) and raptor, and is sensitive to rapamycin (Hara et al., 2002; Kim et al., 2002; Kim et al., 2003). The rapamycin-insensitive complex mTORC2 is composed of mTOR, mLST8 (GβL), rictor, SIN1 and protor (Jacinto et al., 2006; Sarbassov et al., 2004). mTORC1 controls protein synthesis, nutrient import and autophagy (Hay and Sonenberg, 2004). Studies in Drosophila and mammalian cells have shown that two proteins, S6 kinase and 4E-BP1, link mTORC1 to the control of mRNA translation and two proteins, Atg1 and S6K, to the control of autophagy. The downstream functions of mTORC2 are less known than those of mTORC1. mTORC2 appears to be involved in actin cytoskeleton regulation and Akt/PKB regulation through a phosphorylation at serine 473 (Sarbassov et al., 2005b). As Akt/PKB acts upstream of mTORC1, it has been suggested that mTORC2 could be located upstream of mTORC1. However, recent studies have shown that *in vivo* the phosphorylation at Ser473 is not required for the phosphorylation at Thr308, and the phosphorylation of TSC2, an Akt/PKB target in the mTORC1 signaling pathway. These findings strongly suggest that mTORC2 is not in fact located upstream of mTORC1. Interestingly, recent knockout studies of raptor and rictor and have shown that the contributions of mTORC1 and mTORC2 are critical in the early stages of embryogenesis and at midgestation, respectively (Guertin et al., 2006; Shiota et al., 2006).

The first evidence that TOR has a role in regulating autophagy came from experiments involving rat hepatocytes that showed that rapamycin partially reverses the inhibitory effects of amino acids on autophagic proteolysis (Blommaart et al., 1995). The stimulatory effect of rapamycin on autophagy has been confirmed in different models. This would give credence to the observation that TORC2 is not directly involved in the regulation of autophagy. However, the possible relevance of this complex in autophagy remains to be established because TORC2 is sensitized to long-term treatment with rapamycin (Sarbassov et al., 2006).

The first genetic evidence for the role of TOR in autophagy came from studies in yeast demonstrating that a temperature-sensitive TOR mutant induces autophagy at a permissive temperature (Noda and Ohsumi, 1998). Following on from these data, and some of the findings discussed in the preceding section, several studies have shown that signaling pathways that activate TOR also inhibit autophagy, whereas signaling pathways that inhibit TOR stimulate autophagy (Arsham and Neufeld, 2006; Codogno and Meijer, 2005).

Autophagy and cell death

Although strictly speaking, the term autophagy simply means "self-eating", many presume that this cellular self-eating is inevitably a form of cellular self-destruction. Indeed, within the cell death research field, the visualization of autophagosomes in dying cells has led to the belief that autophagy is a form of non-apoptotic, or type II, programmed cell death. However, this concept has been recently challenged by numerous studies evaluating cells and organisms lacking the autophagy genes. Most evidence linking autophagy to cell death is circumstantial and rather indicates that, at least in cells with intact apoptotic machinery, autophagy is primarily a pro-survival rather than a pro-death mechanism. Actually, there are only two *in vivo* examples in model organisms where the ablation of autophagy genes retards cell death: in the involuting Drosophila melanogaster salivary gland (Berry and Baehrecke, 2007) and in nematodes with hyperactive ion channels that undergo necrotic neuronal cell death (Toth et al., 2007). Direct induction of autophagy by overexpression of the Atg1 kinase has also been shown to be sufficient to kill fat and salivary gland cells in Drosophila. In cultured mammalian cells, cell death by canonical autophagy (defined as death that is reduced by genetic inactivation of autophagy genes including beclin-1) has been reported primarily (but not exclusively) in cells that are deficient in apoptosis, either by the virtue of Bax/Bak deletion or caspase inhibition. RNA interference directed against 2 autophagy genes, atg7 and beclin 1, blocked cell death in mouse L929 cells treated with the caspase inhibitor zVAD (Yu et

al., 2004). Further, RNAi against autophagy genes atg5 and beclin 1 blocked death of Bax/Bak double knockout murine embryonic fibroblasts (MEFs) treated with staurosporine or etoposide (Shimizu et al., 2004). Notably, in both of these studies, Atg gene silencing blocked the death of cells whose apoptotic pathway had been crippled. Although these findings exclude the possibility that autophagy is triggering death through apoptosis induction, they raise the question of whether autophagy is a death mechanism in cells whose apoptotic machinery is intact. In addition, in etoposide-treated wild-type MEFs (which die by apoptosis), only minimal autophagic activity and no inhibition of death by 3-MA is seen, indicating that autophagy is not involved in the death process unless apoptosis is blocked. On the other side, the number of works demonstrating the pro-survival function of autophagy, both in vitro and in vivo, is continuously growing. Indeed, most evidence shows that autophagy suppression by genetic knockout/knockdown of essential autophagy genes increases cell death (Kourtis and Tavernarakis, 2009; Maiuri et al., 2007b; Scarlatti et al., 2009). Further, the evidence for cell death by autophagy remains to be demonstrated in mammals; in fact, embryonic mice lacking autophagy genes, including ambra1, beclin-1, and atg5, have been shown to have increased, not decreased, numbers of apoptotic cells.

Aims

Mitochondria are unique organelles within the complex system of subcellular compartments. They are engaged in the regulation of several physiological as well as pathological conditions and the number of cellular processes they are involved in is continuously growing over the years. The outer mitochondrial membrane (OMM) represents the primary interface towards the other cellular structures and should thus be considered a key site for the whole organelle regulation. The Voltage-dependent anion channel (VDAC) is far the most abundant protein located at OMM level and embodies the ideal candidate for understanding the complexity of the mitochondrial regulation of the cell fate. Despite the huge amount of scientific literature covering this topic, many of the long standing notions about this protein have been questioned by several recent works. This project propose to investigate the role of the different VDAC isoforms in the regulation of some fundamental cellular events. In particular we will take advantage from the long standing experience of our group in the analysis of cellular Ca^{2+} signaling in order to precisely characterize the contribution of these proteins to global cellular Ca^{2+} homeostasis. By using the most modern technologies based on both fluorescent and bioluminescent Ca^{2+}-probes, we will also correlate the effects on Ca^{2+} signaling to the their consequences on cell death through apoptosis. Moreover we will also investigates the yet unidentified involvement of mitochondria on novel stress-sensing signaling pathway leading to autophagy.

Materials and Methods

Yeast two-hybrid screening

Yeast two-hybrid screening was carried using the pLexA system according to the protocol of Golemis, E. A. et al. (Gyuris et al., 1993). The full ORF cDNA of rat VDAC-1 (NM_031353) was cloned into the pGilda yeast inducible expression vector fused with the pLexA DNA binding domain. The EGY48 (*leu -/-*) yeast strain was transformed with the pGilda/VDAC-1 vector using the lithium acetate method. The expression of the full length VDAC-1 protein was verified by immunoblotting, while its nuclear localization was shown by the negative repression test (data not shown). Following the validation of the method, the pGilda/VDAC containing yeasts were transformed with the *lacZ* reporter gene plasmid pSH18-34, followed by transformation of approximately 5x106 yeast cells with the pJG4-5 pLexA activation domain fusion vector cDNA libraries (from human embryonic kidney and adult liver, Origene). Positive clones were selected in two runs: first for their ability to grow on plates lacking leucine; second, the remaining clones were assayed for β-galactosidase activity on medium supplemented with 5-bromo-4-chloro-3-indolyl-β-D-galactopyranoside (X-gal). 372 and 104 positive clones were obtained from the kidney and brain cDNA libraries, respectively. The positive clones were first amplified by PCR using yeast stocks homogenized by 3 freeze/thaw cycles as template and primers annealing to the pJG4-5 vector (forward: 5'-CGT AGT GGA GAT GCC TCC-3'; reverse: 5'-CTG GCA AGG TAG ACA AGC CG-3'). The PCR reaction was performed using the Long term PCR kit (Roche). PCR products were first characterized by restriction enzyme mapping using the frequent cutter HaeIII enzyme. Clones were grouped according to their digestion patterns, verified by agarose gel electrophoresis, and one clone from each group was bi-directionally sequenced using the primers applied in the PCR reaction. About 90% of the clones contained a subsequence of the ER resident chaperone heat-

shock 70-kd protein 5 (HSPA5, grp-78, see table), most probable reflecting the requirement of efficient folding of the VDAC-1 protein. The results of sequencing of the remaining clones are shown in the table. One group of the putative interacting proteins were found to be cytoskeletal and signaling elements (shown in bold), while another group (shown in normal) were found to be folding intermediates, presumably underlying the proper function of the VDAC OMM channel. In order to verify the interaction of VDAC-1 with grp-75 (heat-shock 70-kd protein 9b; HSPA9B, shown in bold/italics), the plasmid containing the positive cDNA was isolated from yeast. Cells of the positive clone were resuspended in 1M sorbitol and 50 mM EDTA with the yeast lytic enzyme (2 mg/ml; MP Biomedicals). After 30 min at 37 °C, the yeast cells were centrifuged, and the pellet was dissolved in Hirt's solution (10 mM Tris-HCl (pH 7.5), 50 mM EDTA, and 0.2% SDS) with 0.5 mg/ml proteinase K (Invitrogen) and incubated at 50°C for 6 h. The plasmid DNA was extracted with phenol/chloroform/isoamyl alcohol (25:24:1). The aqueous phase was precipitated with the same volume of 20% polyethylene glycol and 2.5 M NaCl, and the plasmid DNA was pelleted, washed with 70% ethanol, and resuspended in 10 μl of 10mM Tris-HCl (pH 7.5) and 1mM EDTA. The plasmid obtained was transformed into *Escherichia coli* strain DH5α and purified. The isolated PJG4-5/grp-75(aa 471-681) plasmid was then co-transformed with the pGilda/VDAC-1 to the EGY48 (*leu -/-*)/pSH18-34 yeast strain and verified to interact with VDAC-1 by survival on *leu* – medium and by induced galactosidase activity on X-gal plates.

Subcellular fractionation and proteomic analysis

HeLa cells and rat liver were homogenized, and crude mitochondrial fraction (8,000g pellet) was subjected to separation on a 30% self-generated Percoll gradient as described previously (Vance, 1990). A low-density band (denoted as MAM fraction) was collected and analysed by immunoblotting and Blue-Native/SDS-PAGE 2D separation. For SDS-PAGE analysis of MAM fraction proteins 10 μg proteins were loaded on 10% SDS-polyacrilamyde gels. The antibodies used

were: αIP3R, non isotype specific monoclonal antibody, 1:200, Calbiochem; #407140, recognizing all three isoforms; αVDAC1, 1:5 000; Calbiochem, monoclonal anti-porin 31HLHuman, #529534); αgrp-75, 1:500, rabbit polyclonal, Santa Cruz Biotechnology, H-155, sc-13967) and was also present in the MAM, while it was free of contamination from inner membrane proteins (see Supplementary Fig. 1) For coimmunoprecipitation of grp-75 with IP3R and VDAC-1 total cellular proteins were precipitated with a monoclonal grp-75 antibody (3 μg, Affinity Bioreagents, MA3-028) and protein-G-Sepharose™ (Amersham, GE Healthcare), washed with 50 mM Tris-HCl, 1% Nonidet-P40 1% (for the IP3R) or 50 mM Tris-HCl (for VDAC-1) according to the manufacturer's instructions. The precipitated protein fraction was separated on 7 or 10% SDS- polyacrilamyde gels and immunoblotted against IP3R-3 (1:200; goat polyclonal, Santa Cruz Biotechnology, C-20; sc-7277), grp-75 and VDAC-1, as described above. For blue-native and SDS-PAGE two-dimensional separation of the MAM fraction proteins the native MAM fraction was solubilized with 1M aminocaproic acid, and 2% dodecylmaltoside, combined with 5% Serva Blue G and separated on a 4% acrylamide capillary gel in the first dimension. The capillary gel was incubated with a dissociating solution (1% SDS and 1% mercaptoethanol), stacked over a 10 % SDS-PA gel, separated, then the proteins were immunoblotted against the IP3Rs, grp-75 and VDAC-1 using the antibodies described above.

IP$_3$R and grp75 expression constructs

Mouse grp75, cloned into the expression vector pTOPO (Invitrogen) was used (Wadhwa et al., 1993). The constructs encoding the fusion proteins of the PH domain of the p130 (GenBank D45920; residues 95-233) protein and the IP$_3$R-LBD domain (residues 224–605) of the human IP$_3$R-1 with monomeric red (mRFP1), green, or yellow fluorescent proteins, as well as the strategies for ER targeting have been described previously (Lin et al., 2005; Varnai et al., 2005). For OMM tethering, the N-terminal mitochondrial localization sequence of the mouse AKAP1 protein

(GenBank V84389, residues 34-63) was fused to the N-termini of the IP_3R-LBD and p130PH constructs through a short linker (DPTRSR). The OMM-IP_3-LBD_{1-604}-mRFP1 construct was obtained by amplification of the 1-604 fragment of IP_3R-1 cDNA and insertion into the AKAP1/mRFP1 vector. Transient transfection was done by the Ca^{2+}-phosphate precipitation technique. Experiments were carried out 24-36 hours after transfection.

Imaging techniques

For 3D morphological image acquisition the cells were transfected with mRFP1 fused IP_3R-$LBD_{224-605}$ constructs and loaded with 50 nM mitoTracker Green (Molecular Probes, Leiden, Netherlands) for 20 min at 37°C. Kinetic imaging of $[Ca^{2+}]_c$ transients were performed as previously described (Szabadkai et al., 2004). All imaging experiments were carried out on Zeiss Axiovert 200 inverted microscopes, equipped with cooled CCD digital cameras. Z-series of images were acquired at 0.5 μm distance, deconvolved using a custom-made algorithm and 3D reconstructed as described previously (Carrington et al., 1995; Rizzuto et al., 1998b).

Aequorin as a Ca^{2+} indicator

Aequorin is a 21 KDa protein isolated from jellyfish of the genus Aequorea which emits blue light in the presence of calcium. The aequorin originally purified from the jellyfish is a mixture of different isoforms called "heterogeneous aequorin" (Shimomura, 1986). In its active form the photoprotein includes an apoprotein and a covalently bound prosthetic group, coelenterazine. When calcium ions bind to the three high affinity EF hand sites, coelenterazine is oxidized to coelenteramide, with a concomitant release of carbon dioxide and emission of light. Although this reaction is irreversible, in vitro an active aequorin can be obtained by incubating the apoprotein with coelenterazine in the presence of oxygen and 2-mercaptoethanol. Reconstitution of an active aequorin (expressed recombinantly) can be obtained also in living cells by simple addition of

coelenterazine to the medium. Coelenterazine is highly hydrophobic and has been shown to permeate cell membranes of various cell types, ranging from the slime mold Dictyostelium discoideum to mammalian cells and plants.

Different coelenterazine analogues have been synthesized that confer to the reconstituted protein specific luminescence properties (Shimomura et al., 1993). A few synthetic analogues of coelenterazine are now commercially available from Molecular Probes.

The possibility of using aequorin as a calcium indicator is based on the existence of a well-characterized relationship between the rate of photon emission and the free Ca^{2+} concentration. For physiological conditions of pH, temperature and ionic strength, this relationship is more than quadratic in the range of $[Ca^{2+}]$ 10^{-5}-10^{-7} M. The presence of 3 Ca^{2+} binding sites in aequorin is responsible for the high degree of cooperativity, and thus for the steep relationship between photon emission rate and $[Ca^{2+}]$. The $[Ca^{2+}]$ can be calculated from the formula L/L_{max} where L is the rate of photon emission at any instant during the experiment and L_{max} is the maximal rate of photon emission at saturating $[Ca^{2+}]$. The rate of aequorin luminescence is independent of $[Ca^{2+}]$ at very high ($>10^{-4}$ M) and very low $[Ca^{2+}]$ ($< 10^{-7}$ M). However, as described below in more details, it is possible to expand the range of $[Ca^{2+}]$ that can be monitored with aequorin. Although aequorin luminescence is not influenced either by K^{+} or Mg^{2+} (which are the most abundant cations in the intracellular environment and thus the most likely source of interference in physiological experiments) both ions are competitive inhibitors of Ca^{2+} activated luminescence. Aequorin photon emission can be also triggered by Sr^{2+} but its affinity is about 100 fold lower than that of Ca^{2+}, while lanthanides have high affinity for the photoprotein (e.g. are a potential source of artifacts in experiments where they are used to block Ca^{2+} channels). pH was also shown to affect aequorin luminescence but at values below 7. Due to the characteristics described above, experiments with aequorin need to be done in well-controlled conditions of pH and ionic concentrations, notably of Mg^{2+}.

Recombinant aequorins. For a long time the only reliable way of introducing aequorin into living cells has been that of microinjecting the purified protein. This procedure is time consuming and laborious and requires special care in handling of the purified photoprotein. Alternative approaches (scrape loading, reversible permeabilization, etc.) have been rather unsuccessful. The cloning of the aequorin gene has opened the way to recombinant expression and thus has largely expanded the applications of this tool for investigating Ca^{2+} handling in living cells. In particular, recombinant aequorin can be expressed not only in the cytoplasm, but also in specific cellular locations by including specific targeting sequencing in the engineered cDNAs.

Extensive manipulations of the N-terminal of aequorin have been shown not to alter the chemiluminescence properties of the photoprotein and its Ca^{2+} affinity. On the other hand, even marginal alterations of the C-terminal either abolish luminescence altogether or drastically increase Ca^{2+} independent photon emission. As demonstrated by Watkins and Campbell, the C-terminal proline residue of aequorin is essential for the long-term stability of the bound coelenterazine (Watkins and Campbell, 1993). For these reasons, all targeted aequorins synthesized in our laboratory include modifications of the photoprotein N-terminal. Three targeting strategies have been adopted:

1.Inclusion of a minimal targeting signal sequence to the photoprotein cDNA. This strategy was initially used to design the mitochondrial aequorin and was followed also to synthesize an aequorin localized in the nucleus and in the lumen of the Golgi apparatus.

2. Fusion of the cDNA encoding aequorin to that of a resident protein of the compartments of interest. This approach has been used to engineer aequorins localized in the sarcoplasmic reticulum (SR), in the nucleoplasm and cytoplasm (shuttling between the two compartments depending on the concentration of steroid hormones), on the cytoplasmic surface of the endoplasmic reticulum (ER) and Golgi and in the subplasmalemma cytoplasmic rim.

3. Addition to the aequorin cDNA of sequences that code for polypeptides that bind to endogenous proteins. This strategy was adopted to localize aequorin in the ER lumen.

We routinely included in all the recombinant aequorins the HA1 epitope-tag that facilitates the immunocytochemical localization of the recombinant protein in the cell.

Chimeric Aequorin cDNAs Below we briefly describe the constructs produced in our laboratory. A few other constructs have been produced in other laboratories and will not be dealt with in detail here.

Cytoplasm (cytAEQ): an unmodified aequorin cDNA encodes a protein that, in mammalian cells is located in the cytoplasm and, given its small size, also diffuses into the nucleus. An alternative construct is also available that is located on the outer surface of the ER and of the Golgi apparatus. This construct was intended to drive the localization of aequorin to the inner surface of the plasma membrane given that it derives from the fusion of the aequorin cDNA with that encoding a truncated metabotropic glutamate receptor (mgluR1). The encoded chimeric protein, however, remains trapped on the surface of the ER and Golgi apparatus, with the aequorin polypeptide facing the cytoplasmic surface of these organelles. The cytoplasmic signal revealed by this chimeric aequorin is indistinguishable from that of a cytoplasmic aequorin, but it has the advantage of being membrane bound and excluded from the nucleus.

Mitochondria (mtAEQ): mtAEQ was the first targeted aequorin generated in the laboratory, which has been successfully employed to measure the $[Ca^{2+}]$ of the mitochondrial matrix of various cell types. This construct includes the targeting presequence of subunit VIII of human cytochrome c oxidase fused to the aequorin cDNA.

*Endoplasmic Reticulum (erAEQ):*The erAEQ includes the leader (L), the VDJ and Ch1 domains of an Ig2b heavy chain fused at the N-terminus of aequorin. Retention in the ER depends on the presence of the Ch1 domain that is known to interact with high affinity with the luminal ER protein BiP.

41

To expand the range of Ca^{2+} sensitivity that can be monitored with the different targeted aequorins we have also employed in many of our constructs a mutated form of the photoprotein (asp119 → ala). This point mutation affects specifically the second EF hand motive of wild type aequorin. The affinity for Ca^{2+} of this mutated aequorin is about 20 fold lower than that of the wild type photoprotein. Chimeric aequorins with the mutated isoform are presently available for the cytoplasm, the mitochondrial matrix, the ER and SR, the Golgi apparatus and the sub plasmamembrane region.

Cell preparation and transfection

Although in a few cases the aequorin cDNA has been microinjected, the most commonly employed method to obtain expression of the recombinant protein is transfection. Different expression plasmids have been employed, some commercially available (pMT2, pcDNAI and 3) other have been kindly provided by colleagues. The calcium phosphate procedure is by far the simplest and less expensive and it has been used successfully to transfect a number of cell lines, including HeLa, L929, L cells, Cos 7, A7r5 and PC12 cells, as well as primary cultures of neurons and skeletal muscle myotubes. Other transfection procedures have been also employed, such as liposomes, the "gene gun" and electroporation. Viral constructs for some aequorins are also available (Alonso et al., 1998; Rembold et al., 1997). In this section we briefly describe the calcium phosphate procedure, a simple and convenient transfection method for HeLa or Hek293 cells.

One day before the transfection step (two days for Hek293), HeLa cells in Dulbecco Modified Eagle's Medium (DMEM) supplemented with 10% Fetal Calf serum (FCS) are plated on a 13 mm round coverslip (poly-D-lysine coated in the case of Hek293) at 30-50% confluence. Just before the transfection procedure, cells are washed with 1 ml of fresh medium.

Calcium-Phosphate transfection procedure

The following stock solutions need to be prepared and conserved at -20°C until used.

- $CaCl_2$ 2.5 M.

- HEPES Buffered Solution (HBS): NaCl 280mM, Hepes 50 mM, Na_2HPO_4 1.5 mM, pH 7.12.

- Tris-EDTA (TE): Trizma-base 10mM, EDTA 1mM, pH 8.

All solutions are sterilized by filtration using 0.22 μm filters. For 1 coverslip, 5 μl of $CaCl_2$ 2.5 M are added to the DNA disolved in 45 μl of TE. Routinely, 4 μg of DNA are used to transfect 1 coverslip. The solution is then mixed under vortex with 50 μl of HBS and incubated for 20 to 30 minutes at room temperature. The cloudy soultion is then added directly to the cell monolayer. 18-24 hours after addition of the DNA, the cells are washed with PBS (2 or 3 times until the excess precipitate is completely removed). Using this protocol the transfected cells are usually between 30 and 50 %. Although an optimal transfection is obtained after an overnight incubation, we found that a substantial aequorin expression, sufficient for most experimental conditions, is obtained also with an incubation of only 6 hours with the Ca^{2+}-phosphate-DNA complex. Stable clones has be also obtained by cotransfecting with the aequorin cDNA another plasmid encoding the resistance to neomycin and then selecting the cells with 1 mg/ml of neomycin.

Reconstitution of functional aequorin

Once expressed the recombinant aequorin must be reconstituted into the functional photoprotein. This is accomplished by incubating cells with the synthetic coelenterazine for variable periods of time (usually 1-3 hours) and under conditions of temperature and $[Ca^{2+}]$ that depend on the compartment investigated. Practically, coelenterazine is dissolved at 0.5 mM in pure methanol as a 100X stock solution kept at - 80°C. This solution tolerates several freeze-thaw cycles. However, we recommend the supply of coelenterazine solution to be split into small aliquots (50 μl). Coelenterazine must be protected from light.

For compartments with low $[Ca^{2+}]$ under resting conditions (cytosol and mitochondria the cells transfected with the appropriate recombinant aequorins are simply incubated at 37°C in fresh

DMEM medium supplemented with 1% FCS and 5 μM coelenterazine. Higher or lower coelenterazine concentrations can be also used, if necessary. Good reconstitution is achieved with 1 hour incubation, but an optimal reconstitution requires 2 hours.

For compartments endowed with high $[Ca^{2+}]$ under resting conditions (ER), to obtain good reconstitution and interpretable data it is first necessary to reduce the $[Ca^{2+}]$ in the organelle. Otherwise aequorin is immediately consumed after reconstitution and in steady state little functional photoprotein is present in cells. Depletion of Ca^{2+} from the organelles has been (and can be) achieved in different ways. here we describe a simple protocols: cells are incubated at 37°C for 5 minutes in KRB solution (Krebs-Ringer modified buffer: 125 mM NaCl, 5mM KCl, 1mM Na_3PO_4, 1mM $MgSO_4$, 5.5 mM glucose, 20 mM Hepes, pH 7.4) supplemented with 600 μM EGTA, 10 μM ionomycin). After washing with KRB containing 100 μM EGTA, 5% bovine serum albumin, cells are further incubated in the same medium supplemented with 5 μM coelenterazine for 1 hour, but at 4°C.

Slight variations in these depletion protocols have been used both by our group and other investigators. Here it is necessary to stress a few general aspect of the procedure: i) the more efficient the Ca^{2+} depletion, the better the reconstitution; ii) some compartments (e.g. the Golgi and in part the ER) can be grossly altered morphologically by the Ca^{2+} depletion protocol. The incubation at 4°C largely prevents these morphological changes, without altering the efficacy of the reconstitution; iii) if ionophores or SERCA inhibitors are employed for depletion they must be removed completely before starting the experiment. For this reason extensive washing of the cell monolayer with Bovine Serum Albumin (BSA) is recommended at the end of the reconstitution procedure.

Luminescence detection

The aequorin detection system is derived from that described by Cobbold and Lee and is based on

the use of a low noise photomultiplier placed in close proximity (2-3 mm) of aequorin expressing cells. The cell chamber, which is on the top of a hollow cylinder, is adapted to fit 13-mm diameter coverslip. The volume of the perfusing chamber is kept to a minimum (about 200 μl). The chamber is sealed on the top with a coverslip, held in place with a thin layer of silicon. Cells are continuously perfused via a peristaltic pump with medium thermostated via a water jacket at 37°C. The photomultiplier (EMI 9789 with amplifier-discriminator) is kept in a dark box and cooled at 4°C. During manipulations on the cell chamber, the photomultiplier is protected from light by a shutter. During aequorin experiments, the shutter is opened and the chamber with cells is placed in close proximity of the photomultiplier. The output of the amplifier-discriminator is captured by an EMIC600 photon-counting board in an IBM compatible microcomputer and stored for further analysis.

Ca^{2+} measurement

For the cells transfected with cytosolic, mitochondria or nuclear aequorins, the coverslip with the transfected cells is transferred to the luminometer chamber and it is perfused with KRB saline solution in presence of 1 mM $CaCl_2$ to remove the excess coelenterazine. The stimuli or drugs to test are added to the perfusing medium and reach the cells with a lag time that depends on the rate of the flux and the length of the tubes. In order to make the stimulation more rapid and homogeneous the rate of the peristaltic pump is set to its maximum speed. Under these conditions we calculated that the whole monolayer is homogeneously exposed to the stimuli in 2 sec. At the end of the experiments, all the aequorin is discharged by permeabilizing the cells using a hypotonic solution containing digitonin (100 μM) and $CaCl_2$ (10 mM).

For erAEQ transfected cells, unreacted coelenterazine and drugs are removed by prolonged perfusion (3-6 min) with a saline solution containing 600 μM EGTA and 2% BSA. BSA is then

removed from the perfusion buffer and the refilling of the compartments is started by perfusing the medium containing either 1mM $CaCl_2$. To note that BSA increases luminescence background level.

We found that, despite the depletion protocol and the use of a low Ca^{2+} affinity aequorin mutant, the rate of aequorin consumption upon Ca^{2+} refilling is so rapid that most aequorin is consumed in 30 sec and the calibration of the signal in terms of $[Ca^{2+}]$ becomes unreliable. Two alternative solutions to this problem have been developed, i) the use of Sr^{2+} as a Ca^{2+} surrogate and ii) the reconstitution not with the wild type coelenterazine, but with the analogue coelenterazine n that reduces the rate of aequorin photon emission at high $[Ca^{2+}]$. In the latter case $[Ca^{2+}]$ between 10^{-4} and 10^{-3} M can be reliably calibrated (Robert et al., 1998).

Conversion of the luminescent signal into $[Ca^{2+}]$

To transform luminescence values into $[Ca^{2+}]$ values, we have used the method described by Allen and Blink. The method relies on the relationship between $[Ca^{2+}]$ and the ratio between the light intensity recorded in physiological conditions (L, counts/s) and that which would have been reported if all the aequorin was instantaneously exposed to saturating $[Ca^{2+}]$ (L_{max}). Given that the rate constant of aequorin consumption at saturating $[Ca^{2+}]$ is 1.0 s^{-1}, a good estimate of L_{max} can be obtained from the total aequorin light output recorded from the cells after discharging all the aequorin. This usually requires the addition of excess Ca^{2+} and detergents as shown in the preceding section. As aequorin is being consumed continuously, it must be stressed that, for calibration purposes, the value of L_{max} is not constant and decreases steadily during the experiment. The value of L_{max} to be used for $[Ca^{2+}]$ calculations at every time point along the experiment should be calculated as the total light output of the whole experiment minus the light output recorded before that point.

The relationship between the ratio (L/L_{max}) and $[Ca^{2+}]$ has been modeled mathematically. The model postulates that each of the Ca^{2+} binding sites has two possible states, T and R and that light is emitted when all the sites are in the R state. Ca^{2+} is assumed to bind only in the R state. This

46

model contains three parameters: KR, the Ca^{2+} association constant, KTR= [T]/[R], and n, the number of Ca^{2+} binding sites. The values we obtained for the recombinantly expressed recombinant aequorin for each parameter are KR = 7.23 10^6 M^{-1}, KTR = 120, n=3. The equation for the model provides the algorithm we used to calculate the $[Ca^{2+}]$ values at each point where ratio =(L/L_{max})1/n.

$$Ca^{2+} (M) = \frac{Ratio + (Ratio \times KTR) - 1}{KR - (Ratio \times KR)}$$

Results

Chaperone mediated coupling of endoplasmic reticulum and mitochondrial Ca^{2+} channels

Mitochondria and ER of eukaryotic cells form two entwined endomembrane networks, and their dynamic interaction controls metabolic flow, protein transport, intracellular Ca^{2+} signaling, and cell death (Brough et al., 2005; Ferri and Kroemer, 2001; Levine and Rabouille, 2005; Szabadkai and Rizzuto, 2004). Vast knowledge on ER-mitochondrial interaction stems from the analysis of Ca^{2+} signal transmission between these organelles. Ca^{2+} mobilizing hormones and neurotransmitters, as well as proapoptotic stimuli, induce Ca^{2+} release from the ER Ca^{2+} store through the IP_3R Ca^{2+} release channel (Berridge et al., 2003; Patterson et al., 2004). Consequent mitochondrial Ca^{2+} uptake, via a yet unidentified Ca^{2+} channel of the inner mitochondrial membrane (the mitochondrial Ca^{2+} uniporter, MCU), regulates processes as diverse as aerobic metabolism (Hajnoczky et al., 1995), release of caspase cofactors (Pinton et al., 2001a) and feedback control of neighbouring ER or plasma membrane Ca^{2+} channels (Gilabert and Parekh, 2000; Hajnoczky et al., 1999). A corollary of the efficient mitochondrial Ca^{2+} uptake during IP_3 induced Ca^{2+} release is the close apposition of ER and outer mitochondrial membranes (OMM) as demonstrated in a wide variety of cell types using light and electron microscopy studies (Frey et al., 2002; Mannella et al., 1998; Marsh et al., 2001; Rizzuto et al., 1998b). The molecular determinants of this crosstalk, however, are still largely unknown (discussed in (Hajnoczky et al., 2002)). Recently PACS2, an ER-associated vesicular sorting protein was proposed to link the ER to mitochondria (Simmen et al., 2005). The knockdown of PACS2 led to stress-mediated uncoupling of the organelles, reflected also by the inhibition of Ca^{2+} signal transmission.

On the other side, VDAC1, the abundant OMM channel, was also suggested to participate in the interaction. It was shown to be present at ER-mitochondrial contacts and to mediate Ca^{2+}

channeling to the intermembrane space (IMS) from the high $[Ca^{2+}]$ microdomain generated by the opening of the IP$_3$R (Gincel et al., 2001; Rapizzi et al., 2002b). In addition, VDAC1 mediates metabolic flow through the OMM, forming an ATP microdomain close to the ER and sarcoplasmic reticulum Ca^{2+} ATPases (SERCAs) (Vendelin et al., 2004; Ventura-Clapier et al., 2004), and both VDAC1 and VDAC2 take part in metabolic and apoptotic protein complexes (Cheng et al., 2003; Colombini, 2004; Lemasters and Holmuhamedov, 2006).

The transfer and assembly of components of cellular protein complexes were shown to be assisted by molecular chaperones, adding a novel function to their role in nascent protein folding (Soti et al., 2005; Young et al., 2003). Accordingly, Ca^{2+} binding- , heat shock- , and glucose regulated chaperone family members are abundantly present along the Ca^{2+} transfer axis, linking the ER and mitochondrial networks. Well known examples are the Ca^{2+} binding chaperones of the ER lumen (Michalak et al., 2002), immunophilins interacting with ER Ca^{2+} release channels and the mitochondrial permeability transition (MPT) pore (Bultynck et al., 2001; Forte and Bernardi, 2005), and several heat shock family members localized at the mitochondrial membranes, proposed to interact with the components of the MPT pore, such as VDAC (Gupta and Knowlton, 2005; He and Lemasters, 2003; Wadhwa et al., 2005). Still their exact role at the ER-mitochondria interface is not well known, although recently weak links by chaperones were proposed to stabilize signaling and organellar cellular networks (Csermely, 2004; Soti et al., 2005).

Considering the above outlined central position of VDAC at the ER-mitochondrial interface, we used VDAC1 as a starting point for protein biochemical studies, in order to explore molecular interaction pathways between the ER and mitochondrial networks. We found that through the OMM associated fraction of the grp75 chaperone (Zahedi et al., 2006), VDAC1 interacts with the ER Ca^{2+} release channel IP$_3$R. Organellar Ca^{2+} measurements, using targeted recombinant Ca^{2+} probes, confirmed a functional interaction between the IP$_3$R and the mitochondrial Ca^{2+} uptake machinery, which was abolished by grp75 knockdown.

VDAC1, grp75 and IP₃Rs are present in a macromolecular complex at the ER mitochondria interface

We carried out yeast two-hybrid screens of human liver and kidney LexA-AD fused libraries, using a rat VDAC1-LexA-DNA-BD fusion protein as bait. Among the putative interactors, we have found cytoskeletal elements, previously thought to participate in sorting of VDAC or in mitochondrial dynamics (Schwarzer et al., 2002b; Varadi and Rutter, 2004) and a group of chaperone proteins (Table 1).

Name	Accession number
DnaJ (Hsp40) homolog, subfamily A, member 1; DNAJA1	NM_001539
filamin B, beta (actin binding protein 278); FLNB	NM_001457
heat-shock 70-kd protein 5; HSPA5	NM_005347
heat-shock 70-kd protein 9b; HSPA9B	BC024034
protein phosphatase 1g (formerly 2c), magnesium-dependent, gamma isoform; PPM1G	NM_002707
t complex-associated testis-expressed 1-like 1; TCTEL1	D50663
tetratricopeptide repeat domain 1; TCC1	NM_0033114
thioredoxin-like 1; TXNL1	AF052659
tubulin-specific chaperone c; TBCC	BC020170
zinc-finger like protein 9; ZPR9	AY046059

Table 1 VDAC-1 interactors found by yeast two-hybrid screening. Yeast two-hybrid screening was carried using the pLexA system according to the protocol of Gyuris et al. (1993). For details see Supplementary materials and methods. Approximately 90% of the clones contained a sub-sequence of the ER-resident chaperone heat shock 70-kD protein 5 (HSPA5, grp-78), most probably reflecting the requirement of efficient folding of the VDAC1 protein in yeast. The results of sequencing of the remaining clones are shown in the table. One group of the putative interacting proteins were found to be cytoskeletal and signaling elements (underlined); another group (shown in normal) were found to be folding intermediates, presumably underlying the proper function of VDAC1.

In order to investigate whether the chaperones may participate in mediating organelle interactions, we focused our attention on the human heat shock 70kD protein 9B/grp75 (nt 1456-2089, aa 471-681; GenBank ID: BC000478). This chaperone was known to reside in the mitochondrial matrix, taking part of the protein import motor associated with TIM23 (Neupert and Brunner, 2002), but it was also found in the cytosol and in mitochondria-associated high molecular weight protein complexes (Danial et al., 2003; Ran et al., 2000). A recent meticulous proteomic

approach has found grp75 as a member of a conserved matrix protein cluster at the OMM (Zahedi et al., 2006). In addition, two further findings indicated that grp75 may be involved in ER-mitochondria Ca^{2+} transfer: first, its C-terminal domain reduced the voltage dependence and cation selectivity of VDAC1 (Schwarzer et al., 2002), and grp75 overexpression was shown to promote cell proliferation and protect against Ca^{2+} mediated cell death (Liu et al., 2005; Wadhwa et al., 2002).

Based on these findings, we used further biochemical approaches to investigate the role of grp75 at the ER-mitochondria contact sites. We took advantage of a previously developed method to purify a mitochondria-associated ER subfraction (mitochondria associated membrane fraction, denoted as MAM (Vance, 1990)). The MAM was formerly shown to be enriched in lipid synthases and transferases (Vance, 2003), and its potential role in ER-mitochondrial Ca^{2+} transfer was also proposed (Filippin et al., 2003; Szabadkai and Rizzuto, 2004; Yi et al., 2004b). Indeed, immunoblot screening of the MAM fraction, purified from rat liver and HeLa cells, revealed the presence of grp75, as well as Ca^{2+} channels both from the OMM (VDAC1) and the ER (IP$_3$R, Fig. 1A). Then we applied two dimensional blue native - SDS-PAGE protein separation to identify the specific localization of VDAC1, grp75 and the IP$_3$R in higher order protein complexes of the MAM fraction. Samples were separated under non-denaturing conditions on a blue native acrylamide gel (1st dimension), then pulled out into individual protein components by SDS-PAGE (2nd dimension), and screened for the presence of VDAC1, IP$_3$Rs and grp75 by immunoblotting (Fig. 1C). While VDAC1 was present in different amounts in complexes of a wide MW range, we found a specific complex characterized by the presence of both the IP$_3$R and grp75, suggesting their interaction in the native state. The specificity of the complex formation of IP$_3$R and grp75 was corroborated by the finding that SERCA2 showed a different localization in the 2D separation (data not shown).

In order to confirm the existence of a subpopulation of grp75 beyond the abundant matrix content of the protein we applied two approaches. First, 2D separation of the purified, high density
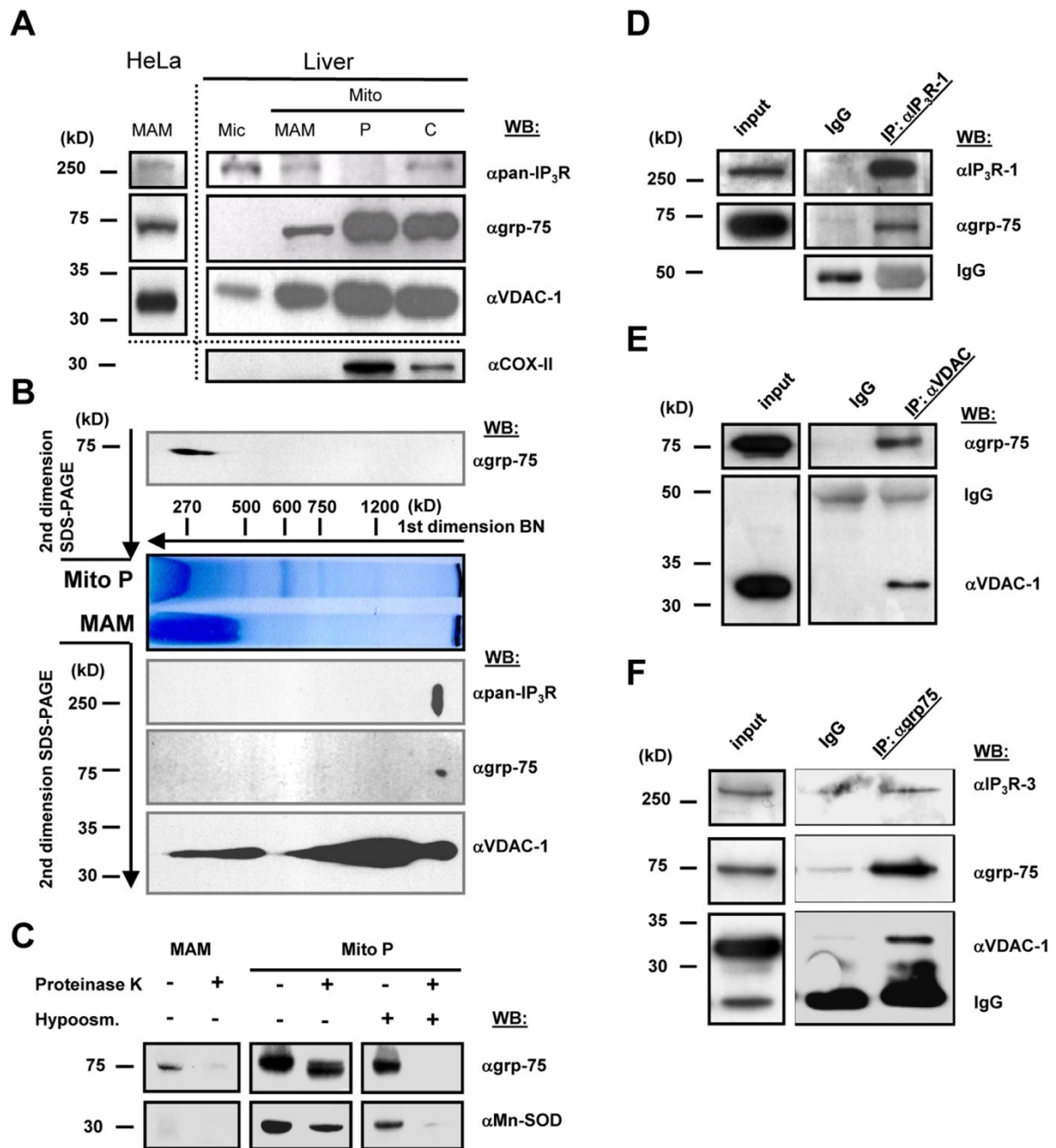
51

Figure 1 IP₃R, VDAC1 and grp75 colocalize on the mitochondria associated membrane fraction. *(A) Immunoblot analysis of protein components of subcellular fractions prepared from rat liver and HeLa cells. Mito: mitochondria; MAM: light mitochondrial fraction, mitochondria-associated membranes; P: heavy mitochondrial fraction, enriched in matrix components; C: crude mitochondrial fraction prior to Percoll gradient separation. 10 μg proteins were loaded on 10% SDS-polyacrilamyde gels. The presence of IP₃Rs was shown by using a non isotype specific monoclonal antibody. VDAC1 and grp75 were both present in the MAM, while it was free of contamination from inner membrane (Cox-II) and matrix (MnSOD, data not shown, see B.) proteins. Different preparations are separated by the dotted line. Blots represent >5 experiments. (B)Blue-native and SDS-PAGE two-dimensional separation of the MAM fraction (below BN) and Mito-P proteins (above BN; for preparation of native subcellular fractions see Materials and Methods and A.).The native fractions were solubilized and separated on an acrylamide capillary gel in the first dimension. The capillary gel was stacked over a 10 % SDS-PA gel, separated, and then the proteins were immunoblotted against the IP₃Rs, grp75 and VDAC1. A typical result of an immunoblot from 3 separate experiments is shown. (C) The MAM and Mito P fractions (50 μg proteins) were subjected to proteinase-K digestion (50 μg/ml) then the presence of grp75 and MnSOD was revealed by immunoblotting. Hypoosmotic shock (50 mM mannitol, Hepes 5mM, EGTA 0.1 mM; 30 min 37°C) was applied to the mito P fraction in order to induce release of matrix proteins.D-F. Co-immunoprecipitation of grp75 with IP₃R and VDAC1. Total cellular proteins were used for immunoprecipitation with a monoclonal IP₃R-1 (D), a polyclonal VDAC (E) and a monoclonal grp75 (F) antibody and the precipitated protein fractions was separated on 10% SDS-polyacrilamyde gels and immunoblotted against IP₃R-3, grp75 and VDAC1. The input homogenate fractions, the IgG controls and the immunoprecipitates are shown.*

52

mitochondrial fraction (containing matrix proteins, Mito P, Fig. 1B), devoid of IP$_3$Rs (see Fig. 1A), revealed a different pattern of grp75 distribution with respect to the 2D separation pattern of the MAM fraction. In Mito P grp75 was found in lower molecular weight complexes (< 400 kD), similarly to previous data in yeast (Dekker and Pfanner, 1997), and confirming that grp75 is involved in specific protein-protein interactions in the MAM. Second, we showed that while the matrix localized grp75 was resistant to proteinase K digestion (similarly to the matrix enzyme MnSOD, Fig. 1C), grp75 was digested by the enzyme in the MAM fraction, confirming its association with the mitochondrial surface.

To further investigate the arrangement of the grp75/VDAC/IP$_3$R complex, we utilized co-immunoprecipitation studies of all three proteins implied. Immunoprecipitation of both VDAC1 and IP$_3$R1 led to the co-precipitation of grp75 (Fig.1D and E, respectively), but no IP$_3$R was found in the VDAC1 precipitate as well as no VDAC1 was detectable in the IP$_3$R1 precipitate. However, immunoprecipitation of grp75 led to the co-purification of both VDAC and the IP$_3$R3, the most abundant subtype of the receptor in HeLa cells (Fig. 1F). These results strongly suggest that grp75 have a central role in setting up the protein complex with VDAC1 and the IP$_3$R. Moreover, the interactions were detected both in the presence and absence of Mg^{2+}-ATP (data not shown), further suggesting the scaffolding rather than chaperoning function of grp75 in the complex.

Direct regulation of mitochondrial Ca^{2+} uptake by the IP$_3$R ligand binding domain

If the ER Ca^{2+} release channel IP$_3$R is directly or indirectly is in physical contact with OMM VDAC channel, we assumed that the mitochondrial Ca^{2+} uptake machinery might be regulated by the large cytoplasmic domain of the IP$_3$R. This scheme was also supported by previous reports, showing that its ligand binding domain (aa 224-605, denoted as IP$_3$R-LBD$_{224-605}$), located on the surface of the bulky cytoplasmic N-terminal part of the receptor, participates in intramolecular interactions with other IP$_3$R domains (Boehning and Joseph, 2000) as well as in linking the receptor

with other protein partners (Bosanac et al., 2004). To assess a direct role of the IP_3R on mitochondrial Ca^{2+} uptake we co-expressed in HeLa cells mRFP1-tagged $IP_3R\text{-}LBD_{224\text{-}605}$ with cytosolic (cytAEQ) or mitochondrially targeted (mtAEQmut) aequorin-based Ca^{2+} probes, and evaluated global and organellar Ca^{2+} responses to agonist stimulation. After reconstitution with the aequorin co-factor coelenterazine, cells were challenged with histamine (in incrementing doses from 1 to 100 µM) and luminescence was measured and converted to $[Ca^{2+}]$. Recombinant expression of the $IP_3R\text{-}LBD_{224\text{-}605}$ caused a marked increase in mitochondrial Ca^{2+} uptake at each agonist concentration applied, in spite of reduced cytoplasmic Ca^{2+} response $([Ca^{2+}]_c)$, due to IP_3 buffering and consequent reduction of IP_3-induced Ca^{2+} release from the ER (Fig. 3A & B). The effect of the $IP_3R\text{-}LBD_{224\text{-}605}$ was presumably exerted on the mitochondrial outer membrane (OMM), since targeting the $IP_3R\text{-}LBD_{224\text{-}605}$ to the OMM surface (by fusing to an N-terminal AKAP1 domain), apparently augmented its stimulatory effect (See Fig. 2 for intracellular localization of the mRFP1 tagged construct and Fig. 3B for the effect on $[Ca^{2+}]_m$). Morphological imaging and mitochondrial loading with the potential sensitive dye teramethyl-rhodamine-methylester (TMRM) showed that the effect was not due to changes in mitochondrial morphology (Fig. 3) or to the modification of mitochondrial membrane potential (data not shown).

In order to confirm that activation of mitochondrial Ca^{2+} uptake can be exerted from the original site of the IP_3R, i.e. from the ER membrane, we expressed $IP_3R\text{-}LBD_{224\text{-}605}$, fused to a C-

OMM-$IP_3R\text{-}LBD_{224\text{-}605}$ **ER-$IP_3R\text{-}LBD_{224\text{-}605}$**

mtTracker   mRFP   overlay   mtTracker   mRFP   overlay
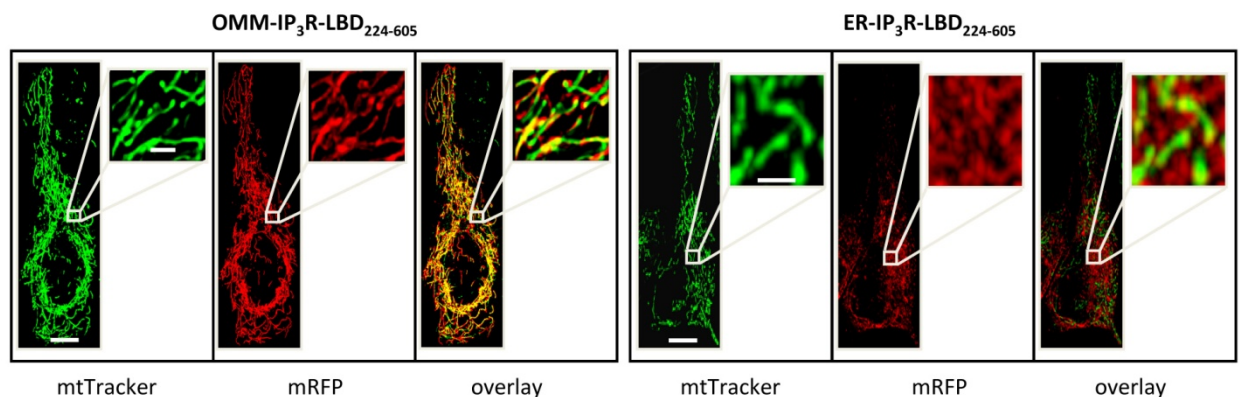
Figure 2 Intracellular localization of OMM-(A) and ER-(B) targeted $IP_3R\text{-}LBD_{224\text{-}605}$, fused with mRFP1 at its C-terminal. Cells were transfected with the respective constructs and loaded with the mitochondrial dye mitoTracker Green (Molecular Probes, Invitrogen). Left panels show mitochondrial structure, middle panels show images of $IP_3R\text{-}LBD_{224\text{-}605}$-mRFP1 fluorescence and right panels show colocalization of the green and red signals (bars=10 μm). Insets show magnified images of the mitochondrial and ER networks (bars=2 μm).

terminal ER-targeting sequence derived from the yeast UBC6 protein (denoted as ER-IP$_3$R-LBD$_{224-605}$) (Varnai et al., 2005). Expression of this construct reduced the steady state ER [Ca^{2+}] ([Ca^{2+}]$_{er}$) and IP$_3$-induced Ca^{2+} release (Fig. 3C), probably due to direct activation of the IP$_3$R, as has been in COS-7 cells (Varnai et al., 2005), although store depletion was incomplete in the HeLa cells at the expression levels used in this study. Still, most importantly, expression of the ER targeted IP$_3$R-LBD$_{224-605}$ augmented mitochondrial Ca^{2+} accumulation following cellular stimulation by histamine similarly as was observed expressing the OMM targeted IP$_3$R-LBD domain (Fig. 2 shows intracellular localization of ER-IP$_3$R-LBD$_{224-605}$; Fig. 3B shows the stimulatory effect of ER-IP$_3$R-LBD$_{224-605}$ on [Ca^{2+}]$_m$). These results strongly suggested that the IP$_3$R, acting from the ER surface regulates mitochondrial Ca^{2+} uptake at an OMM site, independently of its Ca^{2+} channelling function.

Regulation of mitochondrial uptake by the IP$_3$R-LBD is a result of specific protein interactions at the ER-OMM interface

Based on the above conclusions, we further investigated whether the effect of the N-terminal cytosolic domain of the IP$_3$R reflects the specific protein-protein interactions at the ER/mitochondrial contacts. We showed (i) that the K508A mutant of the IP$_3$R-LBD$_{224-605}$, which is unable to bind IP$_3$, increased similarly the [Ca^{2+}]$_m$ rise, but, as expected, did not modify the [Ca^{2+}]$_c$ response (Fig. 3C, D). This suggested that the stimulatory effect, albeit less efficient in the case of the mutant LBD, is independent of IP$_3$ buffering. The reduced efficiency of the OMM targeted mutant LBD was also shown in digitonin permeabilized HeLa cells. In these cells, co-transfected with mtAEQmut and OMM-IP$_3$R-LBD$_{224-605}$ or OMM-IP$_3$R-LBD$_{224-605}$-K508A the Ca^{2+}uptake was measured in the presence of 1 μM extramitochondrial Ca^{2+}. Under these conditions, where the interactions were most probably unbalanced by the application of digitonin, the wild type OMM-IP$_3$R-LBD$_{224-605}$ still exerted a 14.71 ± 4.66 % increase (n = 25, p < 0.01) in Ca^{2+} uptake while the

K508A mutant did not cause a significant increase (6.58±4.23 % increase, n=25, p > 0.05) (ii) The

IP_3R-$LBD_{224-605}$ was shown to play an important role in the regulation of IP_3R channel activity by
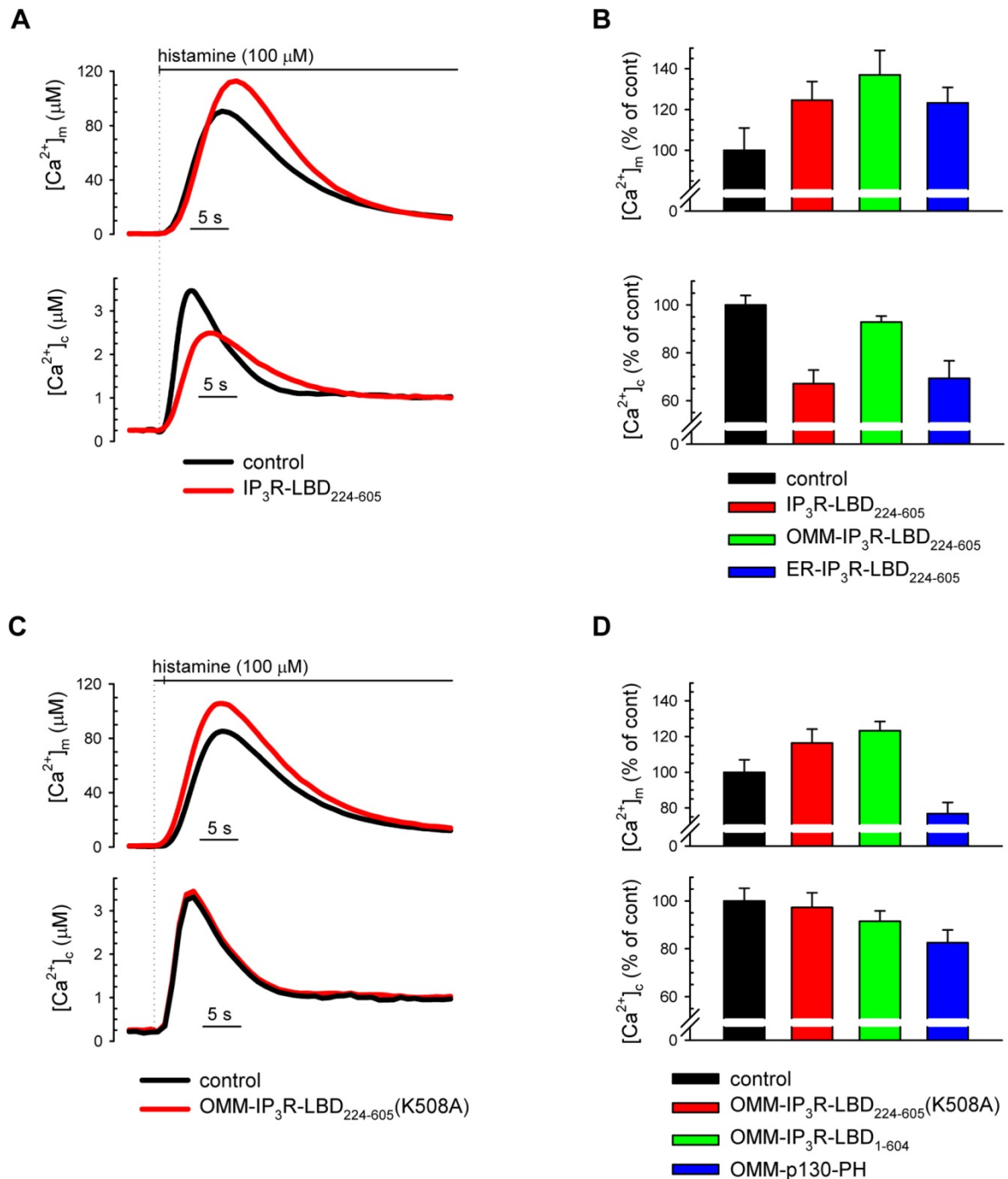

Figure 3 Effect of the IP3R ligand binding domain on mitochondrial Ca2+ uptake. *(A,C) HeLa cells were transfected with mitochondrially targeted (upper panel) and cytosolic aequorin (lower panel). Control traces are shown in black; traces from cells co-transfected with the IP_3R-$LBD_{224-605}$ (A) and the IP_3R-$LBD_{224-605}$ K508 mutant (C) are shown in red. Traces are representative of >15 experiments from >5 preparations. (B) Effect of the cytosolic, OMM and ER targeted IP_3R-$LBD_{224-605}$ (controls, black bar; IP_3R-$LBD_{224-605}$, red bar; OMM-IP_3R-$LBD_{224-605}$, green bar; IP_3R-$LBD_{224-605}$, blue bar; respectively) on peak mitochondrial and cytosolic Ca^{2+} responses (upper and lower panels, respectively). (D) Effect of the OMM-IP_3R-$LBD_{224-605}$(K508A), red bar; the OMM targeted N-terminal (1-604 aa) part of the IP_3R (OMM-IP_3R-LBD_{1-604}), green bar; and the IP_3 binding PH domain of the p130 PLC-like protein (OMM-p130-PH), blue bar; on mitochondrial (upper panel) and cytoplasmic Ca^{2+} responses (lower panel) following 100 μM histamine stimulation. Data in B and D were normalized to mean of the control group, % increase is shown. Cells were transfected and [Ca^{2+}] was measured as described in the Materials and Methods section. Mean ± S.E.M of values are shown.*

56

interacting with the N-terminal repressor domain (aa 1-223)(Boehning and Joseph, 2000; Varnai et al., 2005). Still, expressing the whole N-terminal surface domain of the IP$_3$R, targeted to the exterior of the OMM (OMM-IP$_3$R$_{1-604}$) increased mitochondrial Ca^{2+} (see Fig. 3D). These results exclude that the stimulatory effect of the IP$_3$R-LBD$_{224-605}$ was exerted through unmasking this intramolecular interaction in the endogenous IP$_3$R, but they rather support a model in which the whole N-terminal IP$_3$R exerts direct activation on the mitochondrial Ca^{2+} uptake machinery. (iii) Lastly, we found that a structurally unrelated IP$_3$-binding protein domain, the PH domain of the PLC-like protein, p130 (p130PH)(Lin et al., 2005), targeted to the OMM, reduced both the [Ca^{2+}]$_m$ and [Ca^{2+}]$_c$ responses (Fig. 3D), proving that the stimulatory effect is a specific property of the IP$_3$R-LBD$_{224-605}$, and further confirming that the effect is independent of IP$_3$ binding.

An apparent drawback of the use of the IP$_3$R-LBD$_{224-605}$ is its local IP$_3$ buffering activity when exploring its effect on mitochondrial Ca^{2+} uptake during IP$_3$-induced Ca^{2+} release. Indeed, as shown on Fig. 3A and B, the OMM or ER targeted LBD did not appear to be more efficient in stimulating mitochondrial Ca^{2+} uptake as compared to the non-targeted, cytosolic domain, considering that this construct more efficiently blocked the bulk cytosolic Ca^{2+} response (Fig. 3A and B, lower panels), rendering the ratio of [Ca^{2+}]$_m$:[Ca^{2+}]$_c$ after histamine stimulation identical in IP$_3$R-LBD$_{224-605}$ and OMM/ER-IP$_3$R-LBD$_{224-605}$ expressing cells. Since the expression level of the constructs did not differ significantly (data not shown), we assumed that the lack of higher efficiency reflects higher local IP$_3$ buffering at the ER-mitochondrial interface, not sensed by the bulky cytosolic [Ca^{2+}]$_c$ sensor cytAEQ. Two additional approaches sorted out this complexity. (i) The further use of the p130PH domain, which had no direct effect on the mitochondrial Ca^{2+} uptake machinery (see above), confirmed the assumption of higher local buffering on the OMM surface. Indeed, as shown on (Fig.4A and B), its targeting to the OMM led to significantly higher reduction of mitochondrial Ca^{2+} uptake as compared to its non-targeted, cytosolic counterpart, but equally reduced the [Ca^{2+}]$_c$ response to histamine. (ii) In order to investigate the IP$_3$ independent uptake of Ca^{2+} into mitochondria, we measured [Ca^{2+}]$_m$ after the emptying of the ER Ca^{2+} pool using the

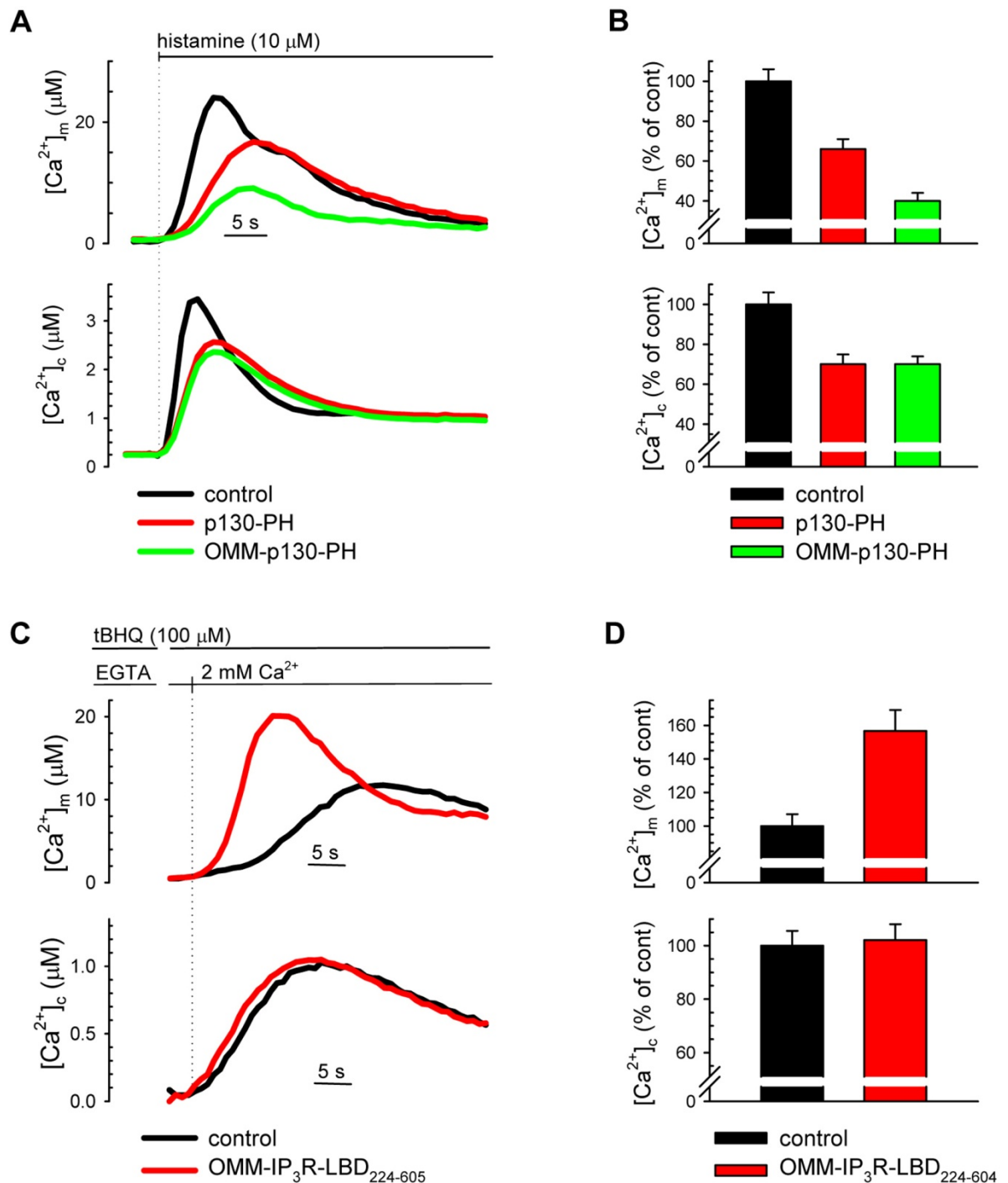SERCA blocker tert-butylhydroquinone (tBHQ) and re-addition of $CaCl_2$ to the extracellular medium.

Figure 4 The effect of IP$_3$R-LBD and p130PH domain on the cytosolic Ca^{2+} responses and mitochondrial Ca^{2+} uptake. *[Ca^{2+}] measurements in HeLa cells, transfected with mitochondrially targeted (upper panels) and cytosolic aequorin (lower panels) are shown. (A) Representative [Ca^{2+}]$_c$ and [Ca^{2+}]$_m$ measurements of control (black traces), cytosolic and OMM targeted p130-PH domain expressing HeLa cells. (B) Comparison of the efficiency of non-targeted and OMM targeted p130-PH on mitochondrial and cytosolic Ca^{2+} responses (normalized to mean of the control group, data are expressed in % increase). (C, D) [Ca^{2+}]$_c$ (upper panels) and [Ca^{2+}]$_m$ (lower panels) were measured after induction of capacitative Ca^{2+} influx, following ER depletion in Ca^{2+} free medium (KRB-EGTA [100 μM], 4 min) and re-addition of 1mM CaCl$_2$. Representative traces of control (black traces) and OMM-IP$_3$R-LBD$_{224-605}$ co-transfected cells (red traces) are shown. ([Ca^{2+}]$_m$ peak in controls: 12.1 ± 2.11 μM, in OMM-IP$_3$R-LBD$_{224-605}$ expressing cells: 21.2 ± 4.00 μM; p = 0.05; [Ca^{2+}]$_c$ peak in controls: 0.96 ± 0.04 μM, in OMM-IP$_3$R-LBD$_{224-605}$ expressing cells: 1.04 ± 0.03 μM). On D, data normalized to the mean of the control group are shown.*

This protocol induces capacitative Ca^{2+} entry and consequent mitochondrial Ca^{2+} uptake from the cytoplasm without IP_3 induced Ca^{2+} release. As shown on Fig. 4C and D, IP_3R-$LBD_{224-605}$ expressing cells showed an ~ 60% increase in the capacitative influx induced $[Ca^{2+}]_m$ response (upper panels), even if the $[Ca^{2+}]_c$ response to Ca^{2+} re-addition remained unaltered (lower panels). This increase in $[Ca^{2+}]_m$ was almost double as compared to the effect following histamine/IP_3 induced Ca^{2+} release from the ER (see Fig. 3B), thus we concluded that local IP_3 buffering masks the stimulatory effect of the IP_3R-$LBD_{224-605}$ during Ca^{2+} release induced mitochondrial Ca^{2+} uptake, and indeed, the effect of the IP_3R-LBD is established at the ER-mitochondrial contacts.

Down-regulation of grp75 abolishes the functional coupling between the IP$_3$R and mitochondria

Since our proteomic studies suggested that the interaction of the VDAC and IP_3R channels is mediated by grp75, we then investigated whether the stimulatory effect of the OMM targeted IP_3R-$LBD_{224-605}$ on mitochondrial Ca^{2+} uptake requires the presence of grp75. Our preliminary experiments shown that strong inhibition of grp75 expression (48 h hours after transfection) in itself strongly reduced mitochondrial Ca^{2+} uptake, most probably due alterations of mitochondrial function due to inhibition of protein import and $\Delta\psi_m$ loss. Thus in the next set of experiments we choose a minor silencing efficiency by conducting experiments after 24h of transfection (see inset of Fig. 5A). We expressed control and grp75 siRNAs in HeLa cells, co-transfecting them with the IP_3R-$LBD_{224-605}$ construct and the mtAEQmut Ca^{2+} probe. As shown on Fig. 5A and B, grp75 siRNA had no significant effect on the $[Ca^{2+}]_m$ response to histamine stimulation. However, the down-regulation of grp75 prevented the stimulatory effect of the IP_3R-$LBD_{224-605}$ on mitochondrial Ca^{2+} uptake, expressed both on the OMM and the ER surface (Fig. 5B). Thus we concluded that the chaperone protein is not only physically associated with the IP_3R/VDAC1 complex, but is also

necessary for functional coupling between these proteins. These results also show that while moderate knock-down of grp75 does not interfere with its function in the mitochondrial matrix, in
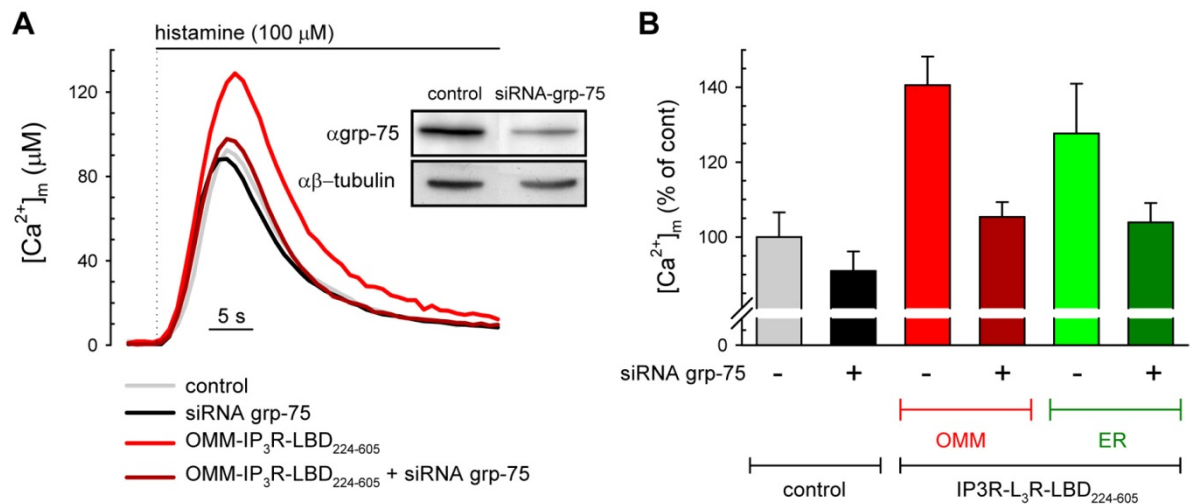

Figure 5 Coupling of the ER and mitochondrial Ca^{2+} channels depends on the presence of grp75. *(A) Mitochondrial Ca^{2+} uptake was measured in control siRNA transfected HeLa cells (grey trace); after siRNA driven down-regulation of grp75 (siRNA-grp75, black trace); control siRNA and OMM-IP$_3$R-LBD$_{224-605}$ transfected cells (red trace); siRNA-grp75 and OMM-IP$_3$R-LBD$_{224-605}$ co-transfected cells (dark red trace). Cells were also co-transfected with the mtAEQmut probe and mitochondrial Ca^{2+} response to 100 μM histamine was measured as described in the Materials and Methods section. (B) Silencing of grp75 reverts the stimulatory effect of IP$_3$R-LBD$_{224-605}$ targeted both to the OMM and ER surface. The percent increase of $[Ca^{2+}]_m$ peaks normalized to the mean of controls are shown in cells co-transfected with mtAEQmut and control siRNA (siRNA-grp75 -; grey bar) and OMM-IP$_3$R-LBD$_{224-605}$ (red bar) or ER-IP$_3$R-LBD$_{224-605}$ (green bar) after stimulation with 100 μM histamine. The stimulatory effect of both the OMM and ER targeted the IP$_3$R-LBD$_{224-605}$ was inhibited after the co-transfection with siRNA-grp75 (+ signs, dark red and dark green bars, respectively), while the control Ca^{2+} peaks remained unaffected (grey bar). (The absolute values find in Supplementary Table 1.) Inset shows immunoblot of grp75 in control siRNA and siRNA-grp75 transfected cells.*

accordance with previous results on mitochondrial protein import (Sanjuan Szklarz et al., 2005), the low amount of grp75 at the ER-mitochondrial contacts is a limiting factor for the stimulatory effect of the IP$_3$R-LBD.

In the final set of experiments we further investigated the role of grp75 in mitochondrial Ca^{2+} uptake regulation by overexpressing the protein. Most likely due to its differentially localized pools, grp75 appeared to modify mitochondrial Ca^{2+} uptake following IP$_3$-induced Ca^{2+} release through diverse mechanisms. Indeed, as shown on Fig. 6A, overexpression of the whole protein led to reduced histamine induced $[Ca^{2+}]_m$ response. However, at the same time, it decreased also the steady state $[Ca^{2+}]_{er}$ level (Fig. 6B), decreasing the driving force for IP$_3$ induced Ca^{2+} release, which in turn might be responsible for the dampened mitochondrial Ca^{2+} accumulation. This parallel reduction of $[Ca^{2+}]_{er}$ and $[Ca^{2+}]_m$ may reflect two different effects of grp75: (i) OMM localized grp75 presumably through the interaction with the IP$_3$R or other members of the ER Ca^{2+} handling
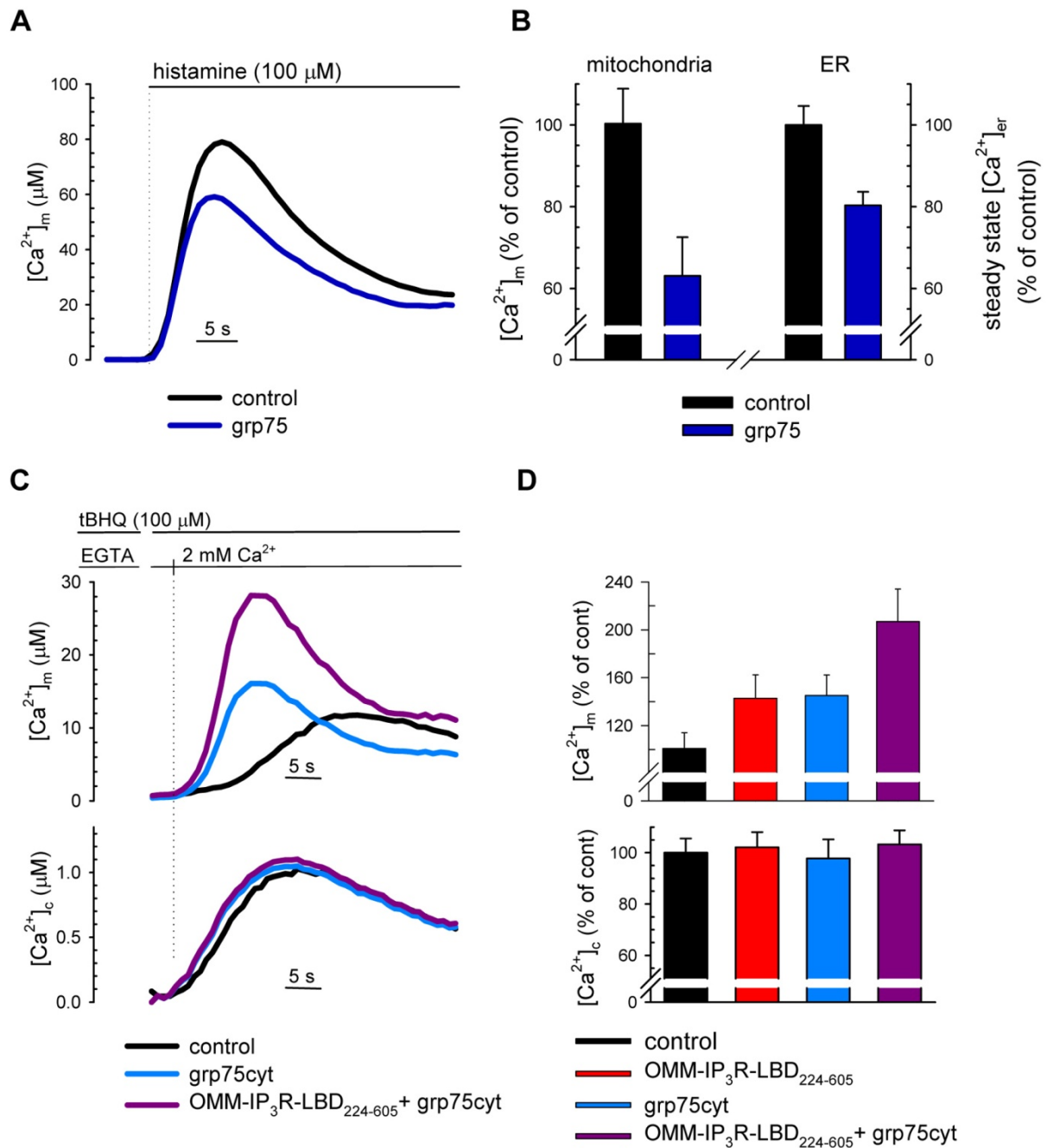
Figure 6 Effect of grp75 overexpression on mitochondrial Ca²⁺ responses and steady state [Ca²⁺]ₑᵣ. *(A, B) HeLa cells were co-transfected with mtAEQmut or erAEQmut probes (controls, black trace and bars) and mouse grp75 (blue trace and bars). [Ca²⁺]ₘ was measured as described above, after stimulation with histamine (100 μM), as indicated on the panel on A. The percent increase (± SEM) of [Ca²⁺]ₘ peaks normalized to the mean of controls are shown on B (left panel), while the effect of grp75 on steady state [Ca²⁺]ₑᵣ is shown on the right panel. Steady state [Ca²⁺]ₑᵣ was measured after refilling of the ER in the presence of 1 mM CaCl₂ in the extracellular medium (n=10, from 4 separate experiments). Prior to measurements, erAEQmut transfected cells were reconstituted with coelenterazine n, following ER Ca²⁺ depletion in a solution containing 0 [Ca²⁺], 600 μM EGTA, 1 μM ionomycin, as previously described (Chiesa et al., 2001). (For [Ca²⁺]ₘ values see Supplementary Table 1. [Ca²⁺]ₑᵣ in controls: 416 ± 19.3 μM, in grp75 overexpressing cells: 334 ± 13.6 μM; p < 0.05).(C, D) [Ca²⁺]ᶜ (upper panels) and [Ca²⁺]ₘ (lower panels) were measured in control and grp75cyt expressing cells, after induction of capacitative Ca²⁺ influx, following ER depletion in Ca²⁺ free medium (KRB-EGTA [100 μM], 4 min) and re-addition of 1mM CaCl₂. Representative traces of control (black traces), co-transfected with OMM-IP₃R-LBD₂₂₄₋₆₀₅ (red traces), grp75cyt (blue) or both (violet traces) are shown. The percent increase (± SEM) of [Ca²⁺]ₘ peaks normalized to the mean of controls are shown on D. [Ca²⁺]ₘ peak in controls: 12.1 ± 2.11 μM, in OMM-IP₃R-LBD₂₂₄₋₆₀₅ expressing cells: 21.2 ± 4.00 μM; p = 0.05; [Ca²⁺]ᶜ peak in controls: 0.96 ± 0.04 μM, in OMM-IP₃R-LBD₂₂₄₋₆₀₅ expressing cells: 1.04 ± 0.03 μM).*

machinery induces Ca^{2+} leak from the ER through the IP_3R, as previously shown for Bcl-2 (Pinton et al., 2000; Bassik et al., 2004). (ii) Matrix localized grp75 may modify mitochondrial parameters (pH, $\Delta\psi_m$) or import of Ca^{2+} handling proteins leading to altered mitochondrial Ca^{2+} uptake as well as the ATP supply for ER Ca^{2+} accumulation through the SERCA pumps. In order to dissect these effects we again used the approach of measuring IP_3 independent mitochondrial Ca^{2+} uptake following capacitative Ca^{2+} influx. In addition, to distinguish OMM based effects from that of the ones in the mitochondrial matrix we expressed a truncated grp75 lacking the N-terminal 51 aa mitochondrial targeting sequence, thus unable to enter into mitochondrial matrix. Ca^{2+} influx was induced by depleting the ER Ca^{2+} store with tBHQ in the absence of extracellular Ca^{2+}, as described in the previous section (see Fig. 4). This 'cytosolic' form of grp75 (grp75$_{cyt}$) did not change the bulk cytosolic $[Ca^{2+}]$ response to re-addition of Ca^{2+} in the extracellular medium, but significantly increased mitochondrial Ca^{2+} accumulation (Fig.6C and D). Moreover, grp75$_{cyt}$ further potentiated the stimulatory effect of IP_3R-$LBD_{224-605}$ (Fig. 6C and D), confirming the results obtained with siRNA grp75, proving that the amount of grp75 present at the OMM in the VDAC/grp75/IP_3R complex is a limiting factor of the positive effect of the IP_3R-LBD on mitochondrial Ca^{2+} uptake. Lastly, by using the co-expression of grp75$_{cyt}$ and IP_3R-$LBD_{224-605}$, we obtained a very high stimulation of mitochondrial Ca^{2+} uptake rate during capacitative Ca^{2+}influx, which leads to a bulk 1 μM $[Ca^{2+}]_c$, we concluded that the VDAC/grp75/IP_3R complex renders mitochondria more sensible at low extramitochondrial $[Ca^{2+}]$, as compared to higher local $[Ca^{2+}]_c$ increases during IP_3 induced Ca^{2+} release (compare the effect of IP_3R-$LBD_{224-605}$ on $[Ca^{2+}]_m$ on Fig.2 and Fig.4 or 6). Indeed, by overexpression of grp75$_{cyt}$ we were not able to observe significant increase in histamine induced $[Ca^{2+}]_m$ responses even if the steady state $[Ca^{2+}]_{er}$ remained unaltered (data not shown).

Effect of different VDAC isoforms on mitochondrial Ca^{2+} homeostasis

The above data and previous work by our group (Rapizzi et al., 2002b) demonstrate that VDAC1 is an essential component of the mitochondrial uptake machinery by modulating OMM permeability to Ca^{2+} ions. In parallel, strong experimental evidences support the notion that mitochondrial Ca^{2+} signals participate in a variety of cellular events, ranging from stimulation of energy production (by maximizing the activity of key enzymes of the Krebs cycle and thus ATP production) to the initiation of the apoptotic process (through the release of caspase cofactors). In this view, investigating the contribution of the different molecular actors mediating mitochondrial Ca^{2+} accumulation could potentially give new insights in the comprehension of how this unique signalling ion can mediate such different cellular outcomes.

In order to dissect the role of Ca^{2+} in apoptosis, many works have examined the influence of intracellular stores on the generation of Ca^{2+} signals leading to cell death. It has been widely demonstrated in many cell types that the Ca^{2+} content of the endoplasmic reticulum is the main determinant of cell sensitivity to many (but not all) apoptotic stimuli. Our group have indeed showed that the overexpression of the anti-apoptotic oncogene Bcl-2 lead to a reduced ER steady state [Ca^{2+}]; as a direct consequence, the [Ca^{2+}] increases caused by inositol-1,4,5-trisphosphate (IP$_3$)-generating agonists or by capacitative Ca^{2+} influx were reduced in amplitude in both the cytosoplasm and the mitochondria (Pinton et al., 2000). Moreover, mimicking the Bcl-2 effect on [Ca^{2+}]$_{er}$ through different pharmacological or molecular approaches indicates that all conditions that lowered [Ca^{2+}] in the ER protected HeLa cells from the Ca^{2+}-dependent apoptotic stimulus C2-ceramide, while treatments that increased [Ca^{2+}]$_{er}$ has the opposite effect (Pinton et al., 2001a). In parallel, Scorrano and Korsmeyer also observed that the genetic ablation of the two pro-apoptotic Bcl-2 family proteins Bax and Bak in mouse fibroblasts causes a reduction in the resting concentration of ER calcium and Bax/Bak double knockout (DKO) cells were resistant to induction of apoptosis by various stimulants, including C2-ceramide and oxidative stress (Scorrano et al., 2003). However, the filling state of the ER only influences the releasable quantity of Ca^{2+} and it is

thus to be considered "upstream" to the real effectors of the apoptotic machinery. The real subcellular compartment responsible for triggering apoptosis is the mitochondrion and in particular its potentially lethal weapons normally residing in the intermembrane space (such as cytochrome C, AIF, Smac/Diablo, HtrA2/Omi and EndoG) (Ravagnan et al., 2002). The activation of the intrinsic apoptotic pathway requires indeed the involvement of this organelle and, in particular, the permeabilization of the outer mitochondrial membrane (OMM) with the consequent release of the above mentioned apoptosis regulators as well as the aperture of the mitochondrial permeability transition pore (mPTP) along with the loss of mitochondrial membrane potential. This permeability transition is controlled by a number of factors (including pH, adenine nucleotides, reactive oxygen species, etc.), suggesting that mitochondria can sense, integrate and decode several different cellular signals and consequently address cell fate. One of the best known mPTP inducers is Ca^{2+}: many experimental works carried out in both isolated mitochondria and living cells clearly show that mitochondrial matrix calcium overload is a key event that precedes the release of caspase cofactors and apoptosome assembly. As a consequence, conditions that enhance mitochondrial Ca^{2+} uptake, generally sensitize cells to several apoptotic stimuli. This is fully supported by our studies about VDAC1, where we showed that it is direct coupled to ER Ca^{2+} releasing channels, thus directly tunneling the cation from one compartment to the other; in parallel, VDAC1 overexpression confers a higher susceptibility to C2-ceramide treatment.

However, in higher multicellular organisms, VDAC exists in three different isoforms that share similar electrophysiological properties (molecular weight cutoff, voltage dependence, etc., see Introduction section) (Xu et al., 1999). In this view, one would expect that all three VDAC isoforms exert the same effect on apoptosis, i.e. enhancing cell death by increasing mitochondrial Ca^{2+} uptake. Unfortunately, this simple model is contradicted by previous work: indeed, Cheng and colleagues demonstrate that VDAC2 is a potent anti-apoptotic protein, and proposed a molecular mechanism where VDAC2 prevents Bak activation by inhibiting its oligomerization and OMM permeability (Cheng et al., 2003). Thus, two different VDAC isoforms are reported to act on

apoptosis in the opposite direction, with VDAC1 being a pro-apoptotic and VDAC2 exerting a protective role against cell death. The notion that these different isoforms are not simply redundant but could potentially being involved in radical different functions is supported by some observations. First of all, the presence of one single archetypical mitochondrial porin in simpler organisms (such as yeasts or *Neurospora Crassa*) and several different isoforms in more complex organisms (ranging from plants to mammals) suggests that gene duplication and divergent evolution likely occurred, conferring specific functions to different isoforms. Moreover, gene ablation of the different isoforms in mice lead to different phenotypes. VDAC1, VDAC3 KO, as well as VDAC1/3 DKO, are viable but with variable defects (see Introduction), while the ablation of VDAC2 is embryonic lethal (Wu et al., 1999). In any case, apart from these clues, a serious and rigorous assessment of the role of the different VDAC isoforms is still missing. We thus exploit the apparent difference in the role of VDAC1 and VDAC2 in the control of cell death through apoptosis as a starting point to study the contribution of mitochondrial porin isoforms. Given the relevance that mitochondrial Ca^{2+} plays in triggering apoptosis we test whether these differences are due to a diverse channeling capacities toward this cation in living cells. We took advantage of the engineered aequorin-based Ca^{2+} probes and carried out an extensive analysis of Ca^{2+} transients in the main intracellular compartments in cells where the levels of VDAC isoforms were selectively modulated through overexpression or RNA interference.

Intracellular localization of VDAC constructs

In collaboration with Prof. Vito De Pinto, we generated several different VDAC chimeras in order to efficiently overexpress the desired isoform. In the previous work by our group we overexpressed rat VDAC1 isoform by introducing in HeLa cells a VDAC1-EGFP chimera, in order to check the correct protein sorting (Rapizzi et al., 2002b). However, this chimera demonstrated to be at least in part missorted, localizing not only in the mitochondrial compartment but also in other subcellular structure. First of all, we thus generate similar DNA constructs by in-frame fusing the

65

cDNA coding for the three different human VDAC isoforms (hVDAC1, hVDAC2 and hVDAC3) with an enhanced yellow fluorescent protein (EYFP), generating as a result three different chimeras: hVDAC1-EYFP, hVDAC2-EYFP and hVDAC3-EYFP. We then transftected HeLa cells with the above vectors and check the localization of protein through high resolution fluorescence microscopy. As shown in figure 7B, VDAC-EYFP chimeras only partially colocalize with mitochondria (here marked with the MitoTracker Red dye), with a pattern very similar to our previous data about rat VDAC1.
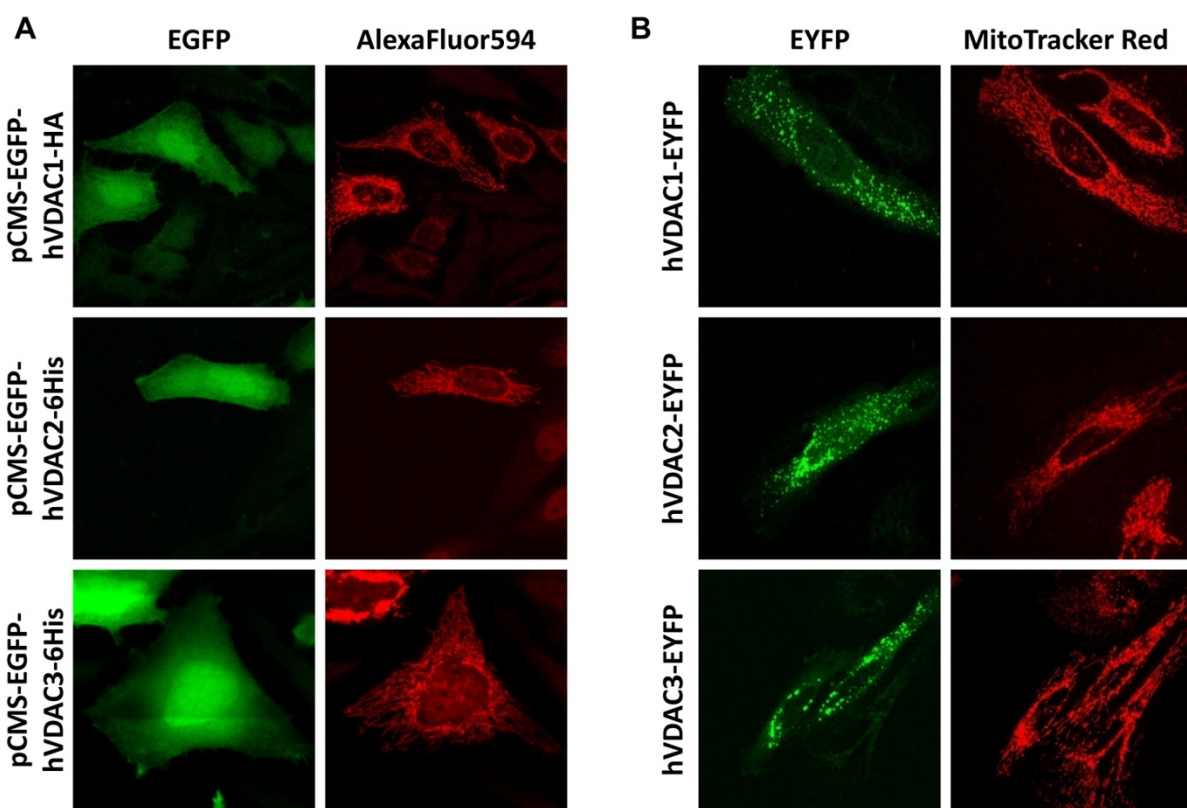

Figure 7 Intracellular localization of VDAC constructs. *HeLa cells have been transfected with the different VDAC-encoding vectors and visualized by confocal fluorescence microscopy. (A) Intracellular localization of hVDAC1-HA, hVDAC2-6His and hVDAC3-6His constructs revealed by immunofluorescence: transfected cells can be seen in the green (thanks to the use of a bicistronic vector encoding for a EGFP) while the subcellular localization of the fusion protein in shown in red. (B) Localization of hVDAC1-EYFP, hVDAC2-EYFP and hVDAC3-EYFP: fluorescence coming from the EYFP fusion proteins is shown in green, while the mitochondrial network was stained with the MitoTracker Red dye. Colocalization analysis reveals that about 30 to 40% of the EYFP signal colocalize with mitochondria (data not shown).*

To solve the relatively poor localization of these EYFP fusion proteins, which is likely to be due to the generous dimension of the fluorescent protein causing a hindrance for the correct insertion into membranes, we tried to generate different construct with VDAC cDNA fused to a smaller tag. We used the bicistronic vector which encodes an EGFP separated from the construct of

interest and we cloned into it the hVDAC1 with a HA-tag (YPYDVPDYA, thus generating hVDAC1-HA) and hVDAC2 or hVDAC3 together with a polyhistidine tag (hVDAC2-6His and hVDAC3-6His). We then checked the localization of these fusion proteins and we thus performed an immunolocalization of the exogenous expressed protein by using a mouse monoclonal antibody against HA-tag (in the case of hVDAC1-HA) or the 6His tag (in the other two cases). The signal was then revealed by using an anti-mouse AlexaFluor594-conjugated antibody and visualized by fluorescence microscopy. As shown in figure 7A, these constructs specifically localize in the mitochondrial compartment, displaying a well-defined mitochondrial network with negligible background. We thus concluded that the fusion of VDAC with a cumbersome fluorescent tag disturbs the correct protein sorting; on the other side, a slighter molecular tag such as HA or 6His do not affect the proper localization. Moreover, none of the fusion proteins used in this work alters mitochondrial overall morphology (which is an important parameter influencing mitochondrial Ca^{2+} uptake).

However, massive protein overexpression, especially at the membrane level, could potentially lead to non-specific toxicity. In addition, several reports shows that VDAC overexpression is *per se* toxic, leading to cell death (Abu-Hamad et al., 2006; De Pinto et al., 2007; Zaid et al., 2005). In particular, VDAC1 overexpression has been demonstrated to induce mitochondrial depolarization. In order to exclude these potentially non-specific effects, we decided to test the effect of VDAC constructs we generated on mitochondrial depolarization. We use the mitochondrial potential-sensitive dye tetramethyl rhodamine methyl ester (TMRM) to count cells with depolarized mitochondria. We expressed the different VDAC-fusion proteins in HeLa cells loaded with TMRM and calculated the percentage of VDAC-overexpressing cells with depolarized mitochondrial (i.e. cells showing no staining with TMRM) under a confocal microscope. Figure 8 shows that hVDA1-HA, hVDAC2-6His and hVDAC3-6His expression causes mitochondrial depolarization to a similar extent (at least 30% of cells), irrespective of what VDAC isoform is overexpressed. Surprisingly, this effect could not be seen when EYFP VDAC-fusion proteins are

expressed or when we downregulate VDACs expression through RNA interference (data not shown). We thus suggest that this effect on mitochondrial membrane potential is non-specific, simply due to the massive expression of the proteins at the outer mitochondrial membrane. Indeed, we propose that the non-perfect VDACs-EYFP localization has the "positive" side effect to cause a milder overexpression at the OMM level when compared to the better localizing VDAC-tagged proteins.
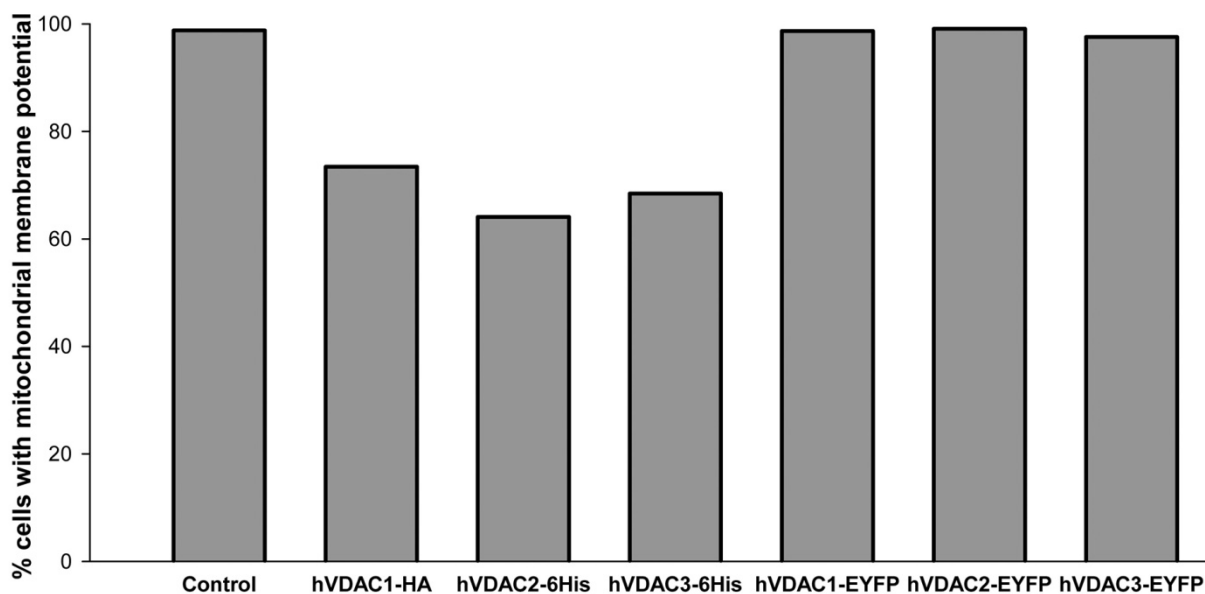

Figure 8 Effect of the different VDAC chimeras on mitochondrial membrane potential. *HeLa cells were transfected with vectors encoding for the different VDAC fusion proteins, loaded with the potential sensitive dye TMRM and visualized by confocal microscopy. At least the 30% of cells expressing hVDAC1-HA, hVDAC2-6His and hVDAC3-6His show an undetectable mitochondrial membrane potential.*

Therefore, VDACs-EYFP fusion proteins, although not perfectly sorted, do not reach toxic expression levels in the OMM, and should be considered a better tool to assess the precise role of the different VDAC isoforms in cellular Ca^{2+} homeostasis and cell death. We decided to use EYFP-VDAC fusion proteins for subsequent experiments.

All VDAC isoforms enhance mitochondrial Ca^{2+} uptake

In order to assess the role of mitochondrial porins on mitochondrial Ca^{2+} homeostasis we co-expressed the various VDAC isoforms with the low affinity mutant of the mitochondrial targeted aequorin Ca^{2+}-probe (mtAeqMut) in HeLa cells and evaluated organellar Ca^{2+} responses to agonist stimulation. . All data have also been confirmed in HEK293 cell line (transfected with the wild-type

probe, mtAeqWT). After reconstitution with the aequorin co-factor coelenterazine, cells were challenged with maximal dose (100 µM) of histamine (or ATP in the case of HEK293) and luminescence was measured and converted to $[Ca^{2+}]$. As shown in figure 9A, VDAC1 overexpression lead to a higher increase of mitochondrial Ca^{2+} transient compared to control, in agreement with our previous published work. In addition, to further demonstrate the specificity of the effect we developed specific siRNA against hVDAC1 and hVDAC2 (siRNA-hVDAC1 and siRNA-hVDAC2 respectively) to downregulate protein level. Accordingly, silencing of VDAC1 exert the opposite effect on mitochondrial Ca^{2+} uptake. We applied than the same experimental setup to investigate the effect of VDAC2 and VDAC3. Surprisingly, VDAC2 (fig 9B) and VDAC3 (fig 9C) demonstrate to have the same effect on mitochondrial Ca^{2+} uptake, i.e. they enhance the
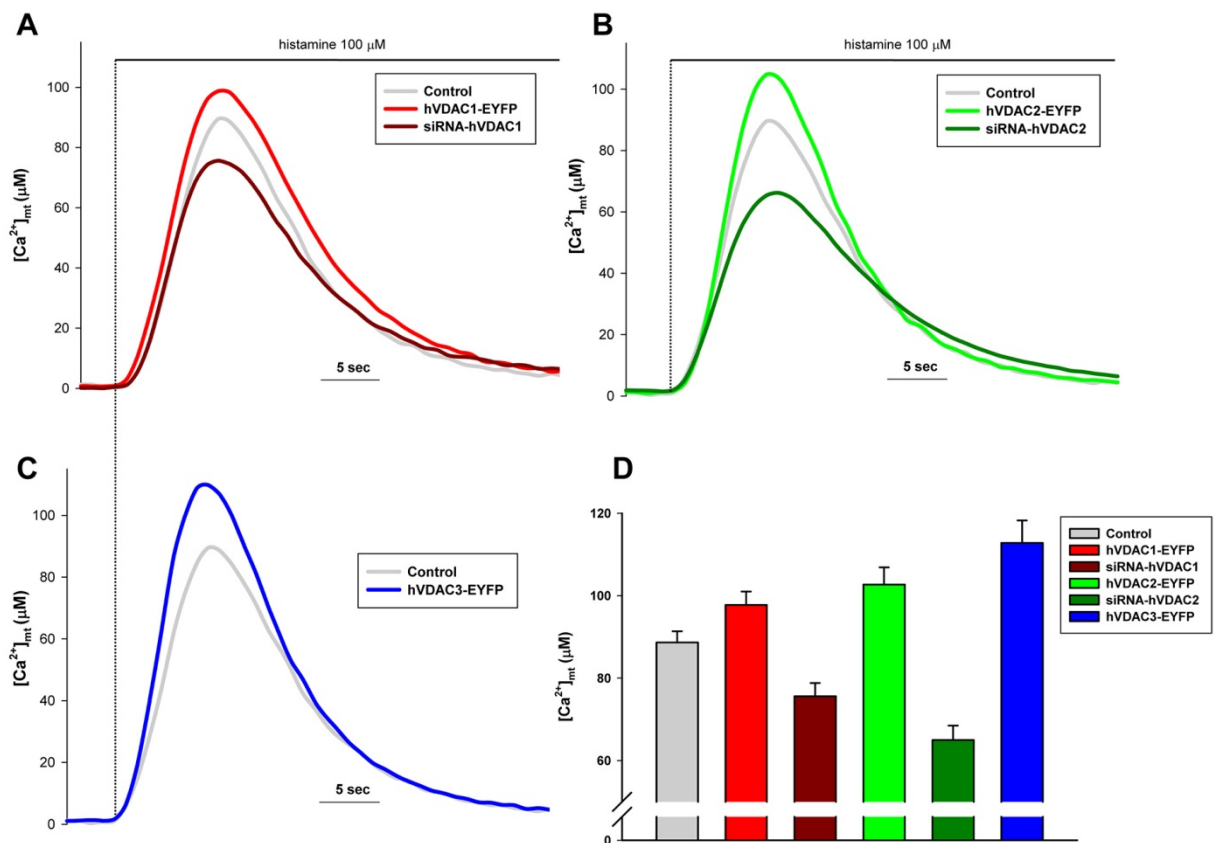

Figure 9 Effect of VDAC isoforms on mitochondrial Ca2+ uptake. *(A,B,C and D) Effects of the modulation of hVDAC1 (A), hVDAC2 (B) and hVDAC3 (C) protein levels on mitochondrial Ca^{2+} uptake. VDAC isoforms were overexpressed through transfection with EYFP fusion proteins and cause the enhancement of mitochondrial Ca^{2+} transients after histamine stimulation compared to control, regardless of the VDAC isoform introduced ($[Ca^{2+}]_{mt}$ peak values are: in controls 88.6±2.7 µM; in hVADC1-EYFP 97.7±3.3 µM; in hVADC2-EYFP102.7±4.2 µM; in hVADC3-EYFP 112.8±5.5 µM). In parallel, agonist induced mitochondrial response in cells where hVDAC1 or hVDAC2 were reduced by RNA interference were decreased when compared to control ($[Ca^{2+}]_{mt}$ peak values are: in siRNA-hVDAC1 75.6±3.2 µM; in siRNA-hVDAC2 64.9±3.5 µM). (D) Data are presented as mean values ± S.E.M.*

amplitude of the agonist-dependent increases in mitochondrial matrix Ca^{2+} concentration. The effect of all VDAC isoforms is thus qualitatively equivalent, suggesting that they share the same Ca^{2+} channeling properties. However, there are minor differences in the extent of the enhancement of mitochondrial Ca^{2+} uptake (hVDAC1 +10%, hVDAC2 +15% and hVDAC3 +25% over control): however, this differences could be due to minor variations in the amount of protein locating at the OMM level. Given that the exact protein quantity actually present in the outer mitochondrial membrane is quite difficult to assess, no conclusions about the Ca^{2+} affinity of the different isoforms can be reached.

VDAC isoforms do not affect cytosolic Ca^{2+} transients

VDAC localization at the OMM level postulate that its effect on Ca^{2+} homeostasis should affect only the mitochondrial compartment, without changing ion homeostasis in the other
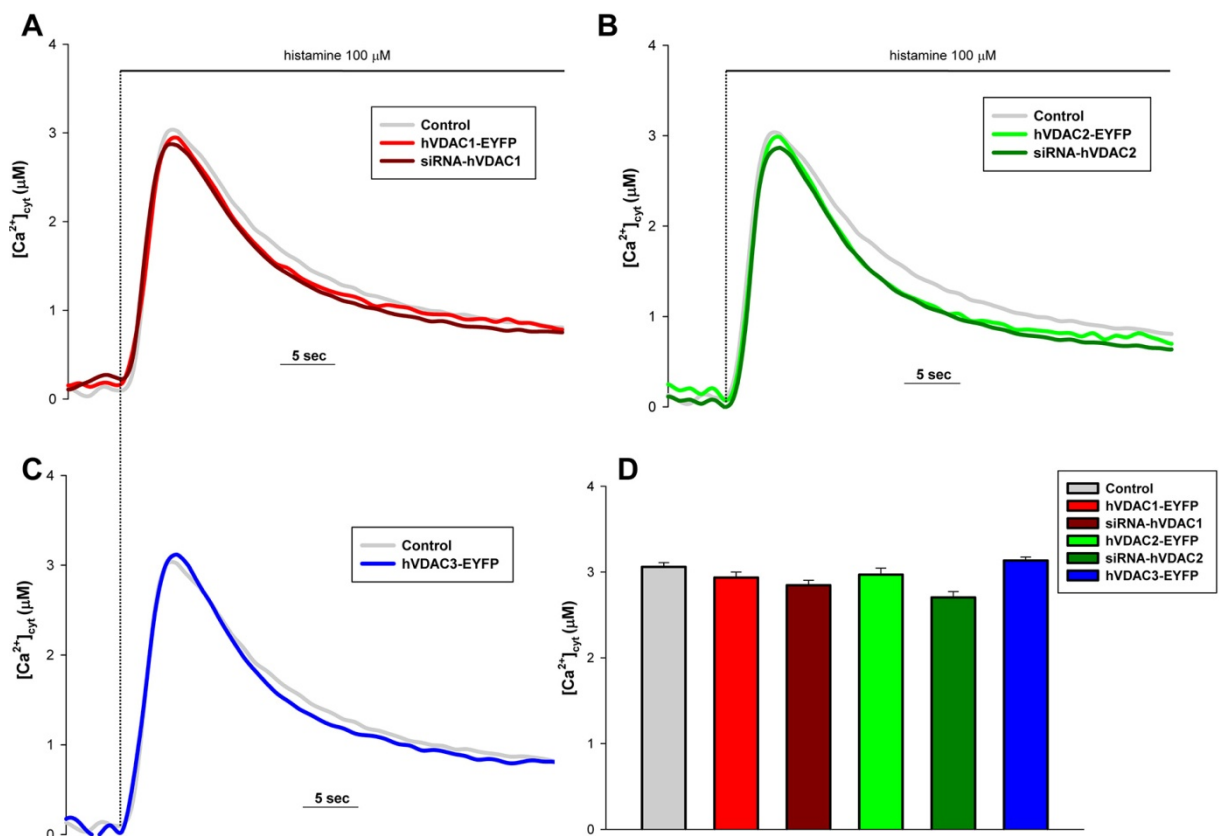

Figure 10 Effect of VDAC isoforms on cytosolic Ca^{2+} transients. *(A,B,C and D) Effects of the modulation of hVDAC1 (A), hVDAC2 (B) and hVDAC3 (C) protein levels on cytosolic Ca^{2+} transients. None of the conditions shows any differences compared to control ($[Ca^{2+}]_{cyt}$ peak values are: in controls 3.06±0.05 μM; in hVADC1-EYFP 2.94±0.06 μM; in siRNA-hVDAC1 2.85±0.06 μM; in hVADC2-EYFP 2.97±0.07 μM; in siRNA-hVDAC2 2.71±0.07 μM; in hVADC3-EYFP 3.12±0.04 μM).). (D) Data are presented as mean values ± S.E.M.*

subcellular locations. We test this hypothesis by performing the previous experiments using the cytosolic localizing aequorin Ca^{2+}-probe (CytAeq). Figure 10 demonstrate that both overexpression and silencing of any VDAC isoforms cannot influence Ca^{2+} transients elicited by agonist stimulation.

This data strongly suggest that VDAC effects on Ca2+ homeostasis is restricted to the mitochondrial compartment.

VDAC has no effect on ER Ca^{2+} content and IP_3 induced Ca^{2+} release

Given that cytosolic and mitochondrial Ca^{2+} transients elicited by IP_3-mobilizing hormones profoundly depend on endoplasmic reticulum Ca^{2+} homeostasis, we finally test the effect of the different VDAC isoforms on ER Ca^{2+} content. To this purpose, we co-transfeted HeLa cells with a low affinity ER targeted aequorin based Ca^{2+}-probe.
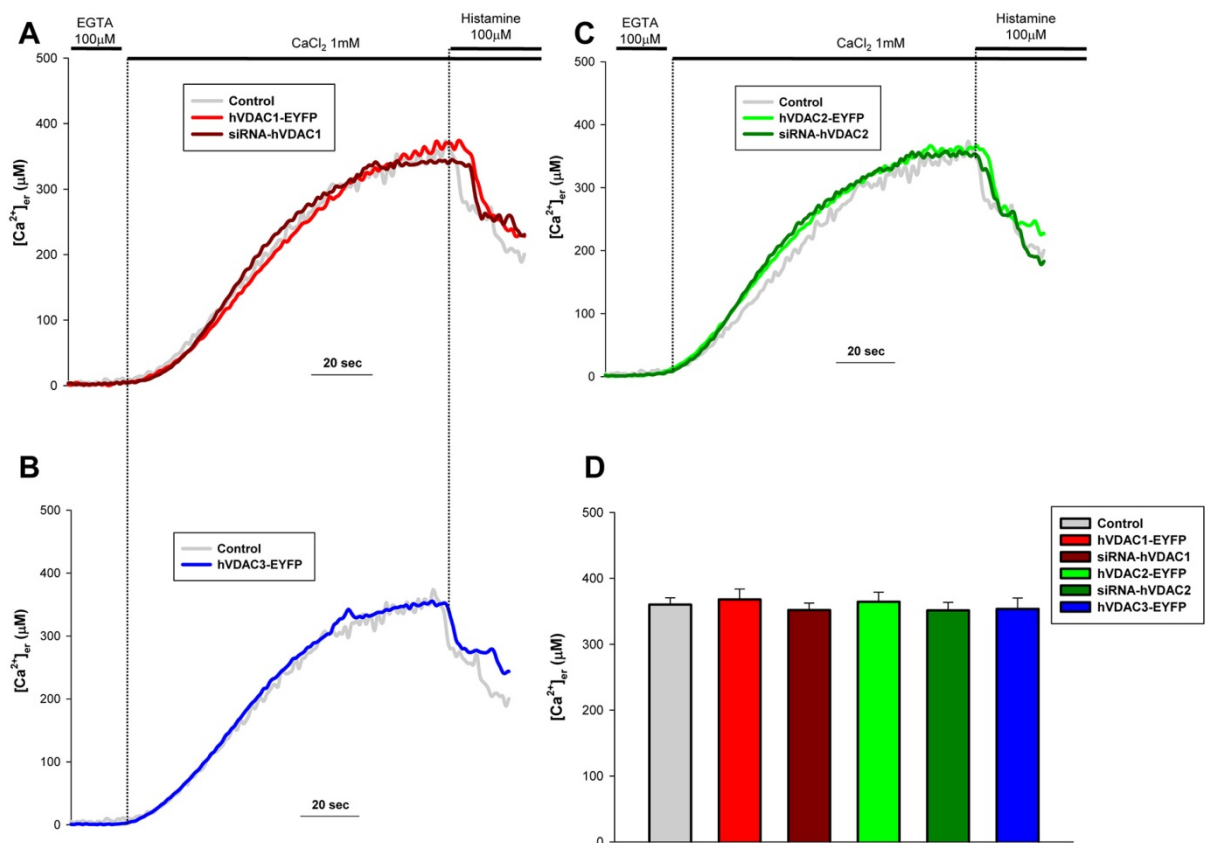

Figure 11 Effect of VDAC isoforms on $[Ca^{2+}]_{er}$ *(A,B,C and D) Effects of the modulation of hVDAC1 (A), hVDAC2 (B) and hVDAC3 (C) protein levels on ER Ca^{2+} steady state levels and IP3 induced release. None of the conditions shows any differences compared to control ($[Ca^{2+}]_{er}$ steady state values are: in controls 360.1±10.6 μM; in hVADC1-EYFP 368±15.6 μM; in siRNA-hVDAC1 351.9±10.6 μM; in hVADC2-EYFP 364.5±14.4 μM; in siRNA-hVDAC2 351.3±12.3 μM; in hVADC3-EYFP 353.6±16.6 μM).). (D) Data are presented as mean values ± S.E.M.*

The experimental protocol for measuring ER [Ca^{2+}] schedule the pre-emptive emptying of the compartment during the reconstitution with a modified coelenterazine to prevent aequorin reaction (by treating cells with the Ca^{2+} ionophore ionomycin in the presence of extracellular EGTA). After reconstitution of the probe, a solution containing 1mM Ca^{2+} is perfused causing an increase in [Ca^{2+}]$_{er}$ until a steady state which represents the filling state of this compartment. After stimulation with histamine [Ca^{2+}]$_{er}$ undergoes to a rapid drop due to the opening of the IP$_3$R, as shown in figure 11. However, as expected from the above data, any of the VDAC isoforms can in any way influence neither ER steady state Ca^{2+} content nor IP$_3$ induced Ca^{2+} release from the ER.

In conclusion, these data demonstrate that VDAC is a fundamental and specific molecular modulator of the mitochondrial Ca^{2+} uptake machinery. Moreover, in our experimental system all the different VDAC isoforms show very similar Ca^{2+} channeling properties. However, these results cannot explain the notion that VDAC1 and VDAC2 differentially regulate sensitivity to apoptotic stimuli. Several consideration can be made about this discrepancy; one possibility is that Ca^{2+} is not an obligatory cell death signal and, at the same time, it isn't the only stimulus acting on mitochondria. Consequently, higher mitochondrial Ca^{2+} uptake capacities does not necessarily result in a higher sensitivity to apoptosis. On the other hand, the experimental system used could not be elegant enough to appreciate subtle diversities in VDAC isoforms functions. To test the latter hypothesis we wonder if the above demonstrated coupling between IP$_3$Rs and VDAC channels could be isoform specific, thus determining a preferential signaling pathway to transfer apoptotic signals.

VDAC isoforms differentially regulate cellular sensitivity to apoptotic stimuli

As a starting point, we first validated previous data published by our group and others in our actual experimental system. To test if the different VDAC isoforms exert a different effect on apoptosis we used a simple bet sensitive assay, the so-called apoptotic counts. In this experiments cells are co-transfected with a reporter gene (such as EGFP) and the constructs of interest: here we

decided to downregulate each isoform through RNA interference techniques in order to get rid of any possible non-specific effect due to overexpression. For each condition (Control, siRNA-hVDAC1, siRNA-hVDAC2, siRNA-hVDAC3) the percentage of GFP-positive cells in the total population is calculated before and after apoptosis induced by C2-ceramide. In the ideal case, although the total number of cells is reduced after cell death induction, the apparent transaction efficiency will be maintained (i.e. transected and non-transfected cells has the same sensitivity to the apoptotic stimulus and will thus die to the same extent). However, when GFP-positive cells are co-transfected with a construct influencing their sensitivity to apoptosis, this will be reflected by a change in the apparent transfection efficiency (i.e. the percentage of fluorescent cells is different before and after treatment with an apoptotic agent). In particular, an increase of transfection efficiency means that fluorescent cells are protected from apoptosis induction (e.g. when an anti-apoptotic protein such as Bcl-2 is overexpressed).
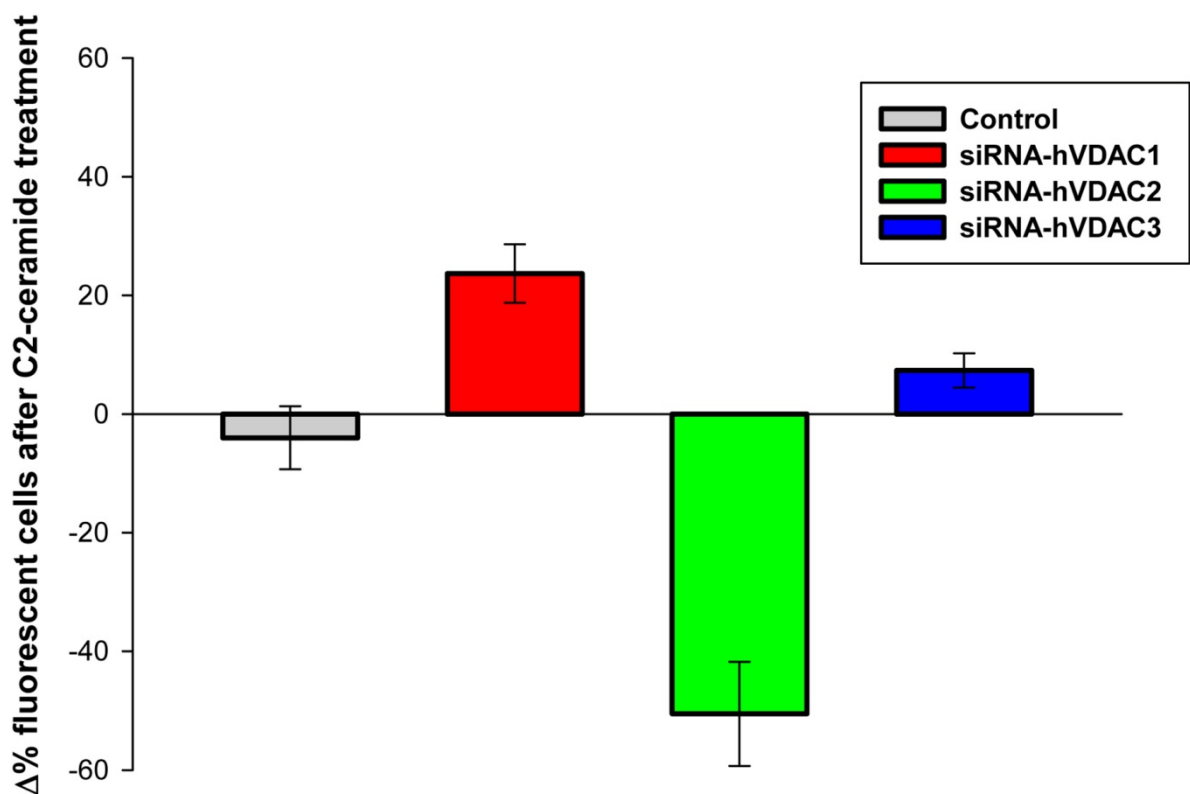

Figure 12 VDAC isoform-specific regulation of apoptosis. *Changes in the apparent number of fluorescent cells reflect different sensitivity to apoptotic stimuli. Data are presented as the percentage difference between transfection efficiencies before and after treatment with 60 μM C2-ceramide for 3h (Control -4±5.3%; siRNA-hVDAC1 +23.7±4.9%; siRNA-hVDAC2 -50.5±8.8%; siRNA-hVDAC3 +7.4±2.9%) .*

73

Conversely, a decrease in fluorescent cells reflects a higher sensitivity to apoptosis. By using this approach, we test the effect of the selective silencing of the different VDAC. As shown in figure 12, hVDAC1 and hVDAC2 have opposite effects on apoptosis sensitivity.

As already reported in literature, VDAC1 is a pro-apoptotic protein (and of course, its silencing is protective), while VDAC2 exert a protective effect (and thus its silencing enhances cell death). The original finding here is that hVDAC3 do not modify in any way cells sensitivity to the apoptotic stimulus C2-ceramide. Therefore, we can conclude that mitochondrial porins, while sharing common Ca^{2+} channeling properties, have evolved different functions in the regulation of cell death. Still, these data do not explain the molecular mechanism through which these different isoforms regulate the decoding of death signals. We thus started from the above demonstrated coupling of ER and mitochondrial Ca^{2+} channels to test the existence of a preferential, isoforms-specific signaling route transferring fine Ca^{2+} pulses from intracellular stores to the effector compartment (i.e. the mitochondria).

VDAC1 specific coupling to ER Ca^{2+} releasing channels

In the previous part of this work, we showed that mitochondria/ER crosstalk is not a merely consequence of physical neighborhood but relies on the existence of macromolecular complexes linking one organelle to the other and that this connection has a functional significance (Szabadkai et al., 2006). However, we didn't investigate in details the fine molecular nature of these complexes, giving no information about the isoforms subtypes involved in this interaction. In the light of our next results, showing that the diverse VDACs differentially contribute to apoptosis while sharing the same Ca^{2+} channeling properties, we wonder whether the molecular basis of these differences could rely on the assembly of highly specialized proteins complexes. Indeed, the existence of a specialized macromolecular complex finely tuning the transfer of Ca^{2+} could account for the selective transmission of certain types of stimuli over others. The emerging picture on the role of mitochondrial Ca^{2+} in the induction of apoptosis shows that the rapid, prompt, large and highly

spatial defined Ca^{2+} increases in the matrix can mediate the stimulation of organellar metabolism; on the other hand, apoptotic stimuli such as C2-ceramide cause instead a more subtle, slower, smaller but sustained Ca^{2+} transfer from the ER to the mitochondria. In this view, during the massive release of the cation occurring when maximal agonist stimulation is imposed, the existence of discrete signaling units can be overwhelmed and masked by the robustness of the response; conversely, when the apoptotic stimuli mobilize small quantities of the cation the existence of fine and preferential routes mediating the direct transfer of Ca^{2+} from one organelle to the other could become relevant. To test this hypothesis we investigated whether the IP_3R is physically coupled to the mitochondrial Ca^{2+} channels in an isoform-specific fashion. We thus performed co-immunoprecipitation experiments using IP_3R type 3 (IP_3R-3) as bait, since the this particular isoform has been shown to be the preferential IP_3R subtype involved in the transmission of apoptotic stimuli (Mendes et al., 2005). We thus test what VDAC isoforms could co-immunoprecipitate with IP_3R-3. Strikingly, figure 13 shows that VDAC1 is the only isoform bound to the IP_3R in stringent conditions. The specificity of the immunoprecipitated complex was assessed by looking for both positive and negative: β-actin has never been shown to interact with ER Ca^{2+} releasing channels, and presumably isn't associated with them; hexokinase-I instead is a known interactor of VDAC1 (Pastorino and Hoek, 2008), but it is not directly associated with IP_3R, most likely making part of a different protein complex; finally, we used the above mentioned grp75 as positive control, since it is a key component of the signaling units responsible for the efficient transfer of Ca^{2+} from the endoplasmic reticulum to the mitochondria. Therefore, the experimental conditions used look strong enough to suggest a selective (or at least a preferential) coupling of IP_3R-3 with VDAC1, since neither VDAC2 or VDAC3 can be found in the co-immunoprecipitate. These results establish the molecular basis for the explanation of the different role of VDAC isoforms in the regulation of cell death, suggesting that VDAC1 exerts its pro-apoptotic activity by transmitting of Ca^{2+} signals from the endoplasmic reticulum to mitochondria through a specific and highly defined macromolecular complex.
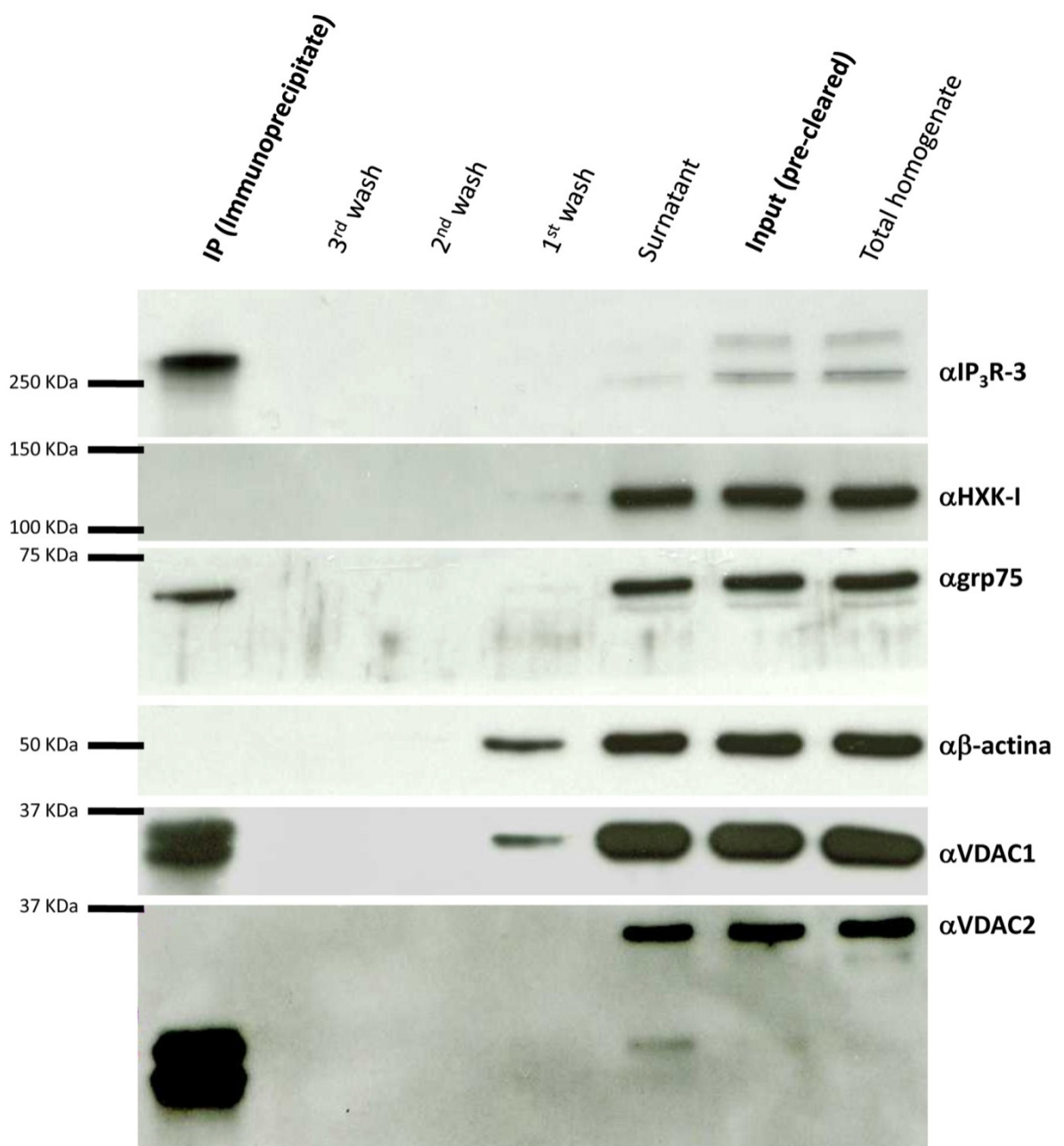
Figure 13 VDAC1 is selectively coupled to IP₃R-3. *IP₃R-3 was immunoprecipitated from total HeLa cells homogenate with an isoform-specific mouse monoclonal antibody. The pre-cleared proteins were incubated overnight with the antibody at 4°C and then incubated with protein G-coated sepharose beads. After 3 washes with RIPA buffer (150 mM NaCl, 1% NP-40, 0.1% SDS, 50 mM Tris, pH 8.0) the immunoprecipitate was collected and all fractions were immunoblotted. β-actin (not known to interact with IP₃Rs) and HXKI (which is bound to VDAC1 but likely making part of a different protein complex, thus further enforcing the specificity of the immunoprecipitated complex) have been used as negative controls. Grp75, a known IP₃R interactor have been used as positive control. In the co-immunoprecipitated fraction, VDAC1 is present in a large amount, while VDAC2 and VDAC3 (data not shown) cannot be revealed.*

VDAC isoforms in the control of autophagy

Data provided so far demonstrate that VDAC is something more than a simple channel, given that its functions isn't limited to the passive and unregulated transit of metabolites from the cytosol to the IMS, but rather it actively participates in the assembly of macromolecular complexes finely shaping cellular signals. However, the existence of different isoforms cannot be explained by simple redundancy, otherwise it would be almost impossible to conciliate the clearly demonstrated opposite roles that VDAC1 and VDAC2 exert on cell death. We thus gave the molecular details about the peculiar pro-apoptotic activity of VDAC1, showing that it is part of a specialized signaling unit that mediate the efficient transfer of Ca^{2+} ions from the ER to mitochondria. Still, these data cannot in any case explain why VDAC2 has a diametrically opposite effect, suggesting that this isoform is involved in other different cellular processes. We thus tried to investigate other potential pathways in which mitochondrial porins could be involved that could help us to explain their role in cell death regulation. One obvious candidate is autophagy, a cellular process deeply involved in cell sensitivity to several kind of stresses (Lum et al., 2005). Indeed, cells evolved a complex intracellular signaling network integrating multiple and occasionally conflicting signals to coordinate the response. The paucity of growth factors, nutrients or the presence of stress stimuli can ultimately result in cell death; however, the primary cellular reaction to these conditions is a survival effort through autophagy, the major cellular catabolic pathway dedicated to self-digestion and recycling of metabolites. Thus, during starvation stimulating macroautophagy provides the fuel required to maintain an active metabolism and the production of ATP. When stress conditions are resolved, or nutrients are restored, cells can revert to normal situation. Conversely, when normal homeostasis cannot be re-established the cell has no other possibility but to die through apoptosis (type I cell death) or the so-called autophagic cell death (type II cell death) (Kroemer et al., 2009). As a consequence, these two processes must be in some way coordinated to ensure the proper response to stress. Indeed, there is now mounting evidences that autophagy and apoptosis share several common regulatory elements (e.g. some Bcl-2 family proteins) (Codogno and Meijer, 2005;

Levine, 2005; Maiuri et al., 2007a; Pattingre and Levine, 2006; Pattingre et al., 2005). Hence, an apparent dysregulation of apoptosis could be, at least in principal, subsequent to an impairment in the regulation of autophagy. We thus wonder if the diverse effects of mitochondrial porins, and in particular VDAC2, in apoptosis could be a consequence of a differential regulation of the autophagic process.

Protein synthesis is a required component of growth and proliferation, and can consume a large amount of the total intracellular energy resources. The process must therefore be tightly regulated, and needs to integrate information from both nutrient abundance and growth factor signaling. This crucial function is carried out by the conserved protein Tor (and its orthologues mTOR in mammals and dTOR in *Drosophila melanogaster*), which functions downstream of PI$_3$K and Akt in growth factor signaling (Hay and Sonenberg, 2004; Sarbassov et al., 2005a). The presence of growth factors or of abundant intracellular amino acids leads to the activation of mTOR and phosphorylation of its targets, ribosomal protein S6 kinase (p70S6K) and the eukaryotic initiation factor 4E binding protein-1 (4EBP-1). Phosphorylation of these targets facilitates cap-dependent translation. mTOR is therefore a component of both growth factor signaling and nutrient-sensing pathways, and induces protein synthesis when metabolic conditions (amino acid availability) are favourable and/or when stimulated by growth factors. In parallel, active mTOR is the main cellular signal that inhibits autophagy; thus, inactivation of mTOR by the removal of growth factor stimulation decreases nutrient use and allows cells to engage the autophagic survival programme. Given its central role as the main cellular nutrient sensor and the relevance that mitochondria play in energy production, we investigated VDAC isoforms as potential modulators of mTOR activity.

VDAC2 is selectively required for mTOR dependent autophagy

In order to study the contribution of the three VDAC isoforms to autophagy, we took advantage of a widely used assay based on LC3-GFP in both resting condition and after autophagy

induction (Kimura et al., 2009). LC3, also known as Atg8, is an essential component of the autophagic machinery and it is recruited to early autophagosomes after lipid-conjugation. Thus, LC3 exists in two forms: LC3-I which is spread in the whole cellular cytoplasm, and LC3-II which strictly associates to autophagosomes. As a consequence, the LC3-GFP chimera reflects this peculiar localization: cells in resting conditions display a pancytoplasmic staining when visualized on a fluorescence microscope; conversely, upon autophagy induction the cytoplasmic stain almost disappears (or at least, decreases), and small, punctuated highly fluorescent structures (corresponding to autophagosomes) become evident. The percentage of cells showing a vacuolar-like distribution of LC3-GFP on the total fluorescent population is a reliable index of autophagy. In our experiments HEK293 cells were seeded onto 24mm glass coverslips and cotransfected with LC3-GFP and various vectors encoding for a specific siRNA against one of the VDAC isoforms (Control, siRNA-hVDAC1, siRNA-hVDAC2 and siRNA-hVDAC3); the percentage of cells with vacuolar LC3-GFP was calculated in resting condition and after autophagy induction. Three different stimuli were used: i) removal of growth factors through serum starvation, ii) rapamycin, the best known mTOR inhibitor and iii) lithium, which is reported to trigger autophagy through a yet unknown but mTOR-independent mechanism (Sarkar et al., 2005). Figure 14 shows that VDAC modulates both basal and induced autophagy in an isoform- and stimulus-dependent manner. Indeed, while VDAC3 knockdown doesn't modify in any way the autophagic process, VDAC1 and VDAC2 exert different effects. RNA interference against VDAC1 indeed shows basal levels of autophagy similar to control cells. After starvation or pharmacological induction, autophagy induction does not increase at the same extent than in controls. This lower capacity of siRNA-hVDAC1 transfected cells to trigger autophagy is however only apparent. We indeed further investigate this phenomenon by performing a time lapse analysis of autophagy induction kinetics by calculating the percentage of autophagic cells at different moments after autophagy induction. Hence, we saw that VDAC1 knockdown cells are perfectly capable to trigger the formation of new autophagosomes but with a much more rapid kinetics, with a significantly higher levels of

autophagic cells after shorter pharmacological treatment (data not shown). Considering that the LC3-GFP is an appropriate marker only of early autophagosomes (because fluorescence disappears during the maturation of the vesicles), the apparent lower levels of autophagic cells after starvation is only a consequence of an higher turnover of these cellular structure. In any case, the most striking effect is caused by the knockdown of VDAC2: these cells show an impressive low level of autophagy not only in resting conditions, but also after serum deprivation or rapamycin treatment.
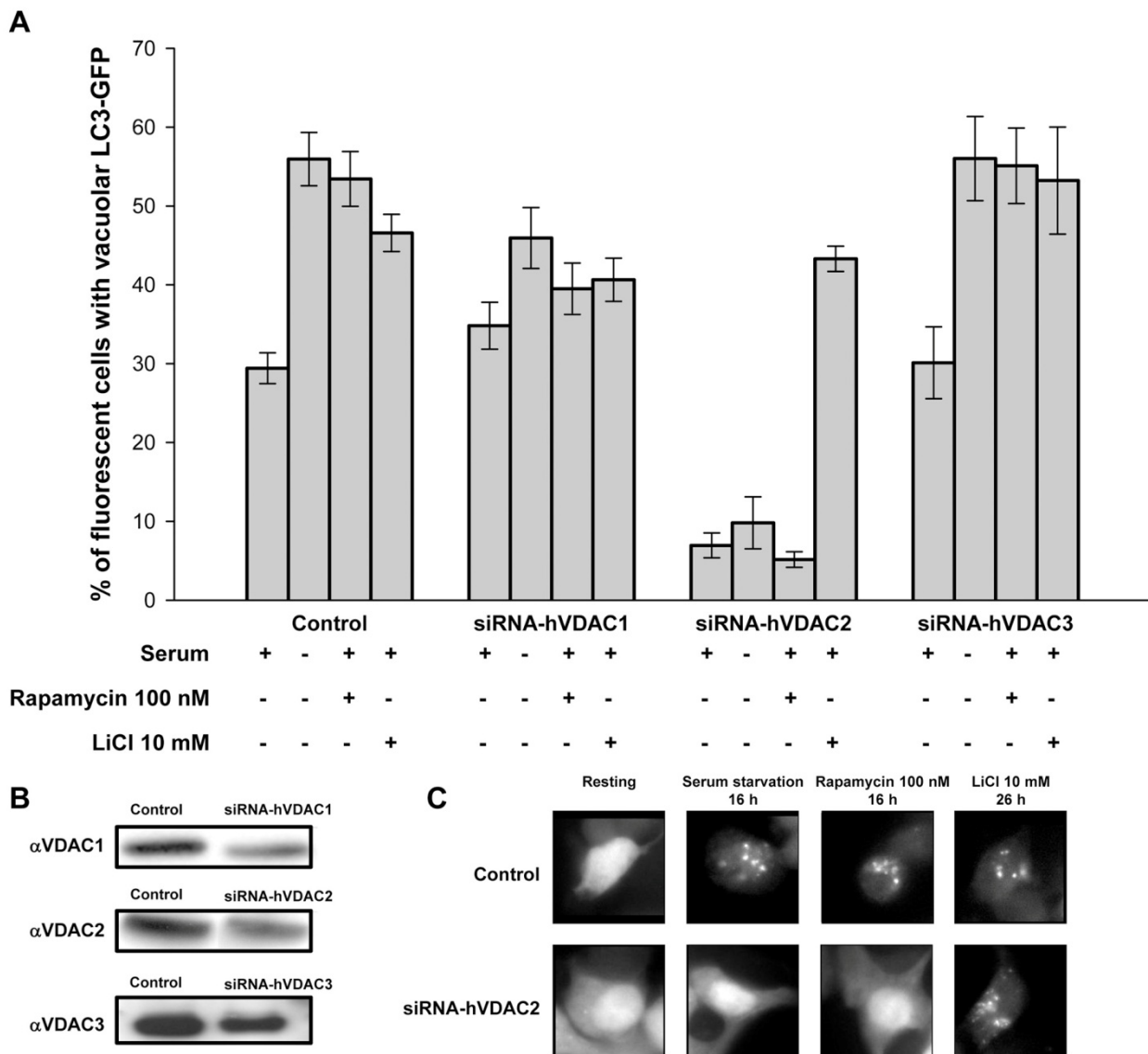

Figure 14 VDAC2 is selectively required for autophagy. *(A) HEK293 cells were cotransfected with plasmids encoding for control, hVDAC1, hVDAC2 or hVDAC3 specific interfering sequences respectively together with LC3-GFP encoding plasmid. The knockdown efficiency has been tested by Western blot as shown in panel B. Cells were then serum starved for 16 h, treated with rapamycin 100 nM for 16 h or LiCl 10 mM for 26 h were indicated. (C) Representative fluorescence images of LC3-GFP in control and siRNA-hVDAC2 transfected cells subjected to the indicated treatment: no gross alteration in cell morphology or autophagic vacuoles can be seen. Data are presented as means ± S.E.M..*

Lithium can instead trigger significant autophagy (similar to control cells) indicating that VDAC2-silenced cells are still autophagy-competent. These data suggest that VDAC2 is an important regulator rather than an essential component of the autophagic machinery. Moreover, VDAC2 seems to be selectively engaged in signaling pathways involving mTOR (such as serum deprivation or rapamycin treatment), being dispensable when other autophagy-inducing signals are activated (as evinced from lithium treatment). In order to further confirm autophagy inhibition in VDAC2 silenced cells, we performed another assay based on the protein degradation: indeed, autophagy (together with the ubiquitin-proteasome system) represents one of the main cellular mechanism for protein quality control and proteolysis. Therefore, monitoring the expression levels of long-living proteins (such as many membrane or organellar proteins) is an indicative index of ongoing autophagy (Kawai et al., 2006). We co-transfected HEK293 with a mitochondrial targeted GFP (mtGFP) with the different VDAC siRNA-encoding plasmids (Control, siRNA-hVDAC1 and siRNA-hVDAC2) and then evaluated mtGFP expression through Western blot before and after autophagy induction by rapamycin. As shown in figure 15, VDAC2 downregulation virtually blocks protein degradation via the lysosomal pathway, thus confirming the strong autophagy inhibition previously detected with the LC3-GFP assay.
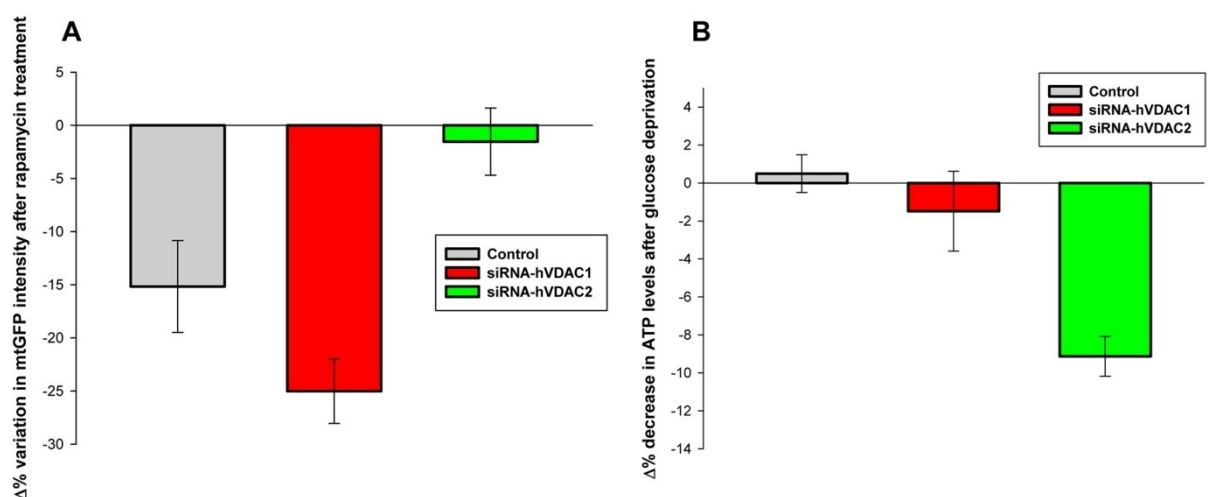

Figure 15 VDAC2 silencing selectively impairs autophagy. *(A) Variations of mtGFP expression levels in control, siRNA-hVDAC1 or siRNA-hVDAC2 transfected cells induced by rapamycin treatment (100 nM for 16 h). Total cell lysate from treated and non-treated cells was immunoblotted and the percentage difference in mtGFP intensity was calculated. (B) Intracellualr ATP decrease after glucose deprivation was monitored in living cells transfected with firely luciferase. Autophagy in control and siRNA-hVDAC1 cells guarantees substrates recycling when glucose is removed for short time periods (up to 10 minutes), while siRNA-hVDAC2 cells undergo to a drop of ATP levels due to the inhibition of autophagy.*

In addition, the VDAC1 silencing causes a slight increase in GFP degradation when compared to control (siRNA-hVDAC1 -25.02 ± 3.04% vs Control -15.16 ± 4.32%): considering that long-living protein degradation represents a late marker of the autophagic process, this data support the hypothesis of an higher turnover of autophagosomes mediated through a VDAC1 dependent mechanism. Finally, in order to test the functional significance of the autophagy regulation by mitochondrial porins we measured intracellular changes in ATP levels under nutrient deprivation in living cells through the firefly luciferase assay (Tasdemir et al., 2008). In resting conditions, cellular ATP production is sustained mainly by glycolysis and mitochondrial respiratory chain through glucose catabolism. However, autophagy allows cells to maintain high ATP levels under conditions of starvation: indeed, in our control cells basal autophagy is sufficient to maintain the normal energy balance even when glucose is removed from the media at least for short periods (e.g. 10 minutes). The same phenomenon can be seen in siRNA-hVDAC1 transfected cells but not in cells where VDAC2 is downregulated, where a significant drop is ATP levels occurs upon glucose withdrawal which can thus be correlated with the absence of autophagy (see figure 15).

Functional data presented so far suggest that VDAC2 can impair autophagy, and selectively mTOR signaling leading to this cellular self-digestion, since VDAC2 silencing inhibits rapamycin- but not lithium-induced formation of cytoplasmic vacuoles. We further confirm this hypothesis by directly measuring mTOR activity. This kinase exists in two main functional units: i) the so-called TORC1 (TOR Complex 1) where mTOR is directly bound to its partner Raptor and positively regulates both translation (by phosphorylating the p70 Ribosomal S6 Kinase, p70S6K) and transcription (through phosphorylation and consequent inactivation of the eukaryotic initiation factor 4E-binding protein 1, 4EBP-1); and ii) the newly identified TORC2 (TOR Complex 2) where mTOR interacts with Rictor and promotes cytoskeletal rearrangements and activates survival pathways by phosphorylating the Akt kinase. Thus, the mTOR activity can be easily monitored by revealing the phosphorylation state of its substrates (p70S6K or 4EBP-1 for complex 1 and Akt for complex 2) through Western blot. Total homogenate where then extracted from cells with normal

(Control) or low (siRNA-hVDAC2) expression levels of VDAC2 under various stimuli and immunoblotted with a phosphorylation-specific antibody. As shown in figure 16, the downregulation of VDAC2 causes an hyper activation of mTORC1 and mTORC2 at resting conditions. Activity of TORC1 is blocked after serum deprivation in control but not in siRNA-hVDAC2 cells (thus correlating with its activity in autophagy regulation), while, as expected, lithium does not cause any variation in its activity. Unfortunately, rapamycin completely blocked p70S6K phosphorylation in both control and VDAC2 silenced cells (that show in turn low levels of autophagy), thus suggesting that the p70S6K pathway is not directly connected with autophagy regulation, or at least that this two pathways can be pharmacologically impaired. Concerning the activity of TORC2, Akt shows a higher degree of phosphorylation in VDAC2-silenced cells in all conditions tested when compared to controls, except for the serum starvation which causes a situation undistinguishable from controls: even for TORC2 activity a strong correlation between its target's phosphorylation and autophagy levels cannot be assessed.
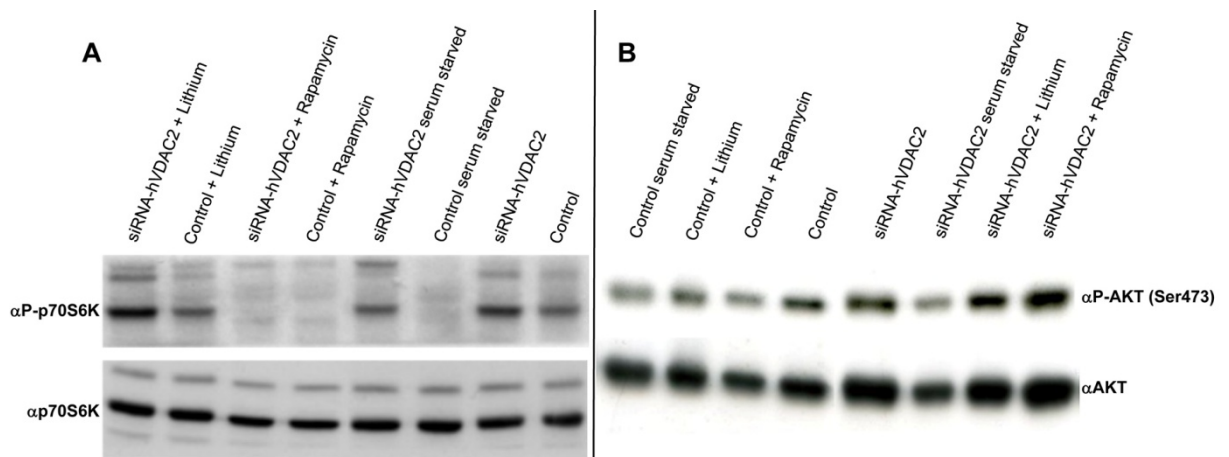
Figure 16 VDAC2 impairs mTOR activity. *(A) Effects of serum starvation (16 h), rapamycin (100 nM for 16 h) and LiCl (10 mM for 26 h) on control and siRNA-hVDAC2 transfected cells. Total homogenate was immunoblotted against phospho-specific (Thr389) or total p70S6K, reflecting the activity of TORC1. (B) The same cellular extracts as in (A) were probed for phospho-specific (Ser473) or total AKT.*

VDAC2 controls mTOR association to mitochondria

Data presented so far strongly argue for a mitochondria dependent regulation of mTOR activity. Despite the huge amount of work carried out on this protein, its relationship with this

organelle is poorly described (Desai et al., 2002; Schieke et al., 2006). Starting from our functional analysis on the role of various VDAC isoforms in controlling mTOR activity we started a biochemical study to understand the molecular foundations of this phenomenon. Initially we checked whether the VDAC2 regulation of mTOR was dependent on a specific protein-protein interaction (similar to what we have previously seen for VDAC1 coupling to IP$_3$Rs). For this purpose, we immunoprecipitated mTOR from HEK293 total cell lysate and looked if the different VDAC isoforms could co-immunoprecipitate with it. Strikingly, we found that only VDAC2 can selectively interact with mTOR. To further confirm the specificity of the assay, we transfected our
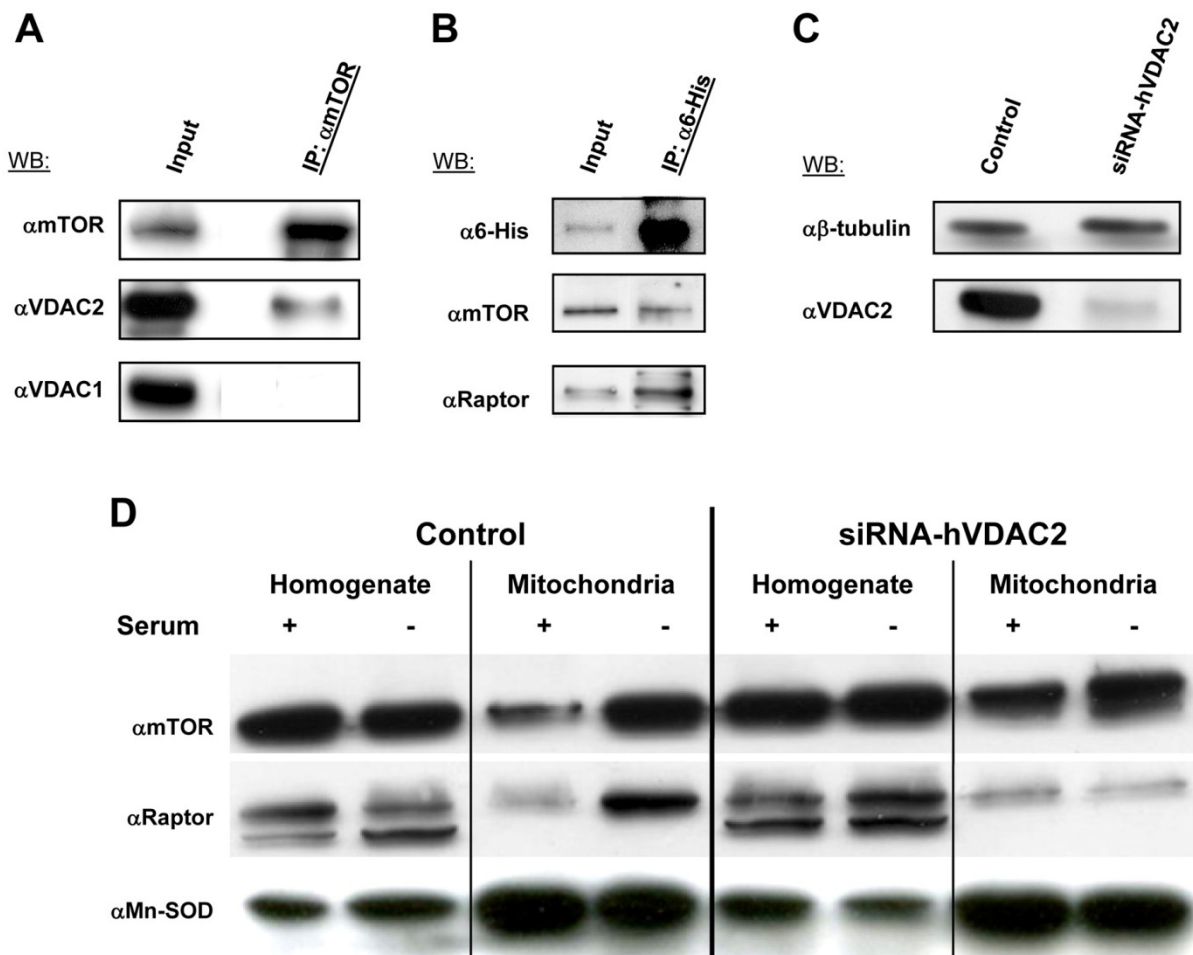
Figure 17 VDAC2 selectively interacts with mTOR and controls its association to mitochondria. (A,B) Characterization of mTOR/VDAC2 interaction through immunoprecipitation studies using mTOR (A) or VDAC2-6His (B) as bait. VDAC2 selectively interacts with mTOR and its associated protein Raptor. (C) Analysis of VDAC2 expression levels in Control and siRNA-hVDAC2 clones. (D) mTOR/Raptor association to mitochondria in Control and siRNA-hVDAC2 clones in resting conditions and after serum deprivation. mTOR/Raptor translocate to mitochondria after serum withdrawal (16h) in control cells, while in VDAC2 deficient cells the mitochondria associated mTOR quantity is significant higher than in controls in resting conditions.

cells with a 6-histidine tagged VDAC2 (see above) and used an anti 6His antibody to immunoprecipitate the exogenously expressed chimera. Again, in the co-immunoprecipitated we were able to find mTOR and proteins associated within its signaling unit such as Raptor (figure 17A,B).

A corollary of this interaction must be at least a partial localization of mTOR and its partners at mitochondria. To test this possibility we performed cellular subfractionation experiments to isolate the mitochondrial fraction. We firstly generated a stable HEK293 clone where VDAC2 levels were downregulated through RNA interference (figure 17C) and their respective controls. We then loaded total homogentates and mitochondrial proteins obtained by differential centrifugation on SDS-PAGE and revealed the presence of mTOR and Raptor. Figure 17D shows that in resting conditions a small fraction of both mTOR and Raptor is associated to mitochondria in control cells. Strikingly, after serum removal the quantity of mTOR and Raptor remains equal in the whole cell lysate but strongly increases the quota allocated in the mitochondrial fraction (in control cells this event is accompanied by an increase in the number of autophagic cells). This data strongly suggest a mitochondrial translocation of mTOR upon stress conditions. Even more remarkably, in VDAC2 deficient cells, the mitochondria-associated mTOR quantity is curiously higher at resting condition when compared to control cells. In addition, serum starvation does not increase the already high organellar mTOR fraction. Unfortunately, these last data are difficult to conciliate with the effects we observed on autophagy. Hence, further studies will be necessary to better assess and clarify the significance of mTOR translocation to mitochondria.

Discussion

Chaperone mediated coupling of endoplasmic reticulum and mitochondrial Ca^{2+} channels. Based on previous observations (Csordas et al., 2002; Gincel et al., 2001; Rapizzi et al., 2002b; Zaid et al., 2005), we used VDAC1 as the start point for proteomic search of interacting proteins and for unraveling the molecular basis of mitochondrial Ca^{2+} homeostasis. An unexpected, but intriguing, finding of our biochemical studies was the central location of the chaperone grp75 in the interaction between ER and mitochondrial Ca^{2+} channels. grp75, a conserved chaperone, has a well studied role in protein import through the IMM. Still, in yeast mitochondria, mtHsp70/Ssc1 was shown to be significantly more abundant than the translocase (TIM23 complex). Thus, only a small fraction of the protein appears to be involved directly in preprotein translocation (Dekker et al., 1997; Sanjuan Szklarz et al., 2005), suggesting the existence of different pools of the protein. Previous work also reported extramitochondrial localization of grp75 (Ran et al., 2000), and its interaction with extramitochondrial proteins such as the cytosolic p53 or the ER luminal grp94 (Takano et al., 2001; Wadhwa et al., 2002b), although the mechanisms that control the differential sorting of the protein are still completely unknown. According to our immunofluorescence and GFP-tagging studies in HeLa cells grp75 shows complete mitochondrial localization, but obviously cannot be discriminated from an OMM-associated pool. Biochemical studies, however, demonstrate that a matrix-localized pool participates in forming complexes in the 200–400-kDa range and represents the major fraction of the total mitochondrial grp75 content, whereas a minor grp75 pool resides in the low-density (MAM) mitochondrial fraction, participating in complexes in the megaDalton range and comprising OMM and ER membrane proteins. To further support an independent function of the nonmatrix pool, we constructed a grp75 mutant lacking the mitochondrial presequence, and thus incompetent for import in the matrix. This protein retained the

capacity to enhance mitochondrial Ca^{2+} accumulation, strongly arguing for the notion that this role of grp75 is not only independent from its chaperone activity in the matrix but also depends on a physically separated protein pool.

How is the newly identified regulatory activity on mitochondrial Ca^{2+} uptake exerted? In principle, two different mechanisms can be envisioned. In the first, grp75 could be involved in scaffolding the ER–mitochondria contacts, and thus determines the number of sites in which mitochondria are exposed to the high $[Ca^{2+}]$ microdomains generated at the mouth of IP_3Rs. Fluorescent labeling studies of the ER and mitochondria revealed a partial (5–20%) colocalization, reflecting these interactions. However, no increase in colocalization has been observed by overexpression of grp75 (or of the IP_3R-$LBD_{224-605}$; unpublished data), suggesting that they do not directly function as structural determinants of the contacts. In a second scenario, grp75 could control the interaction of ER and mitochondrial proteins at the existing organelle contacts, and thus allow crosstalk between signaling partners, e.g., the ion channels of the two membranes. Indeed, grp75, as shown by its knockdown and overexpression models, was necessary and sufficient for the stimulatory effect of the IP_3R-$LBD_{224-605}$ on mitochondrial Ca^{2+} uptake. Moreover, the proteomic data also highlight the central role of grp75 in this interaction. VDAC and IP_3Rs coprecipitate with grp75, and the chaperone is coimmunoprecipitated by both anti-IP_3R and -VDAC antibodies, indicating that it is the key assembling molecule in the loose interaction between the two ion channels.

Within the IP_3R–grp75–VDAC complex, potentiation of mitochondrial Ca^{2+} accumulation by the IP_3R-$LBD_{224-605}$ does not require IP_3 binding, as demonstrated by the fact that it is retained by the K508A mutant, which is unable to bind IP_3 (Varnai et al., 2005). Although the mutant shows the same stimulatory effect (Fig. 2), one should remember that wild-type IP_3R-$LBD_{224-605}$, because of IP_3 buffering, reduces ER Ca^{2+} release, and thus conclude that the wild type is somewhat more effective than the mutant. To further confirm independence from IP_3 buffering, we measured

mitochondrial Ca^{2+} uptake after capacitative influx through the plasma membrane (Figs. 4 and 6). Also, under those experimental conditions, the $IP_3R\text{-}LBD_{224\text{-}605}$ potently stimulated mitochondrial Ca^{2+} uptake.

As for the molecular mechanism of the effect on the mitochondrial Ca^{2+} machinery, different scenarios could be envisioned. In the first, the recombinantly expressed $IP_3R\text{-}LBD$, both from the OMM and ER side, could interact with the endogenous IP_3R itself, and modify the probability of its interaction with grp75/VDAC. Indeed, it was previously shown that intramolecular interactions between different domains of the IP_3R, such as the 224–605 minimal IP_3-binding domain and the 1–223 N-terminal repression domain, regulate IP_3R channel opening upon IP_3 binding. Thus, one could hypothesize that the high expression levels of $IP_3R\text{-}LBD_{224\text{-}605}$ represses an interaction between the extreme N-terminal of the endogenous receptor and grp75/VDAC. To clarify this issue, we expressed the whole (aa 1–604) $IP_3R\text{-}LBD$, which is targeted to the OMM. The $IP_3RLBD_{1\text{-}604}$ had the same effect as $IP_3R\text{-}LBD_{224\text{-}605}$, thus, excluding competition of these two cytoplasmic, N-terminal domains of the IP_3R. In the second, simpler scenario, the $IP_3R\text{-}LBD_{224\text{-}605}$ mimics the effect of the endogenous IP_3R. Thus, it directly enhances mitochondrial Ca^{2+} uptake by maximizing, within the macromolecular complex, the interaction with the mitochondrial VDAC channel. Indeed, the density of the exogenous $IP_3R\text{-}LBD_{224\text{-}605}$, based on fluorescence labeling (Varnai et al., 2005) and Scatchard plot analysis of IP_3 binding (Wibo and Godfraind, 1994), can be assumed to be at least one order of magnitude higher than the endogenous receptor, and indeed, high expression levels were necessary for the effect of IP_3R on mitochondrial Ca^{2+} uptake.

The central role of grp75 in the $IP_3R\text{-}LBD$-induced augmentation of Ca^{2+} uptake was clearly shown by the siRNA driven silencing of the protein, leading to the abolition of the effect. Conversely, high-level expression of grp75 induced a compound effect involving at least three different locations, as follows: i) the ER, decreasing the steady $[Ca^{2+}]_{er}$ level; ii) the OMM, interacting with VDAC, whose permeability/ion selectivity was shown to be modified by grp-75

binding (Schwarzer et al., 2002); and iii) the mitochondrial matrix, modifying mitochondrial parameters, such as pH or Ca^{2+} buffering capacity. Expression of the cytosolic grp75 and measurement of Ca^{2+} influx–induced mitochondrial Ca^{2+} uptake allowed us to eliminate the intramitochondrial effect and changes of ER Ca^{2+} handling. Importantly, mitochondrial Ca^{2+} uptake in this approach was markedly increased, and grp75cyt potentiated the effect of OMM-IP$_3$R-LBD, clarifying the effect of the OMM-associated pool of grp75.

In conclusion, we demonstrated that the IP$_3$R is part of a signaling complex that directly controls Ca^{2+} uptake into mitochondria. Much remains to be understood, but by these results the concept of macromolecular assembly of signaling elements, previously put forward for several plasma membrane channels, can be extended to defined microdomains at the ER-mitochondrial interface. Such an arrangement highlights novel routes for pharmacological intervention that may be used for the modulation of downstream events such as metabolism and apoptosis.

Effect of different VDAC isoforms on mitochondrial Ca^{2+} homeostasis. We thus go deeply in the understanding of the macromolecular complexes located at the ER/mitochondria contact sites. VDAC exists in three distinct isoforms showing similar electro-physiological properties according to several studies carried out in isolated mitochondria. In addition, every mammalian isoforms can, in vivo, restore the impaired growth capacities in yeasts lacking the endogenous VDAC gene. However, these kind of studies fail to precisely address the role of this protein in the complex context of the whole cell, thus underscoring other potential functions. Several observations support the notion that VDAC can finely tune diverse cellular processes in an isoform-specific way: i) selective genetic ablation of the three genes encoding for VDAC cause a diverse phenotype depending on both the isoforms and the genetic context (Graham and Craigen, 2004); ii) VDAC1 and VDAC2 exert diametrically opposite effects on apoptosis (Cheng et al., 2003; Rapizzi et al., 2002b); iii) transcriptional programs controlling the mitochondrial proteome, such as the one triggered by PGC1-α, differentially regulate porins expression in an isoform-specific fashion

(unpublished observation); iv) VDAC1 is selectively upregulated at transcriptional level after some apoptotic stimuli and v) the new anticancer compound erastin, which is selectively active against tumor harboring RAS mutations, has been proposed to act through VDAC2-specific mechanism (Yagoda et al., 2007). We thus started an investigation about the molecular mechanism underlying the diverse role of VDAC1 and VDAC2 in apoptosis. The first, obvious explanation of this diversity can rely on different Ca^{2+} channeling capacities: indeed, given the central role Ca^{2+} plays as sensitizing factor for the release of caspase activators, a differential contribution towards this cation transport (i.e. VDAC1 enhancing mitochondrial Ca^{2+} uptake while VDAC2 not) could account for their opposite effect on apoptosis. Still, such an explanation cannot in any case clarify the anti-apoptotic activity of VDAC2, unless postulating an inhibition of Ca^{2+} uptake of this particular isoforms (which is, based on electro-physiological characteristic, quite unlikely). We thus decided to study IP_3-dependent mitochondrial calcium uptake in living cells where the different isoforms were selectively overexpressed or silenced. Our results clearly shows that all VDAC isoforms share similar Ca^{2+} channeling properties, with some minor differences in the extent of the effect that cannot account for their differential cell death regulation. These minor differences (e.g. VDAC3 being the most effective in increasing Ca^{2+} responses, or VDAC2 knockdown being more effective in decreasing them when compared to VDAC1), could potentially be due to small variations in Ca^{2+} transport capacities. However, as in situ VDAC levels after overexpression or gene silencing are quite difficult to rigorously assess, any conclusion in this direction is at least hazardous. These data simply support the notion that all VDAC isoforms can similarly transport Ca^{2+} in living cells, and this is not correlated to their effect on apoptosis.

How to solve this discrepancy between mitochondrial Ca^{2+} transport and apoptosis regulation? The spontaneous, obvious conclusion is the denial (or, at least the reconsideration) of the classic paradigm linking mitochondrial Ca^{2+} and apoptosis. However, the number of works showing that conditions that enhance (directly or indirectly) mitochondrial Ca^{2+} uptake also

sensitize cells towards cell death is decisively relevant and we are still collecting reports supporting this hypothesis. Moreover, Ca^{2+} in mitochondria represents an intrinsically pleiotropic signal, since the final outcome varies widely depending on the nature of the stimulus and other concomitant signaling pathways. Thus, the transmission and the decoding of cell death signals must be finely regulated in order to trigger the suitable effect. Experimental evidences show that while physiological stimuli regulating normal cellular metabolism causes a massive release of Ca^{2+} from the internal stores, and consequently origins a rapid mitochondrial Ca^{2+} uptake, cell death signals has been shown to induce only a modest (even if sustained) increase in $[Ca^{2+}]$ inside mitochondria. This latter event has been proposed to represent a sort of priming signal that conditions and sensitizes mitochondria to otherwise non-lethal stimuli. In this view, the local coupling between ER and mitochondrial Ca^{2+} channels becomes critically relevant: small Ca^{2+} microdomains elicited by apoptotic stimuli such as C2-ceramide strongly relies on the existence of a preferential route transmitting the signal from the ER to the mitochondrion; on the other side, during physiological signals large $[Ca^{2+}]$ microdomains are generated and the fine channels coupling could be potentially overwhelmed by the vigorous ER Ca^{2+} release. The notion that the accurate discrimination of Ca^{2+} signals mediating diverse effects relies on highly specialized molecular determinants is supported by the observation that the selective knockdown of IP_3R-3 impairs cell death signals transmission while the silencing of the other two isoforms has almost no effect. Based on these observations we thus wonder whether a similar selectivity could exist at mitochondrial level, or, more precisely at ER/mitochondria contact sites. Strikingly, our co-immunoprecipitation studies show that IP_3R-3 selectively (or at least preferably) interacts with VDAC1, while VDAC2 or VDAC3 cannot be revealed in the same experimental conditions. Thus, data presented so far not only give fine details about the complex molecular insights underpinning VDAC Ca^{2+} channeling properties, but also suggest the possible molecular mechanism through which VDAC1 exerts its pro-apoptotic activity. We here propose a model where VDAC represents a fundamental player in mitochondria

physiology, with similar channeling properties shared among its different variants, but concurrently mediating diverse effects through isoform-specific protein-protein interactions and the assembly of highly specialized, higher order protein complexes: This view accounts for most of experimental data available and finally reconciles apparently contrasting evidences, shedding new light on mitochondrial regulation in cell life and death.

VDAC isoforms in the control of autophagy. While VDAC1 effect on apoptosis is a direct consequence of its channeling properties and its selective coupling to ER Ca^{2+} releasing sites, we did not provide any insights on the molecular mechanism underlying the protective activity on cell death exerted by VDAC2. One mechanism has already been proposed, where VDAC2 selectively interacts with the pro-apoptotic Bcl-2 family member Bak and has a critical role in keeping Bak in its monomeric, inactive conformation in viable cells. However, this notion has been recently questioned by the demonstration that both wild-type and VDAC-deficient mitochondria and cells exhibited equivalent cytochrome *c* release, caspase cleavage and cell death in response to the pro-death Bcl-2 family members Bax and Bid (Baines et al., 2007). Moreover we also observed that VDAC2 effect on apoptosis are still visible in Bax/Bak double knockout fibroblasts, suggesting a VDAC2 involvement in some other cellular pathway controlling cellular sensitivity to apoptosis. One obvious candidate is autophagy, considering that autophagy is the primary response to several patho-physiological stimuli and some of the well known apoptotic agents (including C2-ceramide and oxidative stress) have been reported to trigger autophagy before leading to cell death (Chen and Gibson, 2008; Guenther et al., 2008; Moore, 2008; Peralta and Edinger, 2009). In this view, differences in cell death sensitivity could be due, at least in principle, to an impairment in the primary survival cellular effort, i.e. cells where autophagy is inhibited can show an apparent increased sensitivity to several stimuli due to the impossibility to attempt the survival. In addition, considering that the role of mitochondria in this cellular process is abundantly underestimated, we tested the contribution of mitochondrial porins in the control of autophagy. We have thus drawn a

picture where the different VDAC isoforms exert diverse effects on this event, with VDAC3 that demonstrated to be dispensable while VDAC1 and VDAC2 both showed important regulatory functions. In particular, VDAC1-silenced cells seem to have a higher turnover in the formation of autophagic vesicles, apparently due to an increased "on" rate as can be evinced by the faster appearance of autophagosomes and the concomitant increase in long-living proteins degradation (figure 14, 15A and data not shown). However, this observed effect is unlike to place VDAC1 in a signaling pathway directly modulating autophagy, considering that every stimulus used has lead to the same result. Most likely, this outcome could be ascribed to a more general effect, e.g. some aspecific metabolic consequence. The most striking data remains the impressive effect of VDAC2 downregulation, that virtually abolishes autophagy at both basal levels and after the activation of signaling pathway involving mTOR. In particular, serum deprivation and rapamycin treatment do not increase at any extent the number of autophagic cells, while lithium restores the cytoplasmic vacuolarization as observed in control cells, thus suggesting an almost complete inhibition of mTOR signaling that controls autophagy (figure 14 and 15). However, the examination of mTOR activity, through the measurements of its classical substrates (p70S6K or Akt), didn't lead to any conclusive clarification of this phenomenon, since VDAC2 knockdown cells show no p70S6K phosphorylation while still having autophagy inhibited (see figure 16). However, the pharmacological treatment with rapamycin could potentially lead to some misleading artifacts. Due to its not complete inhibition of TORC1 signaling: indeed, despite the connections of TORC1 to the translational machinery, the effects of rapamycin on mammalian cell growth and proliferation are, oddly, less severe than its effects in yeast. In *Saccharomyces cervisiae*, rapamycin treatment induces a starvation-like state that includes a severe G1/S cell cycle arrest and suppression of translation initiation to levels below 20% of non-treated cells (Barbet et al., 1996). Moreover, in yeast rapamycin strongly promotes induction of autophagy (self-eating), a process by which cells consume cytoplasmic proteins, ribosomes and organelles, such as mitochondria, to maintain a

sufficient supply of amino acids and other nutrients (Noda and Ohsumi, 1998). The effects of rapamycin in mammalian cells are similar to those in yeast, but typically much less dramatic and highly dependent on cell type. For instance, rapamycin only causes cell cycle arrest in a limited number of cell types and has modest effects on protein synthesis (Neshat et al., 2001; Pedersen et al., 1997; Shor et al., 2008). Moreover, rapamycin is a relatively poor inducer of autophagy in many cells, and is often used in combination with LY294002, an inhibitor of PI3K and mTOR (Takeuchi et al., 2005). These inconsistent effects may also explain why, despite high expectations, rapamycin has had only limited success as a clinical anti-cancer therapeutic.

VDAC2-dependent regulation of mTOR is likely to require its association with mitochondria. We thus start a biochemical work to find out the molecular mechanism underlying mitochondrial control of mTOR signaling. First we demonstrated a novel and unexpected physical interaction between these two proteins (see figure 17A,B). These data demonstrate that VDAC2 can form higher order macromolecular complexes with mTOR, Raptor and other protein of the TORC1 signaling unit (such as GβL), very similarly to what VDAC1 can do with Ca^{2+} channels. Moreover, we demonstrated through subcellular fractionation, that a small amount of mTOR is associated to mitochondria at resting conditions, and that this quota significantly increases upon autophagy induction, thus suggesting that mTOR mitochondrial translocation is necessary for its inhibition. However, the same experiment carried out in VDAC2 silenced cells strongly argues against this simple mechanism, showing that consistent amount of mTOR are present at mitochondrial levels even at basal conditions (as well as after growth factors withdrawal), when autophagy is virtually absent and mTOR is hyper-activated (figure 17). A possible explanation could rely on the fact the in VDAC2-knockdown cells, the upstream signaling pathway recruiting mTOR at mitochondrial level is still functioning, demonstrating that VDAC2 is not the mitochondrial anchor for mTOR; however, VDAC2 seems to be somewhat necessary for the downstream signaling events and thus

94

its absence keeps mTOR entrapped (and active) at organelle level. However, other experimental work will be necessary to support this hypothesis.

In conclusion this work present some novel and unexpected findings about VDAC: indeed, we suggest that the complexity of the roles exerted through these channel probably relies on isoform-specific protein-protein interactions and on the assembly of highly specialized macromolecular complexes mediating a surprising array of different functions.

References

Abu-Hamad, S., Sivan, S., and Shoshan-Barmatz, V. (2006). The expression level of the voltage-dependent anion channel controls life and death of the cell. Proc Natl Acad Sci U S A *103*, 5787-5792.

Allbritton, N.L., and Meyer, T. (1993). Localized calcium spikes and propagating calcium waves. Cell Calcium *14*, 691-697.

Alonso, M.T., Barrero, M.J., Carnicero, E., Montero, M., Garcia-Sancho, J., and Alvarez, J. (1998). Functional measurements of [Ca2+] in the endoplasmic reticulum using a herpes virus to deliver targeted aequorin. Cell Calcium *24*, 87-96.

Arsham, A.M., and Neufeld, T.P. (2006). Thinking globally and acting locally with TOR. Curr Opin Cell Biol *18*, 589-597.

Bagni, C., Mannucci, L., Dotti, C.G., and Amaldi, F. (2000). Chemical stimulation of synaptosomes modulates alpha -Ca2+/calmodulin-dependent protein kinase II mRNA association to polysomes. J Neurosci *20*, RC76.

Baines, C.P., Kaiser, R.A., Sheiko, T., Craigen, W.J., and Molkentin, J.D. (2007). Voltage-dependent anion channels are dispensable for mitochondrial-dependent cell death. NatCell Biol *9*, 550-555.

Barbet, N.C., Schneider, U., Helliwell, S.B., Stansfield, I., Tuite, M.F., and Hall, M.N. (1996). TOR controls translation initiation and early G1 progression in yeast. Mol Biol Cell *7*, 25-42.

Basso, E., Fante, L., Fowlkes, J., Petronilli, V., Forte, M.A., and Bernardi, P. (2005a). Properties of the permeability transition pore in mitochondria devoid of Cyclophilin D. J Biol Chem *280*, 18558-18561.

Basso, E., Fante, L., Fowlkes, J., Petronilli, V., Forte, M.A., and Bernardi, P. (2005b). Properties of the permeability transition pore in mitochondria devoid of Cyclophilin D. JBiolChem *280*, 18558-18561.

Bayrhuber, M., Meins, T., Habeck, M., Becker, S., Giller, K., Villinger, S., Vonrhein, C., Griesinger, C., Zweckstetter, M., and Zeth, K. (2008). Structure of the human voltage-dependent anion channel. Proc Natl Acad Sci U S A *105*, 15370-15375.

Baysal, K., Jung, D.W., Gunter, K.K., Gunter, T.E., and Brierley, G.P. (1994). Na(+)-dependent Ca2+ efflux mechanism of heart mitochondria is not a passive Ca2+/2Na+ exchanger. Am J Physiol *266*, C800-808.

Bellot, G., Cartron, P.F., Er, E., Oliver, L., Juin, P., Armstrong, L.C., Bornstein, P., Mihara, K., Manon, S., and Vallette, F.M. (2007). TOM22, a core component of the mitochondria outer membrane protein translocation pore, is a mitochondrial receptor for the proapoptotic protein Bax. Cell Death Differ *14*, 785-794.

Berridge, M.J., Bootman, M.D., and Roderick, H.L. (2003). Calcium signalling: dynamics, homeostasis and remodelling. Nat Rev Mol Cell Biol *4*, 517-529.

Berry, D.L., and Baehrecke, E.H. (2007). Growth arrest and autophagy are required for salivary gland cell degradation in Drosophila. Cell *131*, 1137-1148.

Bertolino, M., and Llinas, R.R. (1992). The central role of voltage-activated and receptor-operated calcium channels in neuronal cells. Annu Rev Pharmacol Toxicol *32*, 399-421.

Bezprozvanny, I., and Ehrlich, B.E. (1993). ATP modulates the function of inositol 1,4,5-trisphosphate-gated channels at two sites. Neuron *10*, 1175-1184.

Bhaskar, P.T., and Hay, N. (2007). The two TORCs and Akt. Dev Cell *12*, 487-502.

Blommaart, E.F., Luiken, J.J., Blommaart, P.J., van Woerkom, G.M., and Meijer, A.J. (1995). Phosphorylation of ribosomal protein S6 is inhibitory for autophagy in isolated rat hepatocytes. J Biol Chem *270*, 2320-2326.

Boitier, E., Rea, R., and Duchen, M.R. (1999). Mitochondria exert a negative feedback on the propagation of intracellular Ca2+ waves in rat cortical astrocytes. J Cell Biol *145*, 795-808.

Brookes, P.S., Parker, N., Buckingham, J.A., Vidal-Puig, A., Halestrap, A.P., Gunter, T.E., Nicholls, D.G., Bernardi, P., Lemasters, J.J., and Brand, M.D. (2008). UCPs--unlikely calcium porters. Nat Cell Biol *10*, 1235-1237; author reply 1237-1240.

Brough, D., Schell, M.J., and Irvine, R.F. (2005). Agonist-induced regulation of mitochondrial and endoplasmic reticulum motility. Biochem J *392*, 291-297.

Bugrim, A.E. (1999). Regulation of Ca2+ release by cAMP-dependent protein kinase. A mechanism for agonist-specific calcium signaling? Cell Calcium *25*, 219-226.

Bultynck, G., De Smet, P., Rossi, D., Callewaert, G., Missiaen, L., Sorrentino, V., De Smedt, H., and Parys, J.B. (2001). Characterization and mapping of the 12 kDa FK506-binding protein (FKBP12)-binding site on different isoforms of the ryanodine receptor and of the inositol 1,4,5-trisphosphate receptor. Biochem J *354*, 413-422.

Carrington, W.A., Lynch, R.M., Moore, E.D., Isenberg, G., Fogarty, K.E., and Fay, F.S. (1995). Superresolution three-dimensional images of fluorescence in cells with minimal light exposure. Science *268*, 1483-1487.

Chen, Y., and Gibson, S.B. (2008). Is mitochondrial generation of reactive oxygen species a trigger for autophagy? Autophagy *4*, 246-248.

Cheng, E.H., Sheiko, T.V., Fisher, J.K., Craigen, W.J., and Korsmeyer, S.J. (2003). VDAC2 inhibits BAK activation and mitochondrial apoptosis. Science *301*, 513-517.

Chiara, F., Castellaro, D., Marin, O., Petronilli, V., Brusilow, W.S., Juhaszova, M., Sollott, S.J., Forte, M., Bernardi, P., and Rasola, A. (2008). Hexokinase II detachment from mitochondria triggers apoptosis through the permeability transition pore independent of voltage-dependent anion channels. PLoS ONE *3*, e1852.

Codogno, P., and Meijer, A.J. (2005). Autophagy and signaling: their role in cell survival and cell death. Cell Death Differ *12 Suppl 2*, 1509-1518.

Colombini, M. (1979). A candidate for the permeability pathway of the outer mitochondrial membrane. Nature *279*, 643-645.

Colombini, M. (2004). VDAC: the channel at the interface between mitochondria and the cytosol. Mol Cell Biochem *256-257*, 107-115.

Cortese, J.D., Voglino, A.L., and Hackenbrock, C.R. (1992). The ionic strength of the intermembrane space of intact mitochondria is not affected by the pH or volume of the intermembrane space. Biochim Biophys Acta *1100*, 189-197.

Csermely, P. (2004). Strong links are important, but weak links stabilize them. Trends Biochem Sci *29*, 331-334.

Csordas, G., Madesh, M., Antonsson, B., and Hajnoczky, G. (2002). tcBid promotes Ca(2+) signal propagation to the mitochondria: control of Ca(2+) permeation through the outer mitochondrial membrane. EMBO J *21*, 2198-2206.

Csordas, G., Renken, C., Varnai, P., Walter, L., Weaver, D., Buttle, K.F., Balla, T., Mannella, C.A., and Hajnoczky, G. (2006). Structural and functional features and significance of the physical linkage between ER and mitochondria. J Cell Biol *174*, 915-921.

Csordas, G., Thomas, A.P., and Hajnoczky, G. (1999). Quasi-synaptic calcium signal transmission between endoplasmic reticulum and mitochondria. EMBO J *18*, 96-108.

Danial, N.N., Gramm, C.F., Scorrano, L., Zhang, C.Y., Krauss, S., Ranger, A.M., Datta, S.R., Greenberg, M.E., Licklider, L.J., Lowell, B.B.*, et al.* (2003). BAD and glucokinase reside in a mitochondrial complex that integrates glycolysis and apoptosis. Nature *424*, 952-956.

Darsow, T., Rieder, S.E., and Emr, S.D. (1997). A multispecificity syntaxin homologue, Vam3p, essential for autophagic and biosynthetic protein transport to the vacuole. J Cell Biol *138*, 517-529.

de Brito, O.M., and Scorrano, L. (2008). Mitofusin 2 tethers endoplasmic reticulum to mitochondria. Nature *456*, 605-610.

De Pinto, V., Tomasello, F., Messina, A., Guarino, F., Benz, R., La Mendola, D., Magri, A., Milardi, D., and Pappalardo, G. (2007). Determination of the conformation of the human VDAC1 N-terminal peptide, a protein moiety essential for the functional properties of the pore. Chembiochem *8*, 744-756.

Dekker, P.J., and Pfanner, N. (1997). Role of mitochondrial GrpE and phosphate in the ATPase cycle of matrix Hsp70. J Mol Biol *270*, 321-327.

Desai, B.N., Myers, B.R., and Schreiber, S.L. (2002). FKBP12-rapamycin-associated protein associates with mitochondria and senses osmotic stress via mitochondrial dysfunction. Proc Natl Acad Sci U S A *99*, 4319-4324.

Deter, R.L., and De Duve, C. (1967). Influence of glucagon, an inducer of cellular autophagy, on some physical properties of rat liver lysosomes. J Cell Biol *33*, 437-449.

Duchen, M.R. (2004). Roles of mitochondria in health and disease. Diabetes *53 Suppl 1*, S96-102.

Dyall, S.D., Brown, M.T., and Johnson, P.J. (2004). Ancient invasions: from endosymbionts to organelles. Science *304*, 253-257.

Ferri, K.F., and Kroemer, G. (2001). Organelle-specific initiation of cell death pathways. Nat Cell Biol *3*, E255-263.

Ferris, C.D., Huganir, R.L., Bredt, D.S., Cameron, A.M., and Snyder, S.H. (1991). Inositol trisphosphate receptor: phosphorylation by protein kinase C and calcium calmodulin-dependent protein kinases in reconstituted lipid vesicles. Proc Natl Acad Sci U S A *88*, 2232-2235.

Filippin, L., Magalhaes, P.J., Di Benedetto, G., Colella, M., and Pozzan, T. (2003). Stable interactions between mitochondria and endoplasmic reticulum allow rapid accumulation of calcium in a subpopulation of mitochondria. J Biol Chem *278*, 39224-39234.

Forte, M., and Bernardi, P. (2005). Genetic dissection of the permeability transition pore. J Bioenerg Biomembr *37*, 121-128.

Frey, T.G., Renken, C.W., and Perkins, G.A. (2002). Insight into mitochondrial structure and function from electron tomography. Biochim Biophys Acta *1555*, 196-203.

Funakoshi, T., Matsuura, A., Noda, T., and Ohsumi, Y. (1997). Analyses of APG13 gene involved in autophagy in yeast, Saccharomyces cerevisiae. Gene *192*, 207-213.

Furuichi, T., Kohda, K., Miyawaki, A., and Mikoshiba, K. (1994). Intracellular channels. Curr Opin Neurobiol *4*, 294-303.

Furuichi, T., Yoshikawa, S., Miyawaki, A., Wada, K., Maeda, N., and Mikoshiba, K. (1989). Primary structure and functional expression of the inositol 1,4,5-trisphosphate-binding protein P400. Nature *342*, 32-38.

Galluzzi, L., and Kroemer, G. (2007). Mitochondrial apoptosis without VDAC. Nat Cell Biol *9*, 487-489.

Gilabert, J.A., and Parekh, A.B. (2000). Respiring mitochondria determine the pattern of activation and inactivation of the store-operated Ca(2+) current I(CRAC). EMBO J *19*, 6401-6407.

Gincel, D., Zaid, H., and Shoshan-Barmatz, V. (2001). Calcium binding and translocation by the voltage-dependent anion channel: a possible regulatory mechanism in mitochondrial function. Biochem J *358*, 147-155.

Giorgi, C., Romagnoli, A., Pinton, P., and Rizzuto, R. (2008). Ca2+ signaling, mitochondria and cell death. Curr Mol Med *8*, 119-130.

Graham, B.H., and Craigen, W.J. (2004). Genetic approaches to analyzing mitochondrial outer membrane permeability. Curr Top Dev Biol *59*, 87-118.

Griffiths, E.J., Ocampo, C.J., Savage, J.S., Rutter, G.A., Hansford, R.G., Stern, M.D., and Silverman, H.S. (1998). Mitochondrial calcium transporting pathways during hypoxia and reoxygenation in single rat cardiomyocytes. Cardiovasc Res *39*, 423-433.

Guenther, G.G., Peralta, E.R., Rosales, K.R., Wong, S.Y., Siskind, L.J., and Edinger, A.L. (2008). Ceramide starves cells to death by downregulating nutrient transporter proteins. Proc Natl Acad Sci U S A *105*, 17402-17407.

Guertin, D.A., Stevens, D.M., Thoreen, C.C., Burds, A.A., Kalaany, N.Y., Moffat, J., Brown, M., Fitzgerald, K.J., and Sabatini, D.M. (2006). Ablation in mice of the mTORC components raptor, rictor, or mLST8 reveals that mTORC2 is required for signaling to Akt-FOXO and PKCalpha, but not S6K1. Dev Cell *11*, 859-871.

Gunter, T.E., Buntinas, L., Sparagna, G., Eliseev, R., and Gunter, K. (2000). Mitochondrial calcium transport: mechanisms and functions. Cell Calcium *28*, 285-296.

Gunter, T.E., Buntinas, L., Sparagna, G.C., and Gunter, K.K. (1998). The Ca2+ transport mechanisms of mitochondria and Ca2+ uptake from physiological-type Ca2+ transients. Biochim Biophys Acta *1366*, 5-15.

Gupta, S., and Knowlton, A.A. (2005). HSP60, Bax, apoptosis and the heart. J Cell Mol Med *9*, 51-58.

Gyuris, J., Golemis, E., Chertkov, H., and Brent, R. (1993). Cdi1, a human G1 and S phase protein phosphatase that associates with Cdk2. Cell *75*, 791-803.

Hajnoczky, G., Csordas, G., Madesh, M., and Pacher, P. (2000). The machinery of local Ca2+ signalling between sarco-endoplasmic reticulum and mitochondria. J Physiol *529 Pt 1*, 69-81.

Hajnoczky, G., Csordas, G., and Yi, M. (2002). Old players in a new role: mitochondria-associated membranes, VDAC, and ryanodine receptors as contributors to calcium signal propagation from endoplasmic reticulum to the mitochondria. Cell Calcium *32*, 363-377.

Hajnoczky, G., Hager, R., and Thomas, A.P. (1999). Mitochondria suppress local feedback activation of inositol 1,4, 5-trisphosphate receptors by Ca2+. J Biol Chem *274*, 14157-14162.

Hajnoczky, G., Robb-Gaspers, L.D., Seitz, M.B., and Thomas, A.P. (1995). Decoding of cytosolic calcium oscillations in the mitochondria. Cell *82*, 415-424.

Hansford, R.G. (1994). Physiological role of mitochondrial Ca2+ transport. J Bioenerg Biomembr *26*, 495-508.

Hara, K., Maruki, Y., Long, X., Yoshino, K., Oshiro, N., Hidayat, S., Tokunaga, C., Avruch, J., and Yonezawa, K. (2002). Raptor, a binding partner of target of rapamycin (TOR), mediates TOR action. Cell *110*, 177-189.

Hay, N., and Sonenberg, N. (2004). Upstream and downstream of mTOR. Genes Dev *18*, 1926-1945.

He, L., and Lemasters, J.J. (2003). Heat shock suppresses the permeability transition in rat liver mitochondria. J Biol Chem *278*, 16755-16760.

Hiller, S., Garces, R.G., Malia, T.J., Orekhov, V.Y., Colombini, M., and Wagner, G. (2008). Solution structure of the integral human membrane protein VDAC-1 in detergent micelles. Science *321*, 1206-1210.

Ichimura, Y., Kirisako, T., Takao, T., Satomi, Y., Shimonishi, Y., Ishihara, N., Mizushima, N., Tanida, I., Kominami, E., Ohsumi, M.*, et al.* (2000). A ubiquitin-like system mediates protein lipidation. Nature *408*, 488-492.

Iino, M. (1991). Effects of adenine nucleotides on inositol 1,4,5-trisphosphate-induced calcium release in vascular smooth muscle cells. J Gen Physiol *98*, 681-698.

Iino, M., and Endo, M. (1992). Calcium-dependent immediate feedback control of inositol 1,4,5-triphosphate-induced Ca2+ release. Nature *360*, 76-78.

Iwai, M., Michikawa, T., Bosanac, I., Ikura, M., and Mikoshiba, K. (2007). Molecular basis of the isoform-specific ligand-binding affinity of inositol 1,4,5-trisphosphate receptors. J Biol Chem *282*, 12755-12764.

Iwai, M., Tateishi, Y., Hattori, M., Mizutani, A., Nakamura, T., Futatsugi, A., Inoue, T., Furuichi, T., Michikawa, T., and Mikoshiba, K. (2005). Molecular cloning of mouse type 2 and type 3 inositol 1,4,5-trisphosphate receptors and identification of a novel type 2 receptor splice variant. J Biol Chem *280*, 10305-10317.

Jacinto, E., Facchinetti, V., Liu, D., Soto, N., Wei, S., Jung, S.Y., Huang, Q., Qin, J., and Su, B. (2006). SIN1/MIP1 maintains rictor-mTOR complex integrity and regulates Akt phosphorylation and substrate specificity. Cell *127*, 125-137.

Jacinto, E., Loewith, R., Schmidt, A., Lin, S., Ruegg, M.A., Hall, A., and Hall, M.N. (2004). Mammalian TOR complex 2 controls the actin cytoskeleton and is rapamycin insensitive. Nat Cell Biol *6*, 1122-1128.

Jayaraman, T., and Marks, A.R. (1997). T cells deficient in inositol 1,4,5-trisphosphate receptor are resistant to apoptosis. Mol Cell Biol *17*, 3005-3012.

Jayaraman, T., Ondrias, K., Ondriasova, E., and Marks, A.R. (1996). Regulation of the inositol 1,4,5-trisphosphate receptor by tyrosine phosphorylation. Science *272*, 1492-1494.

Jonas, E.A., Buchanan, J., and Kaczmarek, L.K. (1999). Prolonged activation of mitochondrial conductances during synaptic transmission. Science *286*, 1347-1350.

Jouaville, L.S., Pinton, P., Bastianutto, C., Rutter, G.A., and Rizzuto, R. (1999a). Regulation of mitochondrial ATP synthesis by calcium: evidence for a long-term metabolic priming. Proc Natl Acad Sci U S A *96*, 13807-13812.

Jouaville, L.S., Pinton, P., Bastianutto, C., Rutter, G.A., and Rizzuto, R. (1999b). Regulation of mitochondrial ATP synthesis by calcium: evidence for a long-term metabolic priming. ProcNatlAcadSciUSA *96*, 13807-13812.

Jung, D.W., Baysal, K., and Brierley, G.P. (1996). Properties of the Na(+)-Ca2+ antiport of heart mitochondria. Ann N Y Acad Sci *779*, 553-555.

Kamada, Y., Funakoshi, T., Shintani, T., Nagano, K., Ohsumi, M., and Ohsumi, Y. (2000). Tor-mediated induction of autophagy via an Apg1 protein kinase complex. J Cell Biol *150*, 1507-1513.

Kawai, A., Takano, S., Nakamura, N., and Ohkuma, S. (2006). Quantitative monitoring of autophagic degradation. Biochem Biophys Res Commun *351*, 71-77.

Khan, M.T., Wagner, L., 2nd, Yule, D.I., Bhanumathy, C., and Joseph, S.K. (2006). Akt kinase phosphorylation of inositol 1,4,5-trisphosphate receptors. J Biol Chem *281*, 3731-3737.

Kim, D.H., Sarbassov, D.D., Ali, S.M., King, J.E., Latek, R.R., Erdjument-Bromage, H., Tempst, P., and Sabatini, D.M. (2002). mTOR interacts with raptor to form a nutrient-sensitive complex that signals to the cell growth machinery. Cell *110*, 163-175.

Kim, D.H., Sarbassov, D.D., Ali, S.M., Latek, R.R., Guntur, K.V., Erdjument-Bromage, H., Tempst, P., and Sabatini, D.M. (2003). GbetaL, a positive regulator of the rapamycin-sensitive pathway required for the nutrient-sensitive interaction between raptor and mTOR. Mol Cell *11*, 895-904.

Kim, I., Rodriguez-Enriquez, S., and Lemasters, J.J. (2007). Selective degradation of mitochondria by mitophagy. Arch Biochem Biophys *462*, 245-253.

Kimura, S., Fujita, N., Noda, T., and Yoshimori, T. (2009). Monitoring autophagy in mammalian cultured cells through the dynamics of LC3. Methods Enzymol *452*, 1-12.

Klionsky, D.J., and Ohsumi, Y. (1999). Vacuolar import of proteins and organelles from the cytoplasm. Annu Rev Cell Dev Biol *15*, 1-32.

Kourtis, N., and Tavernarakis, N. (2009). Autophagy and cell death in model organisms. Cell Death Differ *16*, 21-30.

Krauskopf, A., Eriksson, O., Craigen, W.J., Forte, M.A., and Bernardi, P. (2006). Properties of the permeability transition in VDAC1(-/-) mitochondria. Biochim Biophys Acta *1757*, 590-595.

Krieger, C., and Duchen, M.R. (2002). Mitochondria, Ca2+ and neurodegenerative disease. Eur J Pharmacol *447*, 177-188.

Kroemer, G., Galluzzi, L., Vandenabeele, P., Abrams, J., Alnemri, E.S., Baehrecke, E.H., Blagosklonny, M.V., El-Deiry, W.S., Golstein, P., Green, D.R.*, et al.* (2009). Classification of cell death: recommendations of the Nomenclature Committee on Cell Death 2009. Cell Death Differ *16*, 3-11.

Kuma, A., Hatano, M., Matsui, M., Yamamoto, A., Nakaya, H., Yoshimori, T., Ohsumi, Y., Tokuhisa, T., and Mizushima, N. (2004). The role of autophagy during the early neonatal starvation period. Nature *432*, 1032-1036.

Landolfi, B., Curci, S., Debellis, L., Pozzan, T., and Hofer, A.M. (1998). Ca2+ homeostasis in the agonist-sensitive internal store: functional interactions between mitochondria and the ER measured In situ in intact cells. J Cell Biol *142*, 1235-1243.

Lasorsa, F.M., Pinton, P., Palmieri, L., Fiermonte, G., Rizzuto, R., and Palmieri, F. (2003). Recombinant expression of the Ca(2+)-sensitive aspartate/glutamate carrier increases mitochondrial ATP production in agonist-stimulated Chinese hamster ovary cells. J Biol Chem *278*, 38686-38692.

Lee, A.C., Xu, X., and Colombini, M. (1996). The role of pyridine dinucleotides in regulating the permeability of the mitochondrial outer membrane. J Biol Chem *271*, 26724-26731.

Lee, A.C., Zizi, M., and Colombini, M. (1994). Beta-NADH decreases the permeability of the mitochondrial outer membrane to ADP by a factor of 6. J Biol Chem *269*, 30974-30980.

Lee, M.G., Xu, X., Zeng, W., Diaz, J., Kuo, T.H., Wuytack, F., Racymaekers, L., and Muallem, S. (1997a). Polarized expression of Ca2+ pumps in pancreatic and salivary gland cells. Role in initiation and propagation of [Ca2+]i waves. J Biol Chem *272*, 15771-15776.

Lee, M.G., Xu, X., Zeng, W., Diaz, J., Wojcikiewicz, R.J., Kuo, T.H., Wuytack, F., Racymaekers, L., and Muallem, S. (1997b). Polarized expression of Ca2+ channels in pancreatic and salivary gland cells. Correlation with initiation and propagation of [Ca2+]i waves. J Biol Chem *272*, 15765-15770.

Lemasters, J.J., and Holmuhamedov, E. (2006). Voltage-dependent anion channel (VDAC) as mitochondrial governator--thinking outside the box. Biochim Biophys Acta *1762*, 181-190.

Levine, B. (2005). Eating oneself and uninvited guests: autophagy-related pathways in cellular defense. Cell *120*, 159-162.

Levine, T., and Rabouille, C. (2005). Endoplasmic reticulum: one continuous network compartmentalized by extrinsic cues. Curr Opin Cell Biol *17*, 362-368.

Lin, J., Handschin, C., and Spiegelman, B.M. (2005). Metabolic control through the PGC-1 family of transcription coactivators. Cell Metab *1*, 361-370.

Litjens, T., Nguyen, T., Castro, J., Aromataris, E.C., Jones, L., Barritt, G.J., and Rychkov, G.Y. (2007). Phospholipase C-gamma1 is required for the activation of store-operated Ca2+ channels in liver cells. Biochem J *405*, 269-276.

Litsky, M.L., and Pfeiffer, D.R. (1997). Regulation of the mitochondrial Ca2+ uniporter by external adenine nucleotides: the uniporter behaves like a gated channel which is regulated by nucleotides and divalent cations. Biochemistry *36*, 7071-7080.

Liu, X., Kim, C.N., Yang, J., Jemmerson, R., and Wang, X. (1996). Induction of apoptotic program in cell-free extracts: requirement for dATP and cytochrome c. Cell *86*, 147-157.

Liu, Y., Liu, W., Song, X.D., and Zuo, J. (2005). Effect of GRP75/mthsp70/PBP74/mortalin overexpression on intracellular ATP level, mitochondrial membrane potential and ROS accumulation following glucose deprivation in PC12 cells. Mol Cell Biochem *268*, 45-51.

Lum, J.J., DeBerardinis, R.J., and Thompson, C.B. (2005). Autophagy in metazoans: cell survival in the land of plenty. Nat Rev Mol Cell Biol *6*, 439-448.

Maiuri, M.C., Le Toumelin, G., Criollo, A., Rain, J.C., Gautier, F., Juin, P., Tasdemir, E., Pierron, G., Troulinaki, K., Tavernarakis, N.*, et al.* (2007a). Functional and physical interaction between Bcl-X(L) and a BH3-like domain in Beclin-1. EMBO J *26*, 2527-2539.

Maiuri, M.C., Zalckvar, E., Kimchi, A., and Kroemer, G. (2007b). Self-eating and self-killing: crosstalk between autophagy and apoptosis. Nat Rev Mol Cell Biol *8*, 741-752.

Malia, T.J., and Wagner, G. (2007). NMR structural investigation of the mitochondrial outer membrane protein VDAC and its interaction with antiapoptotic Bcl-xL. Biochemistry *46*, 514-525.

Mannella, C.A. (2006). Structure and dynamics of the mitochondrial inner membrane cristae. BiochimBiophysActa *1763*, 542-548.

Mannella, C.A., Buttle, K., Rath, B.K., and Marko, M. (1998). Electron microscopic tomography of rat-liver mitochondria and their interaction with the endoplasmic reticulum. Biofactors *8*, 225-228.

Mao, C., Kim, S.H., Almenoff, J.S., Rudner, X.L., Kearney, D.M., and Kindman, L.A. (1996). Molecular cloning and characterization of SCaMPER, a sphingolipid Ca2+ release-mediating protein from endoplasmic reticulum. Proc Natl Acad Sci U S A *93*, 1993-1996.

Marsh, B.J., Mastronarde, D.N., Buttle, K.F., Howell, K.E., and McIntosh, J.R. (2001). Organellar relationships in the Golgi region of the pancreatic beta cell line, HIT-T15, visualized by high resolution electron tomography. Proc Natl Acad Sci U S A *98*, 2399-2406.

Massey, A.C., Zhang, C., and Cuervo, A.M. (2006). Chaperone-mediated autophagy in aging and disease. Curr Top Dev Biol *73*, 205-235.

McCormack, J.G., Halestrap, A.P., and Denton, R.M. (1990). Role of calcium ions in regulation of mammalian intramitochondrial metabolism. Physiol Rev *70*, 391-425.

McFadzean, I., and Gibson, A. (2002). The developing relationship between receptor-operated and store-operated calcium channels in smooth muscle. Br J Pharmacol *135*, 1-13.

Meldolesi, J., and Pozzan, T. (1987). Pathways of Ca2+ influx at the plasma membrane: voltage-, receptor-, and second messenger-operated channels. Exp Cell Res *171*, 271-283.

Mendes, C.C., Gomes, D.A., Thompson, M., Souto, N.C., Goes, T.S., Goes, A.M., Rodrigues, M.A., Gomez, M.V., Nathanson, M.H., and Leite, M.F. (2005). The type III inositol 1,4,5-trisphosphate receptor preferentially transmits apoptotic Ca2+ signals into mitochondria. J Biol Chem *280*, 40892-40900.

Michalak, M., Robert Parker, J.M., and Opas, M. (2002). Ca2+ signaling and calcium binding chaperones of the endoplasmic reticulum. Cell Calcium *32*, 269-278.

Mignery, G.A., and Sudhof, T.C. (1990). The ligand binding site and transduction mechanism in the inositol-1,4,5-triphosphate receptor. EMBO J *9*, 3893-3898.

Mikoshiba, K. (2007). IP3 receptor/Ca2+ channel: from discovery to new signaling concepts. J Neurochem *102*, 1426-1446.

Missiaen, L., Taylor, C.W., and Berridge, M.J. (1992). Luminal Ca2+ promoting spontaneous Ca2+ release from inositol trisphosphate-sensitive stores in rat hepatocytes. J Physiol *455*, 623-640.

Mitchell, P. (1966). Chemiosmotic coupling in oxidative and photosynthetic phosphorylation. Biol Rev Camb Philos Soc *41*, 445-502.

Mizushima, N., and Klionsky, D.J. (2007). Protein turnover via autophagy: implications for metabolism. Annu Rev Nutr *27*, 19-40.

Mokranjac, D., and Neupert, W. (2005). Protein import into mitochondria. BiochemSocTrans *33*, 1019-1023.

Montero, M., Alonso, M.T., Carnicero, E., Cuchillo-Ibanez, I., Albillos, A., Garcia, A.G., Garcia-Sancho, J., and Alvarez, J. (2000). Chromaffin-cell stimulation triggers fast millimolar mitochondrial Ca2+ transients that modulate secretion. Nat Cell Biol *2*, 57-61.

Montero, M., Lobaton, C.D., Hernandez-Sanmiguel, E., Santodomingo, J., Vay, L., Moreno, A., and Alvarez, J. (2004). Direct activation of the mitochondrial calcium uniporter by natural plant flavonoids. Biochem J *384*, 19-24.

Moore, M.N. (2008). Autophagy as a second level protective process in conferring resistance to environmentally-induced oxidative stress. Autophagy *4*, 254-256.

Moreau, B., Nelson, C., and Parekh, A.B. (2006). Biphasic regulation of mitochondrial Ca2+ uptake by cytosolic Ca2+ concentration. Curr Biol *16*, 1672-1677.

Murthy, K.S., and Zhou, H. (2003). Selective phosphorylation of the IP3R-I in vivo by cGMP-dependent protein kinase in smooth muscle. Am J Physiol Gastrointest Liver Physiol *284*, G221-230.

Nakamura, N., Matsuura, A., Wada, Y., and Ohsumi, Y. (1997). Acidification of vacuoles is required for autophagic degradation in the yeast, Saccharomyces cerevisiae. J Biochem *121*, 338-344.

Neshat, M.S., Mellinghoff, I.K., Tran, C., Stiles, B., Thomas, G., Petersen, R., Frost, P., Gibbons, J.J., Wu, H., and Sawyers, C.L. (2001). Enhanced sensitivity of PTEN-deficient tumors to inhibition of FRAP/mTOR. Proc Natl Acad Sci U S A *98*, 10314-10319.

Neupert, W., and Brunner, M. (2002). The protein import motor of mitochondria. Nat Rev Mol Cell Biol *3*, 555-565.

Noda, T., and Ohsumi, Y. (1998). Tor, a phosphatidylinositol kinase homologue, controls autophagy in yeast. J Biol Chem *273*, 3963-3966.

Nunn, D.L., and Taylor, C.W. (1992). Luminal Ca2+ increases the sensitivity of Ca2+ stores to inositol 1,4,5-trisphosphate. Mol Pharmacol *41*, 115-119.

Oh-hora, M., and Rao, A. (2008). Calcium signaling in lymphocytes. Curr Opin Immunol *20*, 250-258.

Onodera, J., and Ohsumi, Y. (2004). Ald6p is a preferred target for autophagy in yeast, Saccharomyces cerevisiae. J Biol Chem *279*, 16071-16076.

Pacher, P., Sharma, K., Csordas, G., Zhu, Y., and Hajnoczky, G. (2008). Uncoupling of ER-mitochondrial calcium communication by transforming growth factor-beta. Am J Physiol Renal Physiol *295*, F1303-1312.

Parker, I., and Ivorra, I. (1990). Localized all-or-none calcium liberation by inositol trisphosphate. Science *250*, 977-979.

Pastorino, J.G., and Hoek, J.B. (2008). Regulation of hexokinase binding to VDAC. J Bioenerg Biomembr *40*, 171-182.

Patterson, R.L., Boehning, D., and Snyder, S.H. (2004). Inositol 1,4,5-trisphosphate receptors as signal integrators. Annu Rev Biochem *73*, 437-465.

Pattingre, S., and Levine, B. (2006). Bcl-2 inhibition of autophagy: a new route to cancer? Cancer Res *66*, 2885-2888.

Pattingre, S., Tassa, A., Qu, X., Garuti, R., Liang, X.H., Mizushima, N., Packer, M., Schneider, M.D., and Levine, B. (2005). Bcl-2 antiapoptotic proteins inhibit Beclin 1-dependent autophagy. Cell *122*, 927-939.

Pedersen, S., Celis, J.E., Nielsen, J., Christiansen, J., and Nielsen, F.C. (1997). Distinct repression of translation by wortmannin and rapamycin. Eur J Biochem *247*, 449-456.

Peralta, E.R., and Edinger, A.L. (2009). Ceramide-induced starvation triggers homeostatic autophagy. Autophagy *5*.

Petersen, O.H., Burdakov, D., and Tepikin, A.V. (1999). Polarity in intracellular calcium signaling. Bioessays *21*, 851-860.

Pfeiffer, D.R., Gunter, T.E., Eliseev, R., Broekemeier, K.M., and Gunter, K.K. (2001). Release of Ca2+ from mitochondria via the saturable mechanisms and the permeability transition. IUBMB Life *52*, 205-212.

Pinton, P., Ferrari, D., Magalhaes, P., Schulze-Osthoff, K., Di, V.F., Pozzan, T., and Rizzuto, R. (2000). Reduced loading of intracellular Ca(2+) stores and downregulation of capacitative Ca(2+) influx in Bcl-2-overexpressing cells. JCell Biol *148*, 857-862.

Pinton, P., Ferrari, D., Rapizzi, E., Di, V.F., Pozzan, T., and Rizzuto, R. (2001a). The Ca2+ concentration of the endoplasmic reticulum is a key determinant of ceramide-induced apoptosis: significance for the molecular mechanism of Bcl-2 action. EMBO J *20*, 2690-2701.

Pinton, P., Ferrari, D., Rapizzi, E., Di Virgilio, F., Pozzan, T., and Rizzuto, R. (2001b). The Ca2+ concentration of the endoplasmic reticulum is a key determinant of ceramide-induced apoptosis: significance for the molecular mechanism of Bcl-2 action. EMBO J *20*, 2690-2701.

Pinton, P., Leo, S., Wieckowski, M.R., Di Benedetto, G., and Rizzuto, R. (2004). Long-term modulation of mitochondrial Ca2+ signals by protein kinase C isozymes. J Cell Biol *165*, 223-232.

Porcelli, A.M., Ghelli, A., Zanna, C., Pinton, P., Rizzuto, R., and Rugolo, M. (2005). pH difference across the outer mitochondrial membrane measured with a green fluorescent protein mutant. Biochem Biophys Res Commun *326*, 799-804.

Prentki, M., Biden, T.J., Janjic, D., Irvine, R.F., Berridge, M.J., and Wollheim, C.B. (1984). Rapid mobilization of Ca2+ from rat insulinoma microsomes by inositol-1,4,5-trisphosphate. Nature *309*, 562-564.

Qu, X., Zou, Z., Sun, Q., Luby-Phelps, K., Cheng, P., Hogan, R.N., Gilpin, C., and Levine, B. (2007). Autophagy gene-dependent clearance of apoptotic cells during embryonic development. Cell *128*, 931-946.

Ran, Q., Wadhwa, R., Kawai, R., Kaul, S.C., Sifers, R.N., Bick, R.J., Smith, J.R., and Pereira-Smith, O.M. (2000). Extramitochondrial localization of mortalin/mthsp70/PBP74/GRP75. Biochem Biophys Res Commun *275*, 174-179.

Rapizzi, E., Pinton, P., Szabadkai, G., Wieckowski, M.R., Vandecasteele, G., Baird, G., Tuft, R.A., Fogarty, K.E., and Rizzuto, R. (2002a). Recombinant expression of the voltage-dependent anion channel enhances the transfer of Ca2+ microdomains to mitochondria. J Cell Biol *159*, 613-624.

Rapizzi, E., Pinton, P., Szabadkai, G., Wieckowski, M.R., Vandecasteele, G., Baird, G., Tuft, R.A., Fogarty, K.E., and Rizzuto, R. (2002b). Recombinant expression of the voltage-dependent anion channel enhances the transfer of Ca2+ microdomains to mitochondria. JCell Biol *159*, 613-624.

Ravagnan, L., Roumier, T., and Kroemer, G. (2002). Mitochondria, the killer organelles and their weapons. JCell Physiol *192*, 131-137.

Rebecchi, M.J., and Pentyala, S.N. (2000). Structure, function, and control of phosphoinositide-specific phospholipase C. Physiol Rev *80*, 1291-1335.

Rembold, C.M., Kendall, J.M., and Campbell, A.K. (1997). Measurement of changes in sarcoplasmic reticulum [Ca2+] in rat tail artery with targeted apoaequorin delivered by an adenoviral vector. Cell Calcium *21*, 69-79.

Rizzuto, R., Brini, M., Murgia, M., and Pozzan, T. (1993). Microdomains with high Ca2+ close to IP3-sensitive channels that are sensed by neighboring mitochondria. Science *262*, 744-747.

Rizzuto, R., Pinton, P., Carrington, W., Fay, F.S., Fogarty, K.E., Lifshitz, L.M., Tuft, R.A., and Pozzan, T. (1998a). Close contacts with the endoplasmic reticulum as determinants of mitochondrial Ca2+ responses. Science *280*, 1763-1766.

Rizzuto, R., Pinton, P., Carrington, W., Fay, F.S., Fogarty, K.E., Lifshitz, L.M., Tuft, R.A., and Pozzan, T. (1998b). Close contacts with the endoplasmic reticulum as determinants of mitochondrial Ca2+ responses. Science *280*, 1763-1766.

Rizzuto, R., Simpson, A.W., Brini, M., and Pozzan, T. (1992a). Rapid changes of mitochondrial Ca2+ revealed by specifically targeted recombinant aequorin. Nature *358*, 325-327.

Rizzuto, R., Simpson, A.W., Brini, M., and Pozzan, T. (1992b). Rapid changes of mitochondrial Ca2+ revealed by specifically targeted recombinant aequorin. Nature *358*, 325-327.

Robert, V., De Giorgi, F., Massimino, M.L., Cantini, M., and Pozzan, T. (1998). Direct monitoring of the calcium concentration in the sarcoplasmic and endoplasmic reticulum of skeletal muscle myotubes. J Biol Chem *273*, 30372-30378.

Robert, V., Gurlini, P., Tosello, V., Nagai, T., Miyawaki, A., Di Lisa, F., and Pozzan, T. (2001). Beat-to-beat oscillations of mitochondrial [Ca2+] in cardiac cells. EMBO J *20*, 4998-5007.

Rooney, T.A., and Thomas, A.P. (1993). Intracellular calcium waves generated by Ins(1,4,5)P3-dependent mechanisms. Cell Calcium *14*, 674-690.

Rostovtseva, T.K., Antonsson, B., Suzuki, M., Youle, R.J., Colombini, M., and Bezrukov, S.M. (2004). Bid, but not Bax, regulates VDAC channels. J Biol Chem *279*, 13575-13583.

Rostovtseva, T.K., Sheldon, K.L., Hassanzadeh, E., Monge, C., Saks, V., Bezrukov, S.M., and Sackett, D.L. (2008). Tubulin binding blocks mitochondrial voltage-dependent anion channel and regulates respiration. Proc Natl Acad Sci U S A *105*, 18746-18751.

Sandoval, H., Thiagarajan, P., Dasgupta, S.K., Schumacher, A., Prchal, J.T., Chen, M., and Wang, J. (2008). Essential role for Nix in autophagic maturation of erythroid cells. Nature *454*, 232-235.

Saotome, M., Safiulina, D., Szabadkai, G., Das, S., Fransson, A., Aspenstrom, P., Rizzuto, R., and Hajnoczky, G. (2008). Bidirectional Ca2+-dependent control of mitochondrial dynamics by the Miro GTPase. Proc Natl Acad Sci U S A *105*, 20728-20733.

Sarbassov, D.D., Ali, S.M., Kim, D.H., Guertin, D.A., Latek, R.R., Erdjument-Bromage, H., Tempst, P., and Sabatini, D.M. (2004). Rictor, a novel binding partner of mTOR, defines a rapamycin-insensitive and raptor-independent pathway that regulates the cytoskeleton. Curr Biol *14*, 1296-1302.

Sarbassov, D.D., Ali, S.M., and Sabatini, D.M. (2005a). Growing roles for the mTOR pathway. Curr Opin Cell Biol *17*, 596-603.

Sarbassov, D.D., Ali, S.M., Sengupta, S., Sheen, J.H., Hsu, P.P., Bagley, A.F., Markhard, A.L., and Sabatini, D.M. (2006). Prolonged rapamycin treatment inhibits mTORC2 assembly and Akt/PKB. Mol Cell *22*, 159-168.

Sarbassov, D.D., Guertin, D.A., Ali, S.M., and Sabatini, D.M. (2005b). Phosphorylation and regulation of Akt/PKB by the rictor-mTOR complex. Science *307*, 1098-1101.

Saris, N.E., and Carafoli, E. (2005). A historical review of cellular calcium handling, with emphasis on mitochondria. Biochemistry (Mosc) *70*, 187-194.

Sarkar, S., Floto, R.A., Berger, Z., Imarisio, S., Cordenier, A., Pasco, M., Cook, L.J., and Rubinsztein, D.C. (2005). Lithium induces autophagy by inhibiting inositol monophosphatase. J Cell Biol *170*, 1101-1111.

Scarlatti, F., Granata, R., Meijer, A.J., and Codogno, P. (2009). Does autophagy have a license to kill mammalian cells? Cell Death Differ *16*, 12-20.

Schein, S.J., Colombini, M., and Finkelstein, A. (1976). Reconstitution in planar lipid bilayers of a voltage-dependent anion-selective channel obtained from paramecium mitochondria. J Membr Biol *30*, 99-120.

Schieke, S.M., Phillips, D., McCoy, J.P., Jr., Aponte, A.M., Shen, R.F., Balaban, R.S., and Finkel, T. (2006). The mammalian target of rapamycin (mTOR) pathway regulates mitochondrial oxygen consumption and oxidative capacity. J Biol Chem *281*, 27643-27652.

Schinder, A.F., Olson, E.C., Spitzer, N.C., and Montal, M. (1996). Mitochondrial dysfunction is a primary event in glutamate neurotoxicity. J Neurosci *16*, 6125-6133.

Schwarzer, C., Barnikol-Watanabe, S., Thinnes, F.P., and Hilschmann, N. (2002a). Voltage-dependent anion-selective channel (VDAC) interacts with the dynein light chain Tctex1 and the heat-shock protein PBP74. Int J Biochem Cell Biol *34*, 1059-1070.

Schwarzer, C., Barnikol-Watanabe, S., Thinnes, F.P., and Hilschmann, N. (2002b). Voltage-dependent anion-selective channel (VDAC) interacts with the dynein light chain Tctex1 and the heat-shock protein PBP74. IntJBiochemCell Biol *34*, 1059-1070.

Scorrano, L., Oakes, S.A., Opferman, J.T., Cheng, E.H., Sorcinelli, M.D., Pozzan, T., and Korsmeyer, S.J. (2003). BAX and BAK regulation of endoplasmic reticulum Ca2+: a control point for apoptosis. Science *300*, 135-139.

Shimizu, S., Kanaseki, T., Mizushima, N., Mizuta, T., Arakawa-Kobayashi, S., Thompson, C.B., and Tsujimoto, Y. (2004). Role of Bcl-2 family proteins in a non-apoptotic programmed cell death dependent on autophagy genes. Nat Cell Biol *6*, 1221-1228.

Shimizu, S., Shinohara, Y., and Tsujimoto, Y. (2000). Bax and Bcl-xL independently regulate apoptotic changes of yeast mitochondria that require VDAC but not adenine nucleotide translocator. Oncogene *19*, 4309-4318.

Shimomura, O. (1986). Isolation and properties of various molecular forms of aequorin. Biochem J *234*, 271-277.

Shimomura, O., Kishi, Y., and Inouye, S. (1993). The relative rate of aequorin regeneration from apoaequorin and coelenterazine analogues. Biochem J *296 (Pt 3)*, 549-551.

Shiota, C., Woo, J.T., Lindner, J., Shelton, K.D., and Magnuson, M.A. (2006). Multiallelic disruption of the rictor gene in mice reveals that mTOR complex 2 is essential for fetal growth and viability. Dev Cell *11*, 583-589.

Shor, B., Zhang, W.G., Toral-Barza, L., Lucas, J., Abraham, R.T., Gibbons, J.J., and Yu, K. (2008). A new pharmacologic action of CCI-779 involves FKBP12-independent inhibition of mTOR kinase activity and profound repression of global protein synthesis. Cancer Res *68*, 2934-2943.

Smith, J.B., Smith, L., and Higgins, B.L. (1985). Temperature and nucleotide dependence of calcium release by myo-inositol 1,4,5-trisphosphate in cultured vascular smooth muscle cells. J Biol Chem *260*, 14413-14416.

Soti, C., Pal, C., Papp, B., and Csermely, P. (2005). Molecular chaperones as regulatory elements of cellular networks. Curr Opin Cell Biol *17*, 210-215.

Sparagna, G.C., Gunter, K.K., Sheu, S.S., and Gunter, T.E. (1995). Mitochondrial calcium uptake from physiological-type pulses of calcium. A description of the rapid uptake mode. J Biol Chem *270*, 27510-27515.

Steinmann, C., Landsverk, M.L., Barral, J.M., and Boehning, D. (2008). Requirement of inositol 1,4,5-trisphosphate receptors for tumor-mediated lymphocyte apoptosis. J Biol Chem *283*, 13506-13509.

Stone, S.S., Levin, M.C., Zhou, P., Han, J., Walther, T.C., and Farese, R.V., Jr. (2008). The endoplasmic reticulum enzyme, DGAT2, is found in mitochondria-associated membranes and has a mitochondrial targeting signal that promotes its association with mitochondria. J Biol Chem.

Streb, H., Irvine, R.F., Berridge, M.J., and Schulz, I. (1983). Release of Ca2+ from a nonmitochondrial intracellular store in pancreatic acinar cells by inositol-1,4,5-trisphosphate. Nature *306*, 67-69.

Szabadkai, G., Bianchi, K., Varnai, P., De Stefani, D., Wieckowski, M.R., Cavagna, D., Nagy, A.I., Balla, T., and Rizzuto, R. (2006). Chaperone-mediated coupling of endoplasmic reticulum and mitochondrial Ca2+ channels. J Cell Biol *175*, 901-911.

Szabadkai, G., and Rizzuto, R. (2004). Participation of endoplasmic reticulum and mitochondrial calcium handling in apoptosis: more than just neighborhood? FEBS Lett *567*, 111-115.

Szabadkai, G., Simoni, A.M., Chami, M., Wieckowski, M.R., Youle, R.J., and Rizzuto, R. (2004). Drp-1-dependent division of the mitochondrial network blocks intraorganellar Ca2+ waves and protects against Ca2+-mediated apoptosis. MolCell *16*, 59-68.

Szalai, G., Krishnamurthy, R., and Hajnoczky, G. (1999). Apoptosis driven by IP(3)-linked mitochondrial calcium signals. EMBO J *18*, 6349-6361.

Takeuchi, H., Kondo, Y., Fujiwara, K., Kanzawa, T., Aoki, H., Mills, G.B., and Kondo, S. (2005). Synergistic augmentation of rapamycin-induced autophagy in malignant glioma cells by phosphatidylinositol 3-kinase/protein kinase B inhibitors. Cancer Res *65*, 3336-3346.

Tasdemir, E., Maiuri, M.C., Galluzzi, L., Vitale, I., Djavaheri-Mergny, M., D'Amelio, M., Criollo, A., Morselli, E., Zhu, C., Harper, F.*, et al.* (2008). Regulation of autophagy by cytoplasmic p53. Nat Cell Biol *10*, 676-687.

Tateishi, Y., Hattori, M., Nakayama, T., Iwai, M., Bannai, H., Nakamura, T., Michikawa, T., Inoue, T., and Mikoshiba, K. (2005). Cluster formation of inositol 1,4,5-trisphosphate receptor requires its transition to open state. J Biol Chem *280*, 6816-6822.

Thomas, A.P., Renard-Rooney, D.C., Hajnoczky, G., Robb-Gaspers, L.D., Lin, C., and Rooney, T.A. (1995). Subcellular organization of calcium signalling in hepatocytes and the intact liver. Ciba FoundSymp *188*, 18-35.

Thorn, P., Lawrie, A.M., Smith, P.M., Gallacher, D.V., and Petersen, O.H. (1993). Local and global cytosolic Ca2+ oscillations in exocrine cells evoked by agonists and inositol trisphosphate. Cell *74*, 661-668.

Tinel, H., Cancela, J.M., Mogami, H., Gerasimenko, J.V., Gerasimenko, O.V., Tepikin, A.V., and Petersen, O.H. (1999). Active mitochondria surrounding the pancreatic acinar granule region prevent spreading of inositol trisphosphate-evoked local cytosolic Ca(2+) signals. EMBO J *18*, 4999-5008.

Toth, M.L., Simon, P., Kovacs, A.L., and Vellai, T. (2007). Influence of autophagy genes on ion-channel-dependent neuronal degeneration in Caenorhabditis elegans. J Cell Sci *120*, 1134-1141.

Trenker, M., Malli, R., Fertschai, I., Levak-Frank, S., and Graier, W.F. (2007). Uncoupling proteins 2 and 3 are fundamental for mitochondrial Ca2+ uniport. Nat Cell Biol *9*, 445-452.

Tsukada, M., and Ohsumi, Y. (1993). Isolation and characterization of autophagy-defective mutants of Saccharomyces cerevisiae. FEBS Lett *333*, 169-174.

Ujwal, R., Cascio, D., Colletier, J.P., Faham, S., Zhang, J., Toro, L., Ping, P., and Abramson, J. (2008). The crystal structure of mouse VDAC1 at 2.3 A resolution reveals mechanistic insights into metabolite gating. Proc Natl Acad Sci U S A *105*, 17742-17747.

Vance, J.E. (1990). Phospholipid synthesis in a membrane fraction associated with mitochondria. J Biol Chem *265*, 7248-7256.

Vance, J.E. (2003). Molecular and cell biology of phosphatidylserine and phosphatidylethanolamine metabolism. Prog Nucleic Acid Res Mol Biol *75*, 69-111.

Vance, J.E. (2008). Phosphatidylserine and phosphatidylethanolamine in mammalian cells: two metabolically related aminophospholipids. J Lipid Res *49*, 1377-1387.

Vander Heiden, M.G., Li, X.X., Gottleib, E., Hill, R.B., Thompson, C.B., and Colombini, M. (2001). Bcl-xL promotes the open configuration of the voltage-dependent anion channel and metabolite passage through the outer mitochondrial membrane. J Biol Chem *276*, 19414-19419.

Varadi, A., and Rutter, G.A. (2004). Ca2+-induced Ca2+ release in pancreatic islet beta-cells: critical evaluation of the use of endoplasmic reticulum-targeted "cameleons". Endocrinology *145*, 4540-4549.

Varnai, P., Balla, A., Hunyady, L., and Balla, T. (2005). Targeted expression of the inositol 1,4,5-triphosphate receptor (IP3R) ligand-binding domain releases Ca2+ via endogenous IP3R channels. Proc Natl Acad Sci U S A *102*, 7859-7864.

Vendelin, M., Lemba, M., and Saks, V.A. (2004). Analysis of functional coupling: mitochondrial creatine kinase and adenine nucleotide translocase. Biophys J *87*, 696-713.

Ventura-Clapier, R., Kaasik, A., and Veksler, V. (2004). Structural and functional adaptations of striated muscles to CK deficiency. Mol Cell Biochem *256-257*, 29-41.

Vermassen, E., Fissore, R.A., Nadif Kasri, N., Vanderheyden, V., Callewaert, G., Missiaen, L., Parys, J.B., and De Smedt, H. (2004). Regulation of the phosphorylation of the inositol 1,4,5-trisphosphate receptor by protein kinase C. Biochem Biophys Res Commun *319*, 888-893.

Wadhwa, R., Takano, S., Kaur, K., Aida, S., Yaguchi, T., Kaul, Z., Hirano, T., Taira, K., and Kaul, S.C. (2005). Identification and characterization of molecular interactions between mortalin/mtHsp70 and HSP60. Biochem J *391*, 185-190.

Wadhwa, R., Yaguchi, T., Hasan, M.K., Mitsui, Y., Reddel, R.R., and Kaul, S.C. (2002). Hsp70 family member, mot-2/mthsp70/GRP75, binds to the cytoplasmic sequestration domain of the p53 protein. Exp Cell Res *274*, 246-253.

Wang, C.W., and Klionsky, D.J. (2003). The molecular mechanism of autophagy. Mol Med *9*, 65-76.

Watkins, N.J., and Campbell, A.K. (1993). Requirement of the C-terminal proline residue for stability of the Ca(2+)-activated photoprotein aequorin. Biochem J *293 (Pt 1)*, 181-185.

Wojcikiewicz, R.J. (1995). Type I, II, and III inositol 1,4,5-trisphosphate receptors are unequally susceptible to down-regulation and are expressed in markedly different proportions in different cell types. J Biol Chem *270*, 11678-11683.

Wu, S., Sampson, M.J., Decker, W.K., and Craigen, W.J. (1999). Each mammalian mitochondrial outer membrane porin protein is dispensable: effects on cellular respiration. BiochimBiophysActa *1452*, 68-78.

Wullschleger, S., Loewith, R., and Hall, M.N. (2006). TOR signaling in growth and metabolism. Cell *124*, 471-484.

Xu, X., Decker, W., Sampson, M.J., Craigen, W.J., and Colombini, M. (1999). Mouse VDAC isoforms expressed in yeast: channel properties and their roles in mitochondrial outer membrane permeability. J Membr Biol *170*, 89-102.

Yagoda, N., von Rechenberg, M., Zaganjor, E., Bauer, A.J., Yang, W.S., Fridman, D.J., Wolpaw, A.J., Smukste, I., Peltier, J.M., Boniface, J.J.*, et al.* (2007). RAS-RAF-MEK-dependent oxidative cell death involving voltage-dependent anion channels. Nature *447*, 864-868.

Yao, Y., Choi, J., and Parker, I. (1995). Quantal puffs of intracellular Ca2+ evoked by inositol trisphosphate in Xenopus oocytes. J Physiol *482 (Pt 3)*, 533-553.

Yi, M., Weaver, D., and Hajnoczky, G. (2004a). Control of mitochondrial motility and distribution by the calcium signal: a homeostatic circuit. J Cell Biol *167*, 661-672.

Yi, M., Weaver, D., and Hajnoczky, G. (2004b). Control of mitochondrial motility and distribution by the calcium signal: a homeostatic circuit. JCell Biol *167*, 661-672.

Young, J.C., Barral, J.M., and Ulrich Hartl, F. (2003). More than folding: localized functions of cytosolic chaperones. Trends Biochem Sci *28*, 541-547.

Yu, L., Alva, A., Su, H., Dutt, P., Freundt, E., Welsh, S., Baehrecke, E.H., and Lenardo, M.J. (2004). Regulation of an ATG7-beclin 1 program of autophagic cell death by caspase-8. Science *304*, 1500-1502.

Zahedi, R.P., Sickmann, A., Boehm, A.M., Winkler, C., Zufall, N., Schonfisch, B., Guiard, B., Pfanner, N., and Meisinger, C. (2006). Proteomic analysis of the yeast mitochondrial outer membrane reveals accumulation of a subclass of preproteins. Mol Biol Cell *17*, 1436-1450.

Zaid, H., Abu-Hamad, S., Israelson, A., Nathan, I., and Shoshan-Barmatz, V. (2005). The voltage-dependent anion channel-1 modulates apoptotic cell death. Cell Death Differ *12*, 751-760.

Zhang, Y., Qi, H., Taylor, R., Xu, W., Liu, L.F., and Jin, S. (2007). The role of autophagy in mitochondria maintenance: characterization of mitochondrial functions in autophagy-deficient S. cerevisiae strains. Autophagy *3*, 337-346.